UTS UNIVERSITY OF TECHNOLOGY SYDNEY

Safe Optimal Control of Cooperative Multi-Agent Systems

by Boqian Li

Thesis submitted in fulfillment of the requirements for the degree of

Doctor of Philosophy

under the supervision of Prof. Shiping Wen

University of Technology Sydney
Faculty of Engineering and Information Technology

September 2025

CERTIFICATE OF ORIGINAL AUTHORSHIP

I, *Boqian Li* declare that this thesis, is submitted in fulfilment of the requirements for the award of *Doctor of Philosophy*, in the *Australian Artificial Intelligence Institute*, *Faculty of Engineering and Information Technology* at the University of Technology Sydney.

This thesis is wholly my own work unless otherwise referenced or acknowledged. In addition, I certify that all information sources and literature used are indicated in the thesis.

This document has not been submitted for qualifications at any other academic institution.

This research is supported by the Australian Government Research Training Program.

Signature: Production Note:
Signature removed prior to publication.

Date: September 2025

Abstract

The cooperative control of multi-agent systems (MASs) has garnered significant attention due to its broad range of applications, including environmental exploration, area coverage, and more. Two fundamental requirements for MASs are stability, which ensures that the system states converge to desired objectives, and safety, which guarantees that agents operate within safe regions. To meet these requirements, control Lyapunov functions (CLFs) are employed to achieve stability, while control barrier functions (CBFs) are used to enforce safety constraints. These functions are integrated into a unified quadratic programming (QP) framework, where control inputs are computed by solving constrained optimization problems.

In practical applications, external disturbances and modeling uncertainties are often inevitable, thereby necessitating the development of robust control strategies. Within the proposed QP control framework, such uncertainties typically appear as unknown components in the constraint formulations. One conventional approach to address this issue is the use of model-based robustness techniques, which rely on bounds of uncertainties. Alternatively, modern data-driven approaches, such as Gaussian process (GP) modeling, offer possible solution by providing probabilistic approximations of the unknown functions, including mean and variances predictions. This probabilistic characterization enables an estimation of uncertainty, enhancing the robustness and overall reliability of the control framework.

Moreover, MASs frequently operate in resource-constrained environments, where

control performance is of high importance. In such scenarios, system behavior is often influenced by hyperparameters whose effects on performance are complex and difficult to model analytically. To systematically improve long-term control performance, this thesis formulates this problem as a black-box optimization task and proposes a constrained Bayesian optimization (CBO) algorithm, which efficiently explores the hyperparameter space to identify configurations that optimize system performance while ensuring stability and safety.

Building upon the above statement, this thesis investigates the cooperative control of MASs from the following main perspectives. First, establish a constrained QP control framework that ensures both stability and safety for decentralized MASs; Second, enhance robustness to uncertainties by dealing with unknown disturbances, thus enabling the control system to adapt in real time to uncertain dynamics; Third, optimize control performance through a CBO algorithm that explicitly considers both safety and effectiveness under varying hyperparameter settings. The proposed methodologies are validated through extensive simulations and case studies, demonstrating their effectiveness in achieving stable, safe, robust, and high-performing cooperative control in MASs.

Dedication

For Mom and Dad

To the Moon and Beyond...

ACKNOWLEDGMENTS

Embarking on the journey toward a doctoral degree at University of Technology Sydney has been a profound personal endeavor. Throughout this challenging yet rewarding path, I have encountered numerous obstacles that tested my resolve. However, each hurdle surmounted has not only strengthened my character but also deepened my commitment to the pursuit of knowledge. Reflecting upon this journey, I am profoundly grateful for the personal growth and the relentless pursuit of excellence that have culminated in this dissertation.

First of all, I wish to express my deepest gratitude to my principle supervisor, Professor Shiping Wen, for his unparalleled expertise and insightful guidance which have been instrumental in shaping the trajectory of my research. Professor Wen's support has significantly helped me to think critically and innovatively. His patience and encouragement have fostered an environment where I could explore complex ideas with confidence. The countless hours he invested in reviewing my work and providing detailed feedback of my academic research have been invaluable. His dedication to my academic and personal development has left an indelible mark, for which I am always grateful.

I am also thankful to my co-supervisor Dr. Lu Qin, whose collaboration has enriched this research. His diverse perspectives and expertise have significantly contributed to the depth and breadth of this work. The shared experiences, rigorous discussions, and collective problem-solving have been pivotal in achieving our scholarly goals.

I would like to express my deepest gratitude to the administrative staff and faculty members of the School of Computer Science, Faculty of Engineering and Information

Science. Their unwavering support has been the cornerstone of my research journey. From facilitating access to vital scientific resources to providing timely assistance during challenging times, their dedication has been truly invaluable. The seamless operation of our research environment stands as a testament to their hard work and commitment, fostering a space where academic endeavors can thrive.

Lastly, I wish to thank my friends, Feng Xu, Xiaocui Dang, Shengbo Wang, Zhencheng Fan, Linhao Zhao, Ziyu Sheng, Guangyang Tian, Wuzhida Bao, and Shanshan Zhao. Their steadfast support, encouragement, and understanding have been a source of strength throughout this journey. The balance between academic life and personal well-being was achievable because of their presence. Our shared moments of laughter have been the perfect counterbalance to the demands of doctoral research.

In conclusion, this dissertation is not solely the result of individual effort but is a culmination of the collective support, guidance, and love from all those mentioned above. To each of you, I extend my deepest gratitude.

Furthermore, I acknowledge Dr. Chandranath Adak for providing this thesis template.

List of Publications

Related to the Thesis:

1. **B. Li**, Z. Guo, C. Hu, S. Zhu and S. Wen, "Safe Formation Control of Uncertain Multiagent Systems From a Bayesian Perspective," in IEEE Transactions on Automatic Control, vol. 70, no. 3, pp. 1929-1934, March 2025. DOI: 10.1109/TAC.2024.3470928.

2. **B. Li**, Y. Cao, Y. Yang, S. Zhu, Z. Guo, T. Huang and S. Wen, "Quadratic Programming Consensus Tracking Control of Uncertain Multiagent Systems via Event-Triggered Mechanism," in IEEE Transactions on Systems, Man, and Cybernetics: Systems, vol. 54, no. 12, pp. 7861-7870, Dec. 2024. DOI: 10.1109/TSMC.2024.3459850.

3. **B. Li**, S. Wang, Z. Guo, S. Zhu, J. Huang, J. Sun, G. Wen and S. Wen, "Safe Control Framework of Multi-Agent Systems From a Performance Enhancement Perspective," in IEEE Transactions on Automation Science and Engineering, vol. 22, pp. 7622-7631, Oct. 2024. DOI: 10.1109/TASE.2024.3466791.

4. **B. Li**, S. Wen, Z. Yan, G. Wen and T. Huang, "A Survey on the Control Lyapunov Function and Control Barrier Function for Nonlinear-Affine Control Systems," in IEEE/CAA Journal of Automatica Sinica, vol. 10, no. 3, pp. 584-602, March 2023. DOI: 10.1109/JAS.2023.123075.

5. **B. Li**, and S. Wen, "High-Order Control Barrier Function for Safety in Uncertain Multi-Agent Systems," Preparing to submit.

Others:

6. **B. Li**, L. Zhao and S. Wen. "Periodic Event-Triggered Consensus of Stochastic Multi-Agent Systems Under Switching Topology," in Artificial Intelligence Science and Engineering, vol. 1, no. 2, 2025. DOI: 10.23919/AISE.2025.000011.

7. **B. Li**, T. Huang and S. Wen, "Safety Assurance of Connected Agents via Event-Triggered Control Barrier Function," Under review.

8. **B. Li** and S. Wen, "Collision-Free Formation Control of Stochastic Multi-Agent Systems," Under review.

TABLE OF CONTENTS

List of Figures

Figure **Page**

List of Abbreviations

ACS Affine-Control System

ARE Algebraic Riccati Equation

BO Bayesian Optimization

CBF Control Barrier Function

CBO Constrained Bayesian Optimization

CLF Control Lyapunov Function

CMA Convariance Matrix Adaptation

EI Expected Improvement

EIC Expected Improvement with Constraints

ETC Event-Triggered Mechanism

GA Genetic Algorithm

GP Gaussian Process

HOCBF High-Order Control Barrier Function

ISS Input-to-State Stability

ISSf Input-to-State Safety

LQR Linear Quadratic Regulator

MAS Multi-Agent System

NBF Neural Barrier Function

PID Proportional-Integral-Derivative

QP Quadratic Programming

RL Reinforcement Learning

RO Research Objective

RQ Research Question

RS Random Search

List of Notations

$\mathbb{R}$ Set of real numbers

$\mathbb{N}^+$ Set of positive integers

$\mathbb{R}^n$ n-dimensional real vectors space

$\mathbb{R}^{n\times m}$ $n \times m$-dimensional real matrices space

$0_{n\times m}$ $n \times m$-dimensional matrix with all elements as 0

I_n n-dimensional identity matrix

$\mathbf{0}_n$ n-dimensional vector with all elements as 0

$\mathscr{C}$ Closed set: $\{x|h(x) \geqslant 0\}$

$\partial\mathscr{C}$ Boundary of $\mathscr{C}$: $\{x|h(x) = 0\}$

Int($\mathscr{C}$) Interior of $\mathscr{C}$: $\{x|h(x) > 0\}$

inf[$\cdot$] Infimum

sup[$\cdot$] Supremum

$|\cdot|$ Absolute value

$\|\cdot\|$ Euclidean norm

$\|\cdot\|_\infty$ Maximum norm

U Set of all possible control inputs

X Set of all possible system states

$\lambda_{\min}(\cdot)$ Minimal eigenvalue of a matrix

$\lambda_{\max}(\cdot)$ Maximal eigenvalue of a matrix

$\mathbf{I}[m,n]$ Set $\{m, m+1, \cdots, n\}$

CHAPTER 1

INTRODUCTION

1.1 Background and Motivations

Over the past decades, affine-control systems (ACSs) have emerged as a cornerstone in modern control theory due to their broad applications [1–4]. These systems are characterized by dynamics that are subject to control inputs and state variables. A challenge in designing controllers for such systems lies in simultaneously ensuring stability and safety, two fundamental properties that underpin reliable operation.

Stability ensures that system states converge to desired equilibria over time, often analyzed using Lyapunov stability theory. The introduction of control Lyapunov functions (CLFs) has revolutionized stability verification, enabling the formulation of control problems as optimization tasks [5]. Recent advancements, such as deep neural network-based CLF approximation, Gaussian process regression-based modeling, reinforcement learning-based controller design, have further enhanced the adoption of CLF in stability analysis [6–8]. Safety, on the other hand, requires system states to remain within

predefined safe regions during operation [9]. Inspired by CLFs, control barrier functions (CBFs) were proposed to enforce safety through forward invariance principles [10, 11].

The interplay between stability and safety has motivated the integration of CLFs and CBFs into a unified framework. Quadratic programming (QP), a powerful optimization tool, naturally accommodates the linear constraints derived from CLF and CBF conditions [12, 13]. By formulating control design as a QP optimization problem, researchers can synthesize controller that minimizes energy consumption or tracking errors while satisfying stability and safety constraints [14]. However, challenges such as computational efficiency, constraint conflicts, and robustness to external disturbances persist, motivating further research in this domain.

Affine-control systems encompass a broad class of control systems, distinguished by dynamics that are linear in the control inputs. The QP control method has been extensively studied in single-agent systems, where the focus is on an individual agent's trajectory tracking and safety requirements, such as avoiding static obstacles. Beyond single-agent control, multi-agent systems (MASs) have emerged as an important research area due to their wide applications [15]. Cooperative control, including consensus and formation control, is a fundamental topic in MASs, where agents must reach agreements or maintain desired spatial configurations through appropriate control protocols [16, 17]. Extending control strategies to MASs introduces new layers of complexity, particularly due to the distributed control requirement [18]. This necessitates that each agent's control input is determined solely based on local information from its neighboring agents, ensuring system resilience by preventing total failure if a subset of agents malfunctions. Moreover, traditional control approaches have often relied on manually designed control protocols, which may result in suboptimal performance.

The CLF-based QP control framework provides a systematic alternative for controlling MASs. By embedding CLF conditions as constraints within a QP framework,

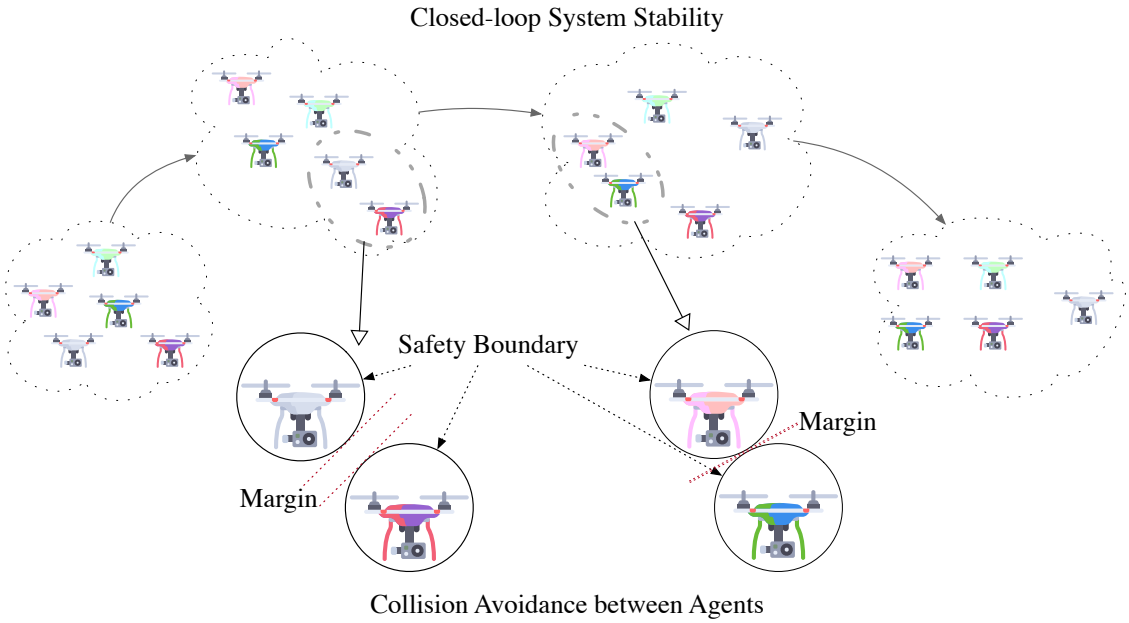

Figure 1.1: Illustration of a MAS highlighting the dual objectives of closed-loop system stability and inter-agent collision avoidance. The upper part of the figure shows groups of agents maintaining state stability and the lower part emphasizes the safety guarantee between agents, where each agent maintains a safe distance from its neighbors.

controllers can be calculated to optimize a given cost function while guaranteeing system stability. In practical MAS deployments, collision avoidance is an important safety requirement, which is typically enforced through CBF constraints within the QP framework [19]. Figure 1.1 illustrates collision avoidance in formation control of MASs. The first challenge of this thesis lies in designing fully distributed CLF and CBF conditions that enable each agent to make control decisions based solely on local information.

Furthermore, it is important to recognize that frequent QP solving introduces significant computational overhead, particularly in MASs. To mitigate this concern, various discontinuous control strategies, such as intermittent control and event-triggered control (ETC) mechanism, have been proposed in the literature to reduce the controller update frequency [20–22]. In the intermittent control strategy, the controller alternates between active and inactive periods, remaining deactivated during resting periods and reacti-

vating during working periods. Differently, the ETC mechanism updates the controller only when necessary, as determined by specific triggering functions. These approaches effectively reduce the computational burden by eliminating the need for continuous controller updates. Motivated by these approaches, we aim to integrate intermittent control and ETC mechanism into the QP control framework to reduce QP solving frequency. The primary challenge, therefore, lies in determining appropriate time instants for activating, deactivating, or updating the controller. This leads to the second key challenge of this thesis: designing intermittent on/off instants or triggering functions for QP control approach while ensuring the MASs still meet their control objectives.

Real-world control systems are inevitably affected by various uncertainties, such as sensor noise, modeling errors, and environmental disturbances [23–25]. A common approach to robustness analysis relies on the upper or lower bounds of disturbance characteristics. This method is relatively straightforward but useful when some prior knowledge about the disturbances is available. For instance, concepts such as input-to-state stability (ISS) and input-to-state safety (ISSf) extend robustness guarantees to systems with disturbances, typically under the assumption of known disturbance bounds. However, such information is not always accessible in practice. At this time, Gaussian process (GP) modeling has emerged as a data-driven alternative for handling uncertainties. By training GP models on collected data, it is possible to obtain probabilistic estimates of unknown disturbances, including both their mean and variance functions. This facilitates an adaptive and less conservative approach to robust CLF and CBF formulations [26]. In this work, we aim to investigate the robustness of the QP framework using these two approaches: one based on disturbance bounds and the other leveraging data-driven GP modeling. The first approach provides theoretical guarantees under known disturbance limits, while the second offers a probabilistic perspective that adapts to uncertainties learned from data. By studying these methods separately, we

aim to gain a comprehensive understanding of their respective strengths and limitations in ensuring stability and safety for uncertain MASs.

In practical MAS deployments, agents often operate under resource limitations, necessitating trade-offs between safety, stability, and optimality. Collision avoidance, a quintessential safety requirement, is typically enforced via CBF constraints in QP frameworks. However, conflicting constraints in multi-agent scenarios can render QP problems infeasible. Recent studies highlight the sensitivity of QP solutions to hyperparameters, such as the CLF decay rates and the CBF parameters, which indirectly influence system performance [27]. To address these challenges, Bayesian optimization (BO) is a useful tool for hyperparameter tuning. By treating QP solvability and system control performance metrics as black-box performance functions, BO iteratively selects hyperparameter values that maximize control efficacy while respecting constraints. The integration of constrained Bayesian optimization (CBO) further ensures feasibility by explicitly incorporating constraint satisfaction into the optimization loop. These advancements bridge the gap between theoretical control design and real-world implementation.

This research aims to advance the theoretical and practical aspects of the QP control approach, providing innovative solutions that enhance stability, safety, robustness, and optimization in MASs. The subsequent chapters delve into the research questions and objectives, development of these techniques, rigorous theoretical analysis, and the corresponding numerical experiments.

1.2 Research Questions and Objectives

1.2.1 Research Questions

This research is structured around two main procedures. The first focuses on short-term optimality, which involves analyzing the stability and safety of MASs through a QP for-

mulation, as well as examining the robustness of the control strategies. Here, 'short-term' refers to control actions that are locally optimal at each time step with respect to a given cost function. The second procedure addresses long-term optimality, which considers the overall control performance over time under specific hyperparameter settings. In this phase, we aim to improve system performance by applying hyperparameter optimization techniques. The key research questions and objectives are outlined below.

Research Question 1 (RQ 1): *How can distributed CLF conditions be designed for each agent to ensure the stability of MASs while considering their interactions?*

The stability of MASs is a fundamental requirement for reliable operation. This research question focuses on the development of distributed CLF conditions that can be applied individually to each agent, allowing them to determine their control actions independently using only local information from neighboring agents. The key challenge lies in ensuring that such decentralized decisions collectively lead to global stability of the entire system, especially when inter-agent couplings or communication constraints are present.

Research Question 2 (RQ 2): *How can distributed CBF conditions be designed for each agent to guarantee collision avoidance with all other agents?*

In addition to stability, safety is an important requirement for MASs. This research question addresses how to construct distributed CBF conditions that enable each agent to ensure collision avoidance in a decentralized manner. The key challenge is to formulate safety constraints that rely solely on local sensing or communication, allowing each agent to make real-time decisions without centralized coordination.

Research Question 3 (RQ 3): *What about the robustness of the proposed control methods in the presence of system uncertainties?*

In real-world MAS applications, various forms of uncertainty, such as modeling

inaccuracies and external disturbances, are inevitable and can significantly degrade control performance if not properly addressed. This research question aims to evaluate and enhance the robustness of the proposed control strategies under such uncertain conditions. It involves studying how sensitive the QP-based controllers are to uncertain dynamics. This question is crucial for ensuring that the MAS remains stable and safe, even when operating under partial knowledge or unexpected perturbations.

Research Question 4 (RQ 4): *How is the control performance evaluated and how can it be enhanced?*

While stability and safety are foundational, the control performance of a MAS, measured by metrics such as energy efficiency, also plays a vital role in practical applications. This research question focuses on developing systematic methods for evaluating and improving the performance of the proposed control strategies. It considers how various factors, including QP update frequency and hyperparameters, influence performance over time. The challenge is to explore methods for performance enhancement from a long-term or system-level perspective.

Together, these four questions form the foundation of this research, providing a structured approach to addressing important issues in the cooperative control of MASs.

1.2.2 Research Objectives

Building upon the identified research questions, this thesis aims to address the key challenges in the cooperative control of MASs through the following six research objectives:

Research Objective 1 (RO 1): *To develop distributed CLF conditions for stability assurance* (Aims to answer RQ 1)

The first objective of this research is to design and implement distributed CLF conditions that can ensure the overall stability of MASs. The aim is to enable each agent

to independently contribute to the system stability without full knowledge of the global dynamics. To address this, designing an observer for each agent enables the estimation of the inaccessible information based on locally combined measurement. Once these estimations are obtained, distributed CLF condition can be formulated for each agent, ensuring that the entire system achieves stability without relying on centralized global information.

Research Objective 2 (RO 2): *To develop distributed CBF conditions for safety enforcement* (Aims to answer RQ 2)

The second objective is to construct distributed CBF conditions that guarantee safety in MASs, particularly focusing on collision avoidance between agents. This entails designing decentralized safety constraints that allow each agent to prevent unsafe behavior using only local observations or neighborhood-level information. In practical scenarios, agents need to navigate in shared environments while avoiding collisions. The research will explore pairwise CBF conditions, and will ensure that these constraints do not conflict with stability requirements, leading to safe yet efficient system behavior.

Research Objective 3 (RO 3): *To develop high-order CBF methods for multiple derivatives* (Aims to answer RQ 2)

In many real-world MASs, agents exhibit high-order dynamics, for example, systems where velocity and acceleration must be controlled explicitly. Traditional first-order CBF formulations may not be sufficient to guarantee safety in such cases. The third objective of this research is to extend the existing CBF framework to high-order systems by developing high-order CBFs. These functions account for multiple derivatives of the system state and enable the enforcement of safety constraints in a mathematically rigorous manner. The research will address the construction of high-order CBFs, analyze their theoretical properties, and demonstrate their effectiveness in ensuring safety for dynamical models.

Research Objective 4 (RO 4): *To develop robust control methods for uncertain systems* (Aims to answer RQ 3)

This objective targets the development of robust control strategies capable of maintaining stability and safety despite uncertainties such as modeling errors and external disturbances. It explores both traditional model-based robustness techniques, which utilize upper or lower bounds of uncertainties, and modern data-driven methods, such as GP modeling, which provide probabilistic estimates of disturbances based on collected data. The research will investigate how these approaches can be integrated into CLF or CBF formulations, either separately or in a hybrid fashion. Emphasis will be placed on analyzing how uncertainty affects the feasibility and performance of the resulting QP-based controllers. This objective is essential for real-world deployment, where systems rarely conform exactly to theoretical models.

Research Objective 5 (RO 5): *To develop strategies for reducing QP computation frequency* (Aims to answer RQ 4)

The fifth objective is to reduce the computational burden of real-time QP-based control by developing discontinuous control strategies, such as intermittent control and event-triggered control. While continuous control updates offer high responsiveness, they can be computationally expensive, especially in large-scale MASs with frequent QP solving. This objective focuses on identifying moments when control updates are most needed, allowing agents to skip unnecessary computations. Event-triggered mechanisms will be designed based on predefined error thresholds or state-dependent conditions. Additionally, the research will examine the stability of such schemes and its impact on system performance.

Research Objective 6 (RO 6): *To develop optimization algorithms for performance enhancement* (Aims to answer RQ 4)

The final objective is to improve the long-term performance of MASs by designing and implementing hyperparameter optimization algorithms. In QP-based control frameworks, hyperparameters such as cost function weights, safety margins, and GP kernel parameters may influence control behavior. Poorly chosen values can lead to suboptimal performance or even instability. This objective involves defining performance metrics such as trajectory tracking error, energy consumption or computation time, and developing optimization algorithms to fine-tune these hyperparameters. Bayesian optimization algorithm is employed as a main approach. The control framework can be made more efficient by systematically optimizing these parameters.

1.3 Research Contributions

This thesis presents a systematic study on QP-based control strategies for MASs, with an emphasis on stability, safety, robustness, and long-term performance optimization. By integrating CLFs and CBFs into a unified constrained optimization framework, the research addresses key challenges in distributed control, uncertainty handling, and computational efficiency. The major contributions are organized according to the structure of the thesis, corresponding to its four core chapters:

Chapter 3: CLF-based QP control for consensus tracking of MASs

- *Development of a distributed CLF-based QP control framework:*
  A novel constrained QP-based control framework is proposed for general linear MASs to achieve consensus tracking. The framework integrates distributed CLF conditions into the QP formulation, enabling each agent to independently achieve cooperative control objectives based on local information.

- *Design of discontinuous control strategies for reduced computation:*
  To alleviate the computational burden associated with continuous QP updates, two

types of discontinuous control strategies, event-triggered control and intermittent control, are incorporated. These strategies significantly reduce the QP solving frequency without compromising system stability.

- *Itegration of GP models into CLF constraints:*
  A data-driven robustness enhancement is achieved by modeling unknown terms in the CLF using one-dimensional GP regression. This eliminates the need for conservative disturbance bounds and enhances adaptability in uncertain environment.

Chapter 4: CLF-CBF-based QP control for safe formation of MASs

- *Formulation of second-order CLF conditions for formation control:*
  A second-order CLF is formulated to guide agents towards a predefined geometric formation, ensuring both distributed requirement and states convergence.

- *Design of pairwise CBF constraints using neighbor sets:*
  A neighboring set construction is introduced, allowing each agent to apply reduced pairwise CBF conditions. This design supports decentralized collision avoidance while reducing the computational and communication complexity.

- *Extension to a GP-CLF-CBF-based QP control framework:*
  Both the CLF and CBF components are modeled using GP regression to handle uncertainty in dynamics and safety boundaries. The resulting GP-CLF-CBF-based QP framework enhances the robustness and adaptability of the system in dynamic environments.

Chapter 5: HOCBF-based QP control for MASs

- *Adoption of HOCBFs with intuitive safety functions:*
  A variant control scheme based on HOCBFs is developed, using a simple relative-

degree-two distance-based safety function. This makes the approach more interpretable and suitable for agent dynamics without requiring complex modeling.

- *Robust safety guarantee under bounded disturbances:*

  The HOCBF formulation is extended to accommodate bounded system disturbances, resulting in a robust safety framework. This allows MASs to maintain constraint satisfaction in worst-case uncertainty conditions, thereby improving its applicability.

Chapter 6: Hyperparameter optimization for performance enhancement

- *Establishment of a unified framework for performance-oriented safety control:*

  A comprehensive optimization framework is proposed to balance safety and performance in MASs. The performance enhancement problem is formulated as a constrained optimization task.

- *Development of the CBF-CBO algorithm:*

  A novel CBF-CBO algorithm is designed to explore the hyperparameter space efficiently. It classifies hyperparameters by their functional roles, identifies feasible regions under safety constraints, and optimizes for desired performance metrics such as tracking accuracy of control effort.

- *Extensive empirical validation in safe control scenarios:*

  The effectiveness of the optimization framework is demonstrated through simulation across various MAS scenarios, showing improvement in long-term control performance while ensuring compliance with safety constraints.

1.4 Research Significance

The significance of this research lies in its dual impact: it contributes novel theoretical tools to the field of safe and robust control, while also offering resource-efficient solutions for the practical deployment of MASs.

Theoretical significance: Theoretically, this research advances the understanding and development of control strategies for MASs by formulating distributed CLF and CBF conditions that enable decentralized implementation while ensuring global system objectives such as consensus, formation tracking, and collision avoidance. Furthermore, by incorporating GP models into CLF and CBF constraints, the work introduces a data-driven mechanism for modeling uncertainties in a probabilistic manner. This bridges the gap between model-based control and learning-based approaches, contributing to the emerging field of learning-enabled control systems. Additionally, the research proposes discontinuous QP control strategies such as event-triggered and intermittent control that significantly reduce computational demands, offering insights into efficient real-time optimization-based control. Finally, the formulation of control performance tuning as a constrained optimization problem, and the development of a CBF-CBO algorithm, present a novel methodology for systematically exploring hyperparameter spaces, thereby integrating long-term performance considerations into the theoretical framework.

Practical Significance: Practically, the proposed QP-based control framework offers effective and scalable solutions for real-world multi-agent applications that require decentralized coordination with guaranteed stability and safety. The framework's robustness is enhanced, which enable real-time adaptation to unknown system disturbances. The research also provides a systematic hyperparameter optimization process that allows engineers and practitioners to fine-tune control performance such as improving tracking accuracy or minimizing control effort while maintaining safety and stability. By addressing key concerns in computational efficiency and performance optimization, the

proposed methods pave the way for more intelligent MASs control in complex real-world environments.

1.5 Thesis Structure

The structure of this thesis is illustrated in Figure 1.2, with the chapters organized as follows:

- CHAPTER 2: This chapter provides a comprehensive review of the foundational theories and recent advancements relevant to this thesis. The chapter is divided into five key subsections. It begins with an overview of CLFs, examining their role in stability analysis and their application in real-time control via QP formulations. The second subsection focuses on CBFs, detailing their use in enforcing safety constraints. The third part introduces HOCBFs, which are essential for handling higher-relative-degree safety constraints. The fourth subsection addresses robustness analysis, introducing bound-based methods and data-driven approaches like GP modeling for uncertainty handling. Finally, the fifth subsection reviews Bayesian optimization techniques and their potential for safe and efficient hyperparameter tuning in control systems.

- CHAPTER 3: This chapter develops a constrained QP control framework to ensure stability in MASs, with a particular focus on consensus tracking problems. A distributed CLF condition is designed such that each agent can make control decisions using only local information, thereby enabling decentralized implementation. A QP problem is formulated that incorporates the CLF condition as a constraint while minimizing control effort. To reduce the computational burden associated with continuous QP solving, the chapter introduces event-triggered and intermittent control strategies that enable discontinuous updates without compromising

stability. Furthermore, a one-dimensional GP model is incorporated into the CLF condition to handle unknown system components. The chapter presents theoretical analysis and simulation results to validate the proposed method's effectiveness in ensuring convergence, robustness, and computational efficiency. This chapter addresses RQ1 and RQ3 to achieve RO1, RO4 and RO5.

- CHAPTER 4: This chapter extends the QP control framework to incorporate safety constraints through the integration of CBFs with CLFs. The focus is on safe formation control, where agents are required to maintain a desired formation shape while avoiding collisions. A neighboring set is introduced to define reduced pairwise CBF constraints that ensure safety with lower computational complexity. To improve adaptability in uncertain environments, GP models are trained for both the CLF and CBF components, resulting in a GP-CLF-CBF-based QP framework that is robust to model disturbances. The chapter provides theoretical guarantees for safety, and validates the approach through simulations involving formation maintenance and collision avoidance. This chapter addresses RQ2 and RQ3 to achieve RO2 and RO4.

- CHAPTER 5: This chapter addresses safety control for MASs which require more sophisticated treatment due to the relative degree of safety constraints. This chapter introduces a HOCBF into the QP framework, using a simple distance-based safety function with relative degree two. This approach simplifies the design process while retaining generality and practical relevance. Robustness to bounded disturbances is analyzed, leading to a robust HOCBF formulation that ensures safety under uncertainty scenarios. The proposed method offers an intuitive way to extend barrier-based safety control to complex MAS models. Simulations are conducted to illustrate the effectiveness and robustness of the proposed HOCBF-based QP approach in scenarios involving external perturbations. This chapter

also addresses RQ2 and RQ3 to achieve RO2 and RO4.

- CHAPTER 6: This chapter shifts focus from short-term control objectives to long-term system performance. A novel hyperparameter optimization framework is proposed to improve control quality over time while maintaining safety guarantees. The performance enhancement problem is formulated as a constrained optimization task, where safety is enforced via CBF conditions, and the objective is to minimize a control cost function. To solve this, the chapter introduces a CBF-CBO algorithm, which explores the hyperparameter space efficiently and systematically identifies optimal and feasible solutions. The framework is evaluated across several MAS scenarios to demonstrate its ability to improve control performance in a safe and data-efficient manner. This chapter addresses RQ4 to achieve RO6.

- CHAPTER 7: This chapter concludes the thesis by summarizing the main contributions and findings across the proposed control framework for MASs. It revisits the key results from the preceding chapters, including the development of distributed CLF/CBF-based QP control strategies, robustness enhancement, and performance optimization via hyperparameter tuning. The second part of the chapter outlines future research directions inspired by the current work. Specifically, it discusses the potential of learning neural barrier functions to automatically capture complex safety constraints using data-driven methods. It also highlights the importance of event-triggered safe control to reduce control update frequency in safe scenarios. Lastly, the concept of transferable barrier functions is proposed to enable safety guarantees across different tasks or environments, enhancing the generalization of the control framework.

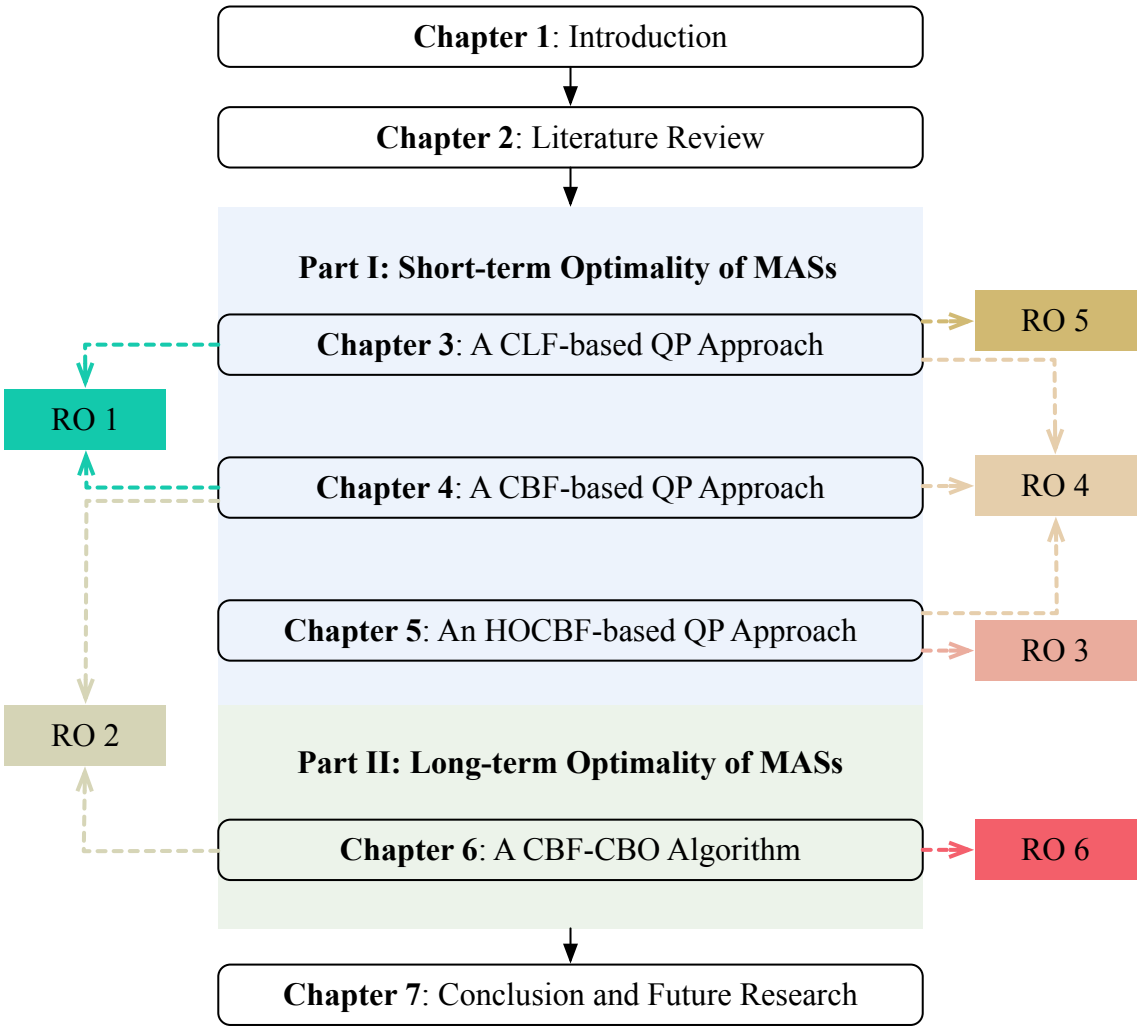

Research Objectives:
1: To develop distributed CLF conditions for stability assurance
2: To develop distributed CBF conditions for safety enforcement
3: To develop high-order CBF methods for multiple derivatives
4: To develop robust control methods for uncertain systems
5: To develop strategies for reducing QP computation frequency
6: To develop optimization algorithms for performance enhancement

Figure 1.2: Thesis Structure.

CHAPTER 2

LITERATURE REVIEW

This chapter reviews the key concepts and recent advances relevant to the control of MASs, focusing on four core aspects: stability, safety, robustness, and control performance. In particular, we examine how CLF or CBF condition can be integrated into a QP framework to address these objectives in a unified manner.

The structure of this chapter is outlined in Figure 2.1. Section 2.1 discusses stability analysis using CLFs and introduces CLF-based QP and discontinuous control strategies. Section 2.2 presents the fundamentals of CBFs, high-order extensions, and their roles in safe control. Section 2.3 covers robustness, including both model-based and data-driven approaches. Section 2.4 focuses on performance optimization and introduces constrained Bayesian optimization algorithm for hyperparameter tuning under safety constraints. This literature review provides the theoretical foundation for the methods developed in subsequent chapters.

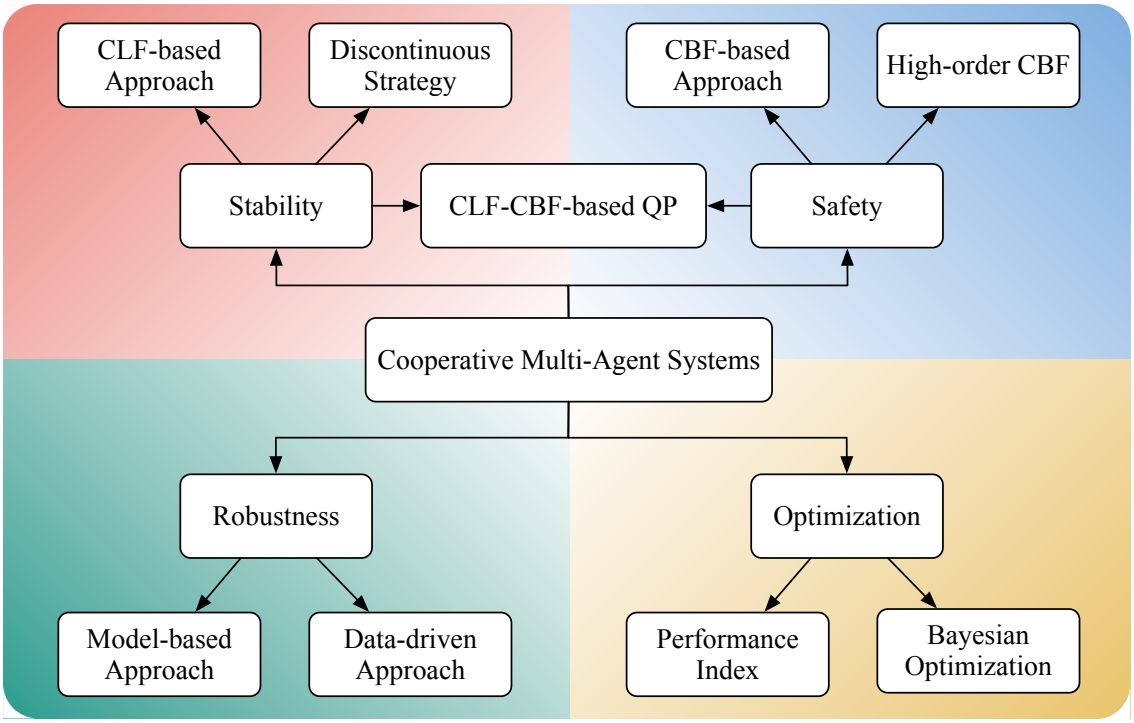

Figure 2.1: Literature Review Structure.

2.1 Control Lyapunov Function

2.1.1 System Stability

Affine-control systems have attracted considerable research interest over the past few decades due to their wide-ranging applications in science and engineering domains [28, 29]. A central challenge in this fields is to design effective controllers that ensure system stability, i.e., guaranteeing that the state trajectories converge to desired equilibrium points despite variations in initial conditions and potential disturbances [30, 31].

To address this challenge, Lyapunov stability theory has long served as a foundational tool. It provides a powerful mathematical framework for analyzing the stability of dynamical systems by constructing appropriate Lyapunov candidate functions [32–36]. Over time, this theory has been extended and adapted to a wide variety of system types, including neural networks, fuzzy systems, and others [37, 38]. These extensions reflect

the flexibility and robustness of Lyapunov-based approaches in handling increasingly complex dynamical systems.

In recent years, the combination of Lyapunov theory with modern computational techniques has led to promising new methodologies. For example, [39] introduced a deep neural network-based method to approximate Lyapunov functions for high-dimensional systems, which helps alleviate the computational burden associated with conventional analytic constructions. This innovation illustrates how classical control theory can benefit from data-driven tools, providing both analytical rigor and enhanced scalability.

In the broader class of ACSs, the cooperative control of MASs has emerged as a vibrant area of study, driven by applications such as coordinated unmanned aerial vehicle fleets, sensor networks, and distributed systems [40]. A fundamental goal in cooperative MAS control is achieving consensus, where agents reach agreement on a common quantity (e.g., position, velocity, or state) through decentralized information exchange [41]. This problem becomes more nuanced in consensus tracking where a group of agents need to track the trajectory of a virtual or physical leader agent [42–45], and formation achievement where the agents are expected to form a formation configuration [46–49]. To address different MAS scenarios, various dynamic models have been explored, including first-order integrator systems [50], second-order dynamics [51], high-order systems [52], and general linear agent models [53]. Across all these types, Lyapunov-based techniques remain indispensable. They are particularly effective in verifying the stability of MAS behaviors under distributed control laws and have been widely applied to problems such as consensus, formation, and containment control [54–56]. These methods not only offer rigorous theoretical guarantees but also accommodate the local interaction structures and decentralized nature of MASs, thereby making them well-suited for real-world deployment.

2.1.2 CLF-based Approach

As highlighted in the aforementioned literature, Lyapunov stability theory remains a cornerstone for validating control protocols. In particular, system stability is ensured when the derivative of a positive-definite Lyapunov function satisfies a specific decay condition. A general condition $\dot{V}(x,t) \leqslant 0$ guarantees asymptotic convergence of system states over time, whereas a stricter condition $\dot{V}(x,t) \leqslant -cV(x,t)$ with $c > 0$ ensures exponential convergence [57]. An explanation of this condition can be found from Figure 2.2(a). Building on this foundation, the concept of control Lyapunov functions (CLFs), initially proposed in [58] and later extended in [59], established a systematic framework for designing stabilizing control laws. Importantly, CLFs form a bridge between classical stability theory and modern control design by linking Lyapunov conditions with optimal control principles, often through integration with cost functions [60–62].

The work of Freeman and Primbs was particularly influential in this regard [63], as it introduced a method to incorporate CLF conditions within a QP formulation. This innovation laid the groundwork for a family of optimization-based control techniques that embed stability constraints directly into the control synthesis process. Subsequent studies have refined and extended this approach, applying CLF-based QP methods to a range of ACSs with demonstrated success in both theoretical and practical settings [64, 65]. These developments underscore the value of CLF-based QP formulations as a means of achieving both control feasibility and performance optimization in a unified framework.

Despite its effectiveness in single-agent systems, the application of CLF-based QP control in multi-agent cooperative scenarios has received relatively limited attention. This represents a gap in the literature that the present work aims to address. In MASs, where distributed agents must collaborate to track reference trajectories or maintain formations, the QP framework offers notable advantages. Specifically, it accommodates

the existence of multiple feasible control solutions and provides a systematic way to select inputs that not only ensure stability but also optimize a given performance criterion [66].

Moreover, the growing availability of efficient numerical solvers and computational resources has further enhanced the practical appeal of CLF-based QP controllers. These solvers facilitate real-time implementation while maintaining the mathematical guarantees provided by Lyapunov-based design [67]. As such, CLF-based QP methods provide a compelling tool for modern MAS control, combining the benefits of rigorous stability analysis with optimization-based flexibility. In this thesis, particular focus is placed on adapting CLF-based QP methods to the distributed control architecture of MASs, exploring their integration with cooperative objectives and resource-aware implementation strategies.

2.1.3 Discontinuous Strategy

While CLF-based QP control offers a compelling framework that simultaneously addresses stability guarantees and optimization, its real-time implementation often encounters significant computational challenges. Specifically, the need to solve a QP problem at every control update introduces considerable computational overhead, which can be especially burdensome in resource-constrained platforms or large-scale MASs. The continuous execution of optimization routines may lead to increased latency, higher energy consumption, and reduced system responsiveness, thus impeding practical deployment in time-sensitive or energy-limited environments [68].

To alleviate this issue, discontinuous control strategies have been developed, aiming to balance control performance with computational efficiency. Among them, intermittent control has emerged as an effective method that reduces the update frequency of QP solvers without severely compromising stability or performance. As proposed in [68], this strategy divides the control timeline into two alternating phases:

- Working periods $[t_k, t_k + \Delta_k)$, during which the controller actively updates the control input by solving the QP to drive the system toward its objective;
- Resting periods $[t_k + \Delta_k, t_{k+1})$, during which the control input is held constant and the QP solver remains idle, thus conserving computational resources.

Intermittent control can be categorized into two primary forms:

- Periodic intermittent control, where the k-th active period duration Δ_k is fixed, allowing for predictable timing patterns and simple implementation [69];
- Aperiodic intermittent control, which adapts Δ_k dynamically based on real-time system states, performance indices, or other criteria [70], offering greater flexibility and responsiveness in dynamic environments.

Regardless of the paradigm, one design consideration lies in ensuring that Δ_k remains above a system-dependent lower bound to avoid excessive delay between updates, which could otherwise lead to degraded control performance or even instability. However, much of the existing literature focuses primarily on offline tuning or overly conservative heuristics, leaving the determination of optimal switching instants t_k an open problem.

To address these limitations, recent studies have proposed event-triggered control mechanisms as an advanced form of discontinuous control [71, 72]. These methods dynamically determine the update instants t_k based on state-dependent conditions rather than fixed schedules. For instance, triggering rules based on Lyapunov function decay rates or deviation thresholds have been employed to initiate control updates only when necessary, ensuring that the system stability margins are preserved without continuous computation [73, 74]. In the context of MASs, event-triggered strategies have demonstrated the ability to significantly reduce communication and computation loads while maintaining consensus or formation objectives [75].

Overall, these discontinuous control strategies offer a promising avenue for enhancing the practical viability of CLF-based QP controllers in MASs. By intelligently reducing update frequency without compromising system stability, these methods lay the groundwork for deploying advanced control algorithms in resource-limited scenarios.

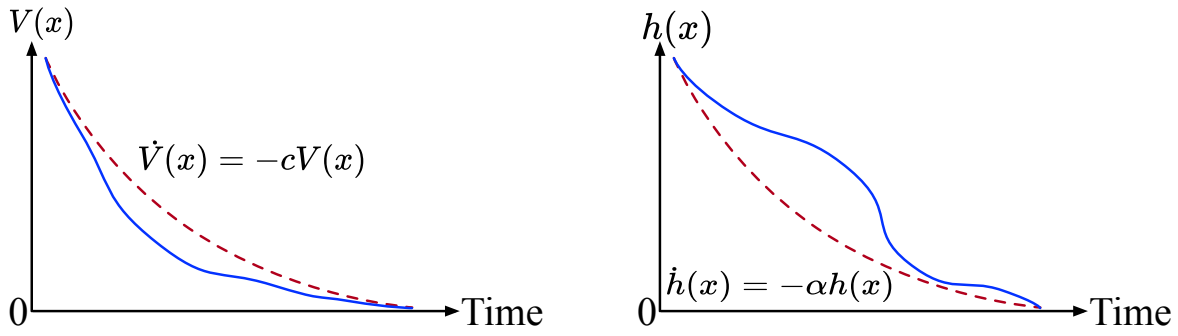

(a) Variation of CLF $V(x)$.

(b) Variation of CBF $h(x)$.

Figure 2.2: An introduction of CLF and CBF conditions.

2.2 Control Barrier Function

2.2.1 System Safety

Safety is a fundamental property in control system design, particularly for ACSs, where it refers to the requirement that system trajectories remain within a designated safe set over time [76–79]. In many real-world applications, this property becomes a main concern and is commonly addressed under the umbrella of safe control [80–83]. Ensuring safety is not only essential for system reliability but also a prerequisite for operational feasibility in dynamic, uncertain environments. For example, Zeng et al. explored safe optimal control in a 2D double-integrator model to achieve obstacle avoidance while satisfying performance goals [84], highlighting the importance of safety constraints in conjunction with control objectives.

In the context of MASs, safety considerations are even more pronounced due to the

increased complexity arising from inter-agent interactions and decentralized decision-making. While stability in the consensus and formation control is crucial, safety must also be maintained to prevent undesirable behaviors such as collisions, boundary violations, or unsafe maneuvers. This is especially true in formation control tasks, where multiple agents coordinate to maintain a prescribed spatial configuration. Such scenarios are common in cooperative surveillance, environmental monitoring, and search-and-rescue missions [85]. In these applications, inter-agent collision avoidance is a core safety requirement that must be enforced throughout the control process.

To address system safety in MASs, several strategies have been proposed. One traditional approach is the use of potential energy fields, as employed by Mondal et al., where artificial repulsive forces are generated around obstacles or neighboring agents to steer the system away from unsafe regions [86]. This method, based on gradient-descent principles, enables obstacle avoidance and convergence to targets but often suffers from local minima and requires careful tuning of boundary conditions. Another line of work by Lashkari et al. proposes spatial computation techniques to generate globally optimal and safe trajectories that satisfy environmental constraints [87]. However, such approaches can be computationally intensive and difficult to scale in real-time applications. As an alternative to these heuristic or computationally expensive methods, a more systematic and theoretically grounded framework is offered by the control barrier function (CBF) approach.

2.2.2 CBF-based Approach

Inspired by the foundational role of CLFs for system stability, the concept of CBFs was introduced to formalize and enforce safety constraints in ACSs [10], with further theoretical advancements presented in [11]. The central idea of CBFs is to guarantee the forward invariance of a designated safe set, ensuring that system trajectories starting

within the safe set remain there for all future times [88, 89]. This makes CBFs a natural and rigorous tool for safe control.

The typical formulation of a safety constraint using a CBF is expressed as an inequality of the form $\dot{h}(x,u) \geqslant -\alpha h(x)$, where $h(x)$ is a continuously differentiable function that defines the safe set $\{x : h(x) \geq 0\}$, and α is a positive constant or an extended class $\mathscr{K}$ function. An explanation of this condition can be found from Figure 2.2(b). This inequality condition is then embedded as a constraint within a QP framework, allowing the controller to optimize performance while satisfying safety guarantees in real time. In this setup, the CBF constraint serves as a safety filter: it minimally modifies a nominal control input when the safety boundary is approached, effectively steering the system away from unsafe states without significantly disrupting the underlying control objectives [90].

This paradigm is particularly beneficial in MASs, where the complexity of distributed interactions, dynamic environments, and inter-agent collision risks necessitate real-time safety enforcement. In this regard, distributed pairwise CBFs were first proposed in [91] to enforce collision avoidance between agents, forming the basis for later developments in coordinated MAS control. The framework was further extended in [55] to support formation navigation tasks that integrate collision avoidance into collective motion planning. Additionally, obstacle avoidance capabilities have been addressed in works like [92], which generalized the CBF framework to include external environmental hazards.

Beyond static obstacle avoidance, researchers have also tackled safety in more complex MAS scenarios [93]. For instance, safe consensus tracking under state constraints has been realized using the CBF-based QP approach [94], where agents are required not only to follow a reference trajectory but also to avoid unsafe states throughout the mission. Furthermore, repetitive-task settings have motivated the development of iterative learning CBFs [95], where safety knowledge is accumulated across task repetitions to

improve performance and robustness over time.

Overall, the integration of CBFs into QP formulations enables a principled and computationally tractable way to achieve real-time safety assurance in MASs. This approach has shown considerable promise across a wide range of scenarios, from distributed coordination to adaptive obstacle avoidance, and serves as a foundational technique for the safe control frameworks developed in this thesis.

2.2.3 High-order CBF

The previously discussed concept of CBF provides a powerful tool for safe control. However, its classical formulation is only directly applicable to systems where the relative degree of the safety function with respect to the control input is one. This constraint limits the applicability of standard CBF methods, particularly in systems with high-order dynamics [96]. For instance, in many studies involving second-order systems, such as multi-agent dynamics described in [91, 97], the safety constraints are carefully designed to ensure the relative degree remains one. This ensures that the derivative of the barrier function explicitly depends on the control input, thus rendering the CBF condition directly enforceable in a QP framework.

To overcome the limitation imposed by the relative degree condition, several methodologies have been developed. A notable approach is the use of back-stepping techniques, as proposed in [98], which decomposes the system into lower-order subsystems to effectively manage higher-relative-degree constraints. Another significant contribution is the direct construction of relative-degree-two CBFs, as detailed in [99]. These works laid the foundation for extending barrier function theory to a broader class of systems.

To handle even more general cases, especially those involving arbitrary relative degrees, high-relative-degree safety constraints were introduced in [100] and further formalized in [101]. These studies provided a systematic framework for extending the

CBF methodology beyond the traditional setting, enabling the control of more complex systems with safety requirements that depend on high-order derivatives of the system state.

A significant breakthrough came with the introduction of the high-order control barrier function (HOCBF) by Xiao et al [102]. Unlike earlier methods that often relied on restrictive conditions such as exponential convergence rates, the HOCBF framework generalizes standard CBF theory while offering a more tractable and flexible implementation. Specifically, the HOCBF ensures the forward invariance of a safety set by recursively constructing a sequence of inequality constraints derived from high-order derivatives of the barrier function. This allows systems with arbitrary relative degrees to be safely controlled in a unified QP-based formulation. The HOCBF can be viewed as a generalization of the zeroing CBFs introduced in [103, 104], and has been further validated through theoretical analysis and experimental implementations in scenarios such as motion planning and adaptive cruise control systems [105]. Moreover, further extensions of the HOCBF concept have been made in discrete-time domains. For example, [106] formulated discrete-time HOCBFs to address high-relative-degree constraints in sampled-data systems, with subsequent refinements presented in [107]. In this thesis, the HOCBF approach is adopted to enable safety assurance in MASs where only simple pairwise distance functions are available, and where the relative degree of these functions exceeds one.

2.2.4 CLF-CBF-based QP

As discussed above, both stability and safety are fundamental properties in the design of control systems. A system that lacks stability is inherently unreliable, while safety is an important requirement in real-world applications. Traditionally, control system design follows a two-step procedure: first, a candidate controller is proposed to fulfill

the desired objective; then, its performance is validated through theoretical analysis and experimental evaluation. Examples include state-feedback protocols that guarantee stability [108], and potential function-based methods that ensure safety [109].

However, it is well recognized that control solutions are not unique: multiple control inputs can yield the same system performance. Specifically, any control input that satisfies a CLF constraint ensures stability, while any input satisfying a CBF constraint ensures safety. This flexibility motivates the use of optimization-based frameworks that can systematically select among the admissible control inputs based on performance criteria.

To handle these constraints effectively, several control architectures have been developed. These include model predictive control, the reference governor strategy, and the invariance control principle [110, 111]. In model predictive control and reference governor methods, a high-level controller generates admissible reference trajectories to ensure that low-level controllers respect constraints. The invariance control principle, on the other hand, adopts a switching-based mechanism to enforce constraints by modifying control laws based on the system state. In parallel, efforts have been made to unify CLF and CBF frameworks for simultaneous achievement of stability and constraint satisfaction. Early works such as [112, 113] attempted this integration but encountered limitations: specifically, near the boundary of the safe set, the CLF may become unbounded, leading to numerical instability or infeasibility in the optimization problem. To address this, a more generalized formulation was developed in [114], which integrates CLF and CBF constraints without inducing singularities or unboundedness near constraint boundaries.

To resolve the ambiguity of selecting among multiple admissible controllers, QP-based formulations are often employed. These methods define a cost function that penalizes undesirable system behavior such as excessive control effort or deviation

from a nominal controller, thus guiding the optimization toward the most desirable solution. The flexibility of QP formulations allows for both single and multiple constraint enforcement. For example, a unified CLF-CBF-based QP framework was proposed in [115], where both safety and stability constraints were encoded in a single optimization problem. Importantly, the CBF constraint was assigned higher priority to ensure safety feasibility, while stability was achieved within the admissible region defined by the CBF. This integrated CLF-CBF-based QP approach represents a powerful and systematic methodology for control-affine systems, combining the strengths of Lyapunov-based stability theory and barrier-based safety enforcement with the performance optimization capabilities of QP solvers. The resulting control law ensures that system trajectories remain within safe bounds while converging toward the desired equilibrium, all while optimizing for control efficiency or task-specific objectives [116].

Given the increasing relevance of distributed and safe control in MASs, further exploration of CLF-CBF-based QP frameworks in this context is both timely and essential. This forms the core motivation of this thesis, which aims to extend and apply the CLF-CBF-QP methodology to MASs with both theoretical rigor and practical applicability.

2.3 Robustness Analysis

In real-world deployments, MASs invariably operate in environments permeated by unmodeled dynamics, sensor noise and exogenous disturbances. Such uncertainty can seriously degrade the performance of controllers that rely on nominal models. Consequently, a substantial body of work has focused on robustifying methods to deal with system uncertainty [117, 118].

Disturbances manifest in multiple ways. For example, researchers considered additive noise on the control input introduced by sensor encoding/decoding processes and cast

robustness in terms of input-to-state stability (ISS) and its safety analogue, input-to-state safety (ISSf) [119, 120]. Zhao et al. investigated matched disturbances acting directly on the system dynamics; they constructed a disturbance observer and incorporated its estimate into modified, robust CLF and CBF conditions [121]. For more general, possibly time-varying disturbances, state-of-the-art filtering techniques such as the unscented Kalman filter have proved useful for online mean-variance estimation [122].

2.3.1 Model-based Approach

Classical robust and adaptive control methods exploit a priori information, typically bounds on unknown uncertainties. Within the CBF framework, a common method is to insert a robustifying term that compensates for the worst-case effect of the disturbance. This idea was formalized in the work [123], and subsequent studies have sought to reduce the resulting conservativeness by deploying disturbance observers, estimators and identifying techniques [124–128].

A related research topic here is the balance between safety and performance. That is to say, overly conservative bounds may guarantee safety but at the cost of energy-inefficient behavior. To mitigate this, recent work has explored safe adaptive controllers that update uncertainty estimates on-line, tightening the gap between guaranteed bounds and actual disturbance levels [129, 130]. This thesis adopts this perspective, and later chapters will focus on the choice of some hyperparameters in the QP framework, thereby improving performance without sacrificing safety.

2.3.2 Data-driven Approach

Model-based techniques presuppose reliable bounds or parametric structures. When these information is unavailable or overly conservative, data-driven methods offer an attractive alternative. One line of research formulates sufficient conditions directly in

terms of statistical properties of the disturbance, sidestepping explicit bounds [131–133]. Within this paradigm, reinforcement-learning (RL) algorithms have been integrated with CLF-CBF constructs, yielding RL-CLF-CBF controllers that iteratively improve performance while respecting safety constraints [134–136]. The episodic learning framework of [137] extends this idea. A limitation of many RL-based schemes, however, is their sensitivity to measurement noise and the difficulty of providing a priori safety guarantees during exploration.

As a less exploratory but more statistically grounded alternative, Gaussian Process (GP) regression treats the unknown dynamics as a random function and returns both mean and variance predictions. Early GP-CBF studies focused on single-agent systems [138, 139], typically employing multi-dimensional GPs to model vector disturbances. Later, [67] showed that even a one-dimensional GP, embedded in a CLF constraint, can effectively compensate unknown dynamics while keeping computational complexity low. The GP-CLF-CBF framework proposed in [140] generalized these ideas and laid the groundwork for extensions to multi-agent settings.

For MASs, probabilistic techniques have recently gained traction. In [141], GP-based uncertainty estimates were fused with distributed CBFs to enforce collision avoidance under stochastic disturbances. A particularly notable contribution is [142], where the learned model was embedded in robust CBF constraints, enabling reliable collision avoidance in uncertain environments. These advances demonstrate that learning-based estimation, when combined with formal barrier conditions, can deliver adaptive and certifiably safe control, which is an approach further elaborated in this thesis.

Collectively, the model-based and data-driven strategies reviewed above provide a rich toolkit for safeguarding CLF-CBF controllers against uncertainty. The subsequent chapters build on both paradigms, and we will see how it becomes a key step toward more adaptive and resilient MASs.

2.4 Bayesian Optimization

2.4.1 Control Performance

As previously discussed, while system stability and safety are essential, control performance is also an important consideration. The linear quadratic regulator (LQR) is a classical and widely adopted performance index. It formulates control objectives as a quadratic cost function, balancing system state deviations and control effort. The resulting optimal control law depends on some hyperparameters, making parameter tuning important for achieving desirable performance. To reduce energy consumption while maintaining stability, many studies have designed optimal controllers that minimize LQR costs [143, 144]. In addition, distributed LQR-based strategies have been explored in MASs for tasks such as consensus tracking and autonomous driving [145, 146].

Conventionally, the LQR problem is solved via the algebraic Riccati equation. However, this approach becomes inapplicable when structural or feasibility constraints are imposed on the gain matrices. To address such limitations, alternative methods have emerged, including gradient projection for structural constraints [147], Gaussian principle of least constraint for constrained dynamics [148], and dynamic adjustment of control gains [149]. Despite these advances, most existing approaches focus exclusively on performance optimization, often overlooking safety considerations. The need to integrate safety constraints into performance-aware optimization frameworks motivates the exploration of new methodologies. Additionally, a key challenge in the CBF-based QP control framework is maintaining the feasibility of the QP problem, especially when multiple CBF constraints conflict in multi-agent settings. While previous studies have shown that CBF-related parameters can significantly influence QP solvability [119], few works have explicitly investigated the relationship between the QP solution and its hyperparameters.

2.4.2 Constrained Bayesian Optimization

To tackle the aforementioned challenges, we propose leveraging Bayesian optimization (BO) to optimize hyperparameters and enhance control performance. BO is a data-driven global optimization method suited for black-box functions, particularly those that are expensive or difficult to evaluate analytically [150]. BO comprises two main components:

- Surrogate function, typically a GP regression, that approximates the true but unknown performance function based on sample evaluations, and

- Acquisition function that guides the exploration-exploitation trade-off by suggesting the next observation point [151].

To ensure QP feasibility during the optimization process, we adopt the constrained Bayesian optimization (CBO) framework introduced in [152], where QP solvability is treated explicitly as a constraint. By evaluating both the performance (e.g., LQR cost) and the feasibility status of the QP at each iteration, the CBO algorithm systematically identifies hyperparameter configurations that balance performance and safety feasibility.

In recent work, CBO has been successfully used to tune proportional-integral-derivative (PID) gain parameters for nonlinear systems [153]. Similarly, preference-based optimization techniques have been developed within the CBO setting to tune CBF parameters, enabling users to learn safe and effective control policies based on qualitative preferences while respecting safety constraints [154]. In this thesis, we aim to show a framework that enables the integration of black-box performance into a unified control design pipeline. This framework offers a promising direction for achieving simultaneous performance optimization and safety assurance in MASs.

2.5 Graph Theory

Before proceeding to the following chapters, we present some fundamental concepts of graph theory relevant to the control of MASs.

The weighted graph $\mathscr{G} = \{\mathscr{V}, \mathscr{E}, \mathscr{A}\}$ describes the information exchange in MASs. Individual agents are represented as nodes, and $\mathscr{V} = \{1, 2, \cdots, N\}$ denotes the set of nodes. The edge set $\mathscr{E}$ includes the connections between agents, where $(i, j) \in \mathscr{E}$ indicates that agent i can receive information from agent j. A path, denoted as $j_1 \to j_n$, is defined as a sequence of $(j_1, j_2) \in \mathscr{E}, \cdots, (j_{n-1}, j_n) \in \mathscr{E}$. If there exists a path from one node to all other nodes, the graph is said to possess a spanning tree. The adjacency matrix $\mathscr{A} = [a_{ij}]_{N\times N}$ and Laplacian matrix $\mathscr{L} = [l_{ij}]_{N\times N}$ are used to represent the properties of the graph $\mathscr{G}$. The elements of these matrices are defined as follows:

$$a_{ij} = \begin{cases} 1, & \text{if } (i,j) \in \mathscr{E} \\ 0, & \text{otherwise} \end{cases} \quad \text{and} \quad l_{ij} = \begin{cases} -a_{ij}, & \text{if } i \neq j \\ \sum_{i\neq j} a_{ij}, & \text{otherwise.} \end{cases} \tag{2.1}$$

Additionally, for a function $\alpha : [0, a) \to [0, \infty)$ with $\alpha(0) = 0$ and constant $a > 0$, if α is continuous and strictly increasing, then it is said to be a $\mathscr{K}$-class function. For a function $\beta : [-b, a) \to (-\infty, \infty)$ with $\beta(0) = 0$ and constants $a, b > 0$, if β is continuous and strictly increasing, then it is said to be an extended $\mathscr{K}$-class function [155].

CHAPTER 3

STABILITY UNDER CLF-BASED QP APPROACH

This chapter will address the tracking control of MASs via a QP optimization framework, where the CLF condition serves as a constraint. The optimal controllers, derived through the QP solver, not only ensure the tracking control objective but also minimize the cost functions of agents. To enhance energy efficiency, discontinuous control methods, such as intermittent control strategy and event-triggered mechanism, are employed in the control framework. The CLF-based QP controllers are only updated at specific time instants, in order to reduce the frequency of QP problem-solving. In addition to considering optimization, the proposed methods are extended to uncertain MASs to enhance robustness, where the uncertainty is modeled by GP regression. In the end, simulation results are provided to demonstrate the feasibility of the theoretical analysis.

This chapter is based on the academic paper "Quadratic Programming Consensus Tracking Control of Uncertain Multiagent Systems via Event-Triggered Mechanism," in IEEE Transactions on Systems, Man, and Cybernetics: Systems, 2024. DOI: 10.1109/TSMC.2024.3459850.

3.1 Background and Preliminaries

3.1.1 Background

Stability is the most fundamental requirement in this work, forming the basis upon which other objectives, such as safety, robustness, and optimality, can be reliably pursued. For MASs, stability analysis has been extensively studied through a variety of approaches, including state-feedback consensus protocols, distributed observer designs and others [156, 157]. While these classical methods are well-developed and theoretically sound, they often focus solely on stability without considering optimization aspects. In this chapter, beginning with the consensus tracking control, we revisit the stability in MASs from the CLF-based QP perspective. The central idea is to move beyond traditional controller design, and instead, treat the control process as an optimization problem constrained by CLF conditions [158]. This enables not only the guarantee of system stability but also the simultaneous optimization of agent behavior with respect to predefined cost functions.

Most importantly, the QP formulation offers a significant structural advantage: extensibility. Once the CLF constraint is embedded in a QP problem, it becomes straightforward to incorporate additional control objectives or constraints, such as safety (via CBFs) or input saturation (simply by adding corresponding constraints to the QP). This modular nature eliminates the need to redesign controllers from scratch whenever new requirements arise. As control problems grow more complex with real-world considerations like obstacle avoidance, input bounds, or cooperative task prioritization, this flexibility becomes a major advantage. Although the CLF approach has been studied in the open literature [159], its application in MASs requires further extension and in-depth investigation to meet the requirements of distributed control, which is the main motivation of this chapter.

3.1.2 CLF and QP Formulation

Consider an ACS described as follows:

$$\dot{x} = f(x) + g(x)u(t), \tag{3.1}$$

where $x(t) \in \mathbb{R}^n$ represents the state variable, $u(t) \in U \subset \mathbb{R}^m$ denotes the control input, and the vector functions $f : \mathbb{R}^n \to \mathbb{R}^n$ and $g : \mathbb{R}^n \to \mathbb{R}^{n\times m}$ are assumed to be continuous. Designing feasible control input $u(t)$ to achieve specific objectives in the system (3.1) is a topic of interest. In this subsection, the control Lyapunov function will be introduced to study the stability properties of the system (3.1).

Definition 3.1. [160] Considering a function $V(x) : \mathbb{R}^n \to \mathbb{R}$ and the dynamical system (3.1), if $V(x)$ is continuous differentiable and for any $x(0) \in \mathbb{R}^n$ and $t \geqslant 0$, there is

$$\begin{aligned} &\underline{c}\|x\|^2 \leqslant V(x) \leqslant \bar{c}\|x\|^2, \\ &\inf_{u\in U}[L_f V(x) + L_g V(x)u(t)] \leqslant -cV(x), \end{aligned} \tag{3.2}$$

where $\underline{c}$, $\bar{c}$, and c are positive constants, $L_f V(x) = \frac{\partial V}{\partial x} f(x)$, $L_g V(x) = \frac{\partial V}{\partial x} g(x)$, then $V(x)$ is a control Lyapunov function.

Remark 3.1. *The Lyapunov stability theory is widely recognized for its utility in verifying system stability and establishing feasible control input. Specifically, for the ACS* (3.1)*, any control input* $u(t)$ *satisfying the condition* (3.2) *will lead to*

$$V(x) \leqslant e^{-ct}V(x(0)) \leqslant \bar{c}e^{-ct}\|x(0)\|^2 \tag{3.3}$$

and

$$\|x(t)\|^2 \leqslant \frac{1}{\underline{c}}V(x) \leqslant \frac{\bar{c}}{\underline{c}}e^{-ct}\|x(0)\|^2, \tag{3.4}$$

which implies

$$\|x(t)\| \leqslant \sqrt{\frac{\bar{c}}{\underline{c}}}\, e^{-\frac{c}{2}t}\|x(0)\| \to 0, \quad t \to \infty. \tag{3.5}$$

In other words, $\|x(t)\|$ is exponentially convergent with the rate $e^{-\frac{c}{2}t}$ under any control input from the following set:

$$\{u \in U | L_f V(x) + L_g V(x) u(t) + cV(x) \leqslant 0\}. \tag{3.6}$$

Based on the analysis in *Remark* 3.1, multiple control inputs are feasible in achieving system stability. To determine the optimal one, we can employ a QP framework to minimize the cost function. In this paper, the minimal norm of $u(t)$ is considered, which was also discussed in [60] and is shown as follows

$$\begin{aligned} u^* = &\arg\min_{u \in U} \frac{1}{2} u^T u \\ \text{s.t.} \quad &L_f V(x) + L_g V(x) u \leqslant -cV(x). \end{aligned} \tag{3.7}$$

Remark 3.2. *In the QP problem* (3.7)*, u^* represents the minimal controller required to realize system stability. Note that the specific form of the cost function can vary, depending on different quadratic terms related to u. For instance, the cost function was extended to $u^* = \arg\min_{u \in U} \frac{1}{2} u^T H(x) u$ in [103] and $u^* = \arg\min_{u \in U} \frac{1}{2}(u - u_d)^T (u - u_d)$ in [116], where $H(x)$ is a positive definite function and u_d represents a pre-designed control input that may not necessarily ensure stability. These variations reflect the flexibility in considering specific control performance or constraints.*

3.1.3 Intermittent Control

In this paper, an intermittent control strategy is employed to reduce the updating frequency of the QP controller (3.7). The time axis is partitioned into alternating working periods $[t_k^{on}, t_k^{off})$ and resting periods $[t_k^{off}, t_{k+1}^{on})$, where $k = 1, 2, \cdots$. Within each time interval, control actions are active from t_k^{on} to t_k^{off} and inactive from t_k^{off} to t_{k+1}^{on}. It is assumed that $t_1^{on} = 0$ and $t_k \to +\infty$ as $k \to +\infty$. Hence, the intermittent controller is

formulated as follows:

$$u(t) = \begin{cases} u(t), & t \in [t_k^{on}, t_k^{off}) \\ 0, & t \in [t_k^{off}, t_{k+1}^{on}). \end{cases} \tag{3.8}$$

The control on and off instants t_k^{on} and t_k^{off} will be determined later to ensure that the system remains under control on the whole and does not experience loss of stability.

3.1.4 GP Regression

GP is a widely used machine learning method for tasks such as regression analysis, classification, and model estimation. It can establish a mapping relationship between the input and output. Specifically, the Gaussian process considers both the input and output as random variables and assumes that their relationship follows a Gaussian distribution. As a result, the Gaussian process is capable of probabilistic modeling of unknown functions while providing confidence evaluations for the predicted results.

Specifically, consider an unknown function $y(\theta)$, $\theta \in \Theta \subset \mathbb{R}$ and the dataset $\mathscr{D} = \{\theta_l, y(\theta_l)\}_{l=1}^{s}$ with s samples. Define $\bar{\theta} = (\theta_1, \cdots, \theta_s)^T$ and $\bar{y} = (y(\theta_1), \cdots, y(\theta_s))^T$. Suppose the mean of the GP model is zero, then for any test value $\theta_0 \in \Theta$, the prediction of $y(\theta_0)$ is provided with its mean and variance as follows

$$\begin{aligned} \mu[y(\theta_0)|\mathscr{D}] &= k^T(\theta_0, \bar{\theta}) K^{-1}(\bar{\theta}, \bar{\theta}) \bar{y}, \\ \sigma^2[y(\theta_0)|\mathscr{D}] &= ker(\theta_0, \theta_0) - k^T(\theta_0, \bar{\theta}) K^{-1}(\bar{\theta}, \bar{\theta}) k(\theta_0, \bar{\theta}), \end{aligned} \tag{3.9}$$

where $k(\cdot,\cdot)$ is the covariance vector, $K(\cdot,\cdot)$ is the covariance matrix and $ker(\cdot,\cdot)$ is the kernel function.

Commonly used kernel functions include the Radial Basis Function, Linear kernel, Sigmoid kernel, *etc*. In this thesis, the radial basis function is adopted [151].

3.2 Deterministic Systems

Firstly, we begin with the deterministic MASs without uncertainty. Consider N followers and one leader in MASs. The system dynamics of agents are described as follows:

$$\dot{x}_i(t) = Ax_i(t) + Bu_i(t), \quad i \in \mathbf{I}[0,N]. \tag{3.10}$$

The state and control input of follower i, $i \in \mathbf{I}[1,N]$ are $x_i(t) \in \mathbb{R}^n$ and $u_i(t) \in U \subset \mathbb{R}^m$, respectively. The system matrices are $A \in \mathbb{R}^{n\times n}$ and $B \in \mathbb{R}^{n\times m}$. The leader is labeled as 0, whose state is $x_0(t) \in \mathbb{R}^n$ and control input is $u_0(t) = 0_m$. It is assumed that only a subset of the followers can establish communication with the leader. Without loss of generality, consider followers denoted by $i \in \mathbf{I}[1,M]$ as the informed followers who have the knowledge of the leader's state. Conversely, the remaining followers denoted by $i \in \mathbf{I}[M+1,N]$ are uninformed ones.

Definition 3.2. [161] The achievement of tracking control of the MAS (3.10) is described as the convergence of the tracking error

$$e_i(t) = x_i(t) - x_0(t), \quad i \in \mathbf{I}[1,N] \tag{3.11}$$

for follower i, i.e., for $\forall x_i(0) \in \mathbb{R}^n$, there is $\lim_{t\to\infty} e_i(t) = 0_n$.

Assumption 3.1. *Every uninformed follower within the system has at least one informed follower connected to them through a directed path.*

Assumption 3.2. (A,B) *is stabilizable.*

To simplify the communication structure, it is assumed that the informed followers, thanks to their direct access to the leader, do not require communication with other followers to achieve consensus tracking. Consequently, these informed followers have no neighbors apart from the leader. Based on this assumption, the Laplacian matrix

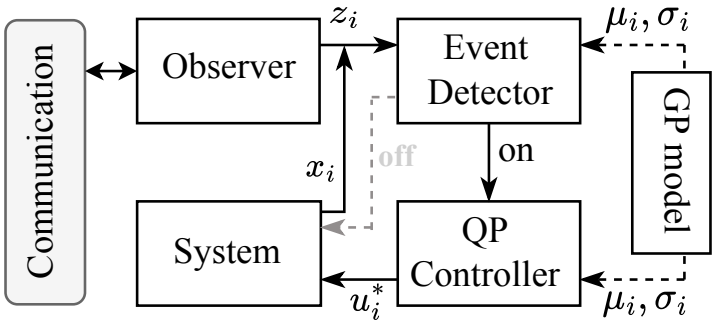

Figure 3.1: An overview of distributed CLF-based QP control method of MASs.

$\mathscr{L} \in \mathbb{R}^{N\times N}$ representing the interconnection among N followers is expressed as

$$\mathscr{L} = \begin{bmatrix} 0_{M\times M} & 0_{M\times(N-M)} \\ \mathscr{L}_1 & \mathscr{L}_2 \end{bmatrix}. \tag{3.12}$$

According to *Assumption* 3.1, the eigenvalues of $\mathscr{L}_2$ have positive real parts. Furthermore, $\mathscr{L}_2$ is a non-singular M-matrix.

Lemma 3.1. *[162] For the M-matrix $\mathscr{L}_2$, there exists a positive diagonal matrix $G = \text{diag}\{g_{M+1}, \cdots, g_N\} \in \mathbb{R}^{(N-M)\times(N-M)}$ such that $G\mathscr{L}_2 + \mathscr{L}_2^T G > 0$.*

This section focuses on the tracking control of MAS (3.10). Firstly, adaptive observers are developed for uninformed followers to estimate $x_0(t)$ to compensate for their limited access. Secondly, a CLF-based QP controller is constructed utilizing the designed observers. Thirdly, an intermittent event-triggering control strategy is incorporated into the proposed QP controller to alleviate the computational burden. An overview of the control methods can be found in Figure 3.1.

3.2.1 CLF-based QP Controller Design

To achieve consensus tracking with the leader, as outlined in *Definition* 3.2, it is evident that each follower requires the leader's information x_0. However, this information is

not accessible to uninformed followers. To address this constraint, a fully distributed observer denoted by $z_i \in \mathbb{R}^n$ is employed for uninformed followers to estimate x_0.

Denote $z_i = x_0$ for informed follower i, $i \in \mathbf{I}[1,M]$. For uninformed follower i, $i \in \mathbf{I}[M+1,N]$, the observer z_i is designed as follows:

$$\begin{cases} \dot{z}_i = Az_i - BB^TP(c_i+\rho_i)\eta_i \\ \eta_i = \sum_{j=1}^{N} a_{ij}(z_i - z_j) \\ \dot{c}_i = \eta_i^T PBB^T P\eta_i \\ \rho_i = \eta_i^T P\eta_i, \end{cases} \tag{3.13}$$

where $P \in \mathbb{R}^{n\times n}$ comes from the algebraic Riccati equation (ARE) solution:

$$PA + A^TP - PBB^TP + I_n = 0_{n\times n}. \tag{3.14}$$

Denoting the observation error

$$\epsilon_i = z_i - x_0, \quad i \in \mathbf{I}[M+1,N] \tag{3.15}$$

for follower i, one can get the following conclusion.

Lemma 3.2. *Under Assumptions 3.1-3.2, if $c_i(0) \geqslant 1$, then there is $\lim_{t\to\infty}\epsilon_i = 0$, $i \in \boldsymbol{I}[M+1,N]$.*

Proof: According to the definition of $\epsilon_i = z_i - x_0$, the η_i in (3.13) can be rewritten as

$$\eta_i = \sum_{j=M+1}^{N} a_{ij}(\epsilon_i - \epsilon_j). \tag{3.16}$$

Denoting $\eta = (\eta_{M+1}^T, \cdots, \eta_N^T)^T$, there is

$$\eta = (\mathscr{L}_2 \otimes I_n)(\epsilon_{M+1}^T, \cdots, \epsilon_N^T)^T. \tag{3.17}$$

As detailed in (3.12), $\mathscr{L}_2$ is a non-singular M-matrix. Hence, we only need to demonstrate $\lim_{t\to\infty}\eta = 0$ to infer $\lim_{t\to\infty}\epsilon_i = 0$, $i \in \mathbf{I}[M+1,N]$. Firstly, defining

$$\begin{aligned} \hat{\rho} &= \mathrm{diag}(\rho_{M+1}, \cdots, \rho_N), \\ \hat{c} &= \mathrm{diag}(c_{M+1}, \cdots, c_N), \end{aligned} \tag{3.18}$$

one can calculate the derivative of η as follows:

$$\dot{\eta} = [I_{N-M} \otimes A - \mathscr{L}_2(\hat{c}+\hat{\rho}) \otimes BB^T P]\eta. \tag{3.19}$$

Based on *Lemma* 3.1, a matrix $G = \mathrm{diag}\{g_{M+1}, \cdots, g_N\}$ exists such that $G\mathscr{L}_2 + \mathscr{L}_2^T G > 0$. Denote $\lambda_0 = \lambda_{\min}(G\mathscr{L}_2 + \mathscr{L}_2^T G) > 0$, and construct the following Lyapunov function:

$$V_0 = \frac{1}{2}\sum_{i=M+1}^{N}[g_i(2c_i+\rho_i)\rho_i + \frac{\lambda_0}{2}(c_i - c_0)^2]. \tag{3.20}$$

Combining with (3.13), the derivative of V_0 is calculated as

$$\begin{aligned}
\dot{V}_0 &= \sum_{i=M+1}^{N}[g_i\rho_i\dot{c}_i + g_i(c_i+\rho_i)\dot{\rho}_i + \frac{\lambda_0}{2}(c_i-c_0)\dot{c}_i] \\
&= \eta^T[\hat{\rho}G \otimes PBB^TP + (\hat{c}+\hat{\rho})G \otimes (PA + A^TP) \\
&\quad - (\hat{c}+\hat{\rho})(G\mathscr{L}_2 + \mathscr{L}_2^T G)(\hat{c}+\hat{\rho}) \otimes PBB^TP \\
&\quad + \frac{\lambda_0}{2}(\hat{c} - c_0 I_{N-M}) \otimes PBB^TP]\eta \\
&\leqslant \eta^T[(\hat{c}+\hat{\rho})G \otimes (PA + A^TP) + \hat{\rho}G \otimes PBB^TP \\
&\quad - \lambda_0(\hat{c}+\hat{\rho})^2 \otimes PBB^TP + \frac{\lambda_0}{2}(\hat{c} - c_0 I_{N-M}) \otimes PBB^TP]\eta \\
&= \eta^T[(\hat{c}+\hat{\rho})G \otimes (PA + A^TP) + \Phi \otimes PBB^TP]\eta,
\end{aligned} \tag{3.21}$$

where

$$\Phi = \hat{\rho}G - \lambda_0(\hat{c}+\hat{\rho})^2 + \frac{\lambda_0}{2}(\hat{c} - c_0 I_{N-M}). \tag{3.22}$$

If $c_i(0) \geqslant 1$, then $c_i(t) \geqslant 1$ for $t \geqslant 0$, since $\dot{c}_i(t)$ is always positive. Hence, there is $\hat{c} \leqslant \hat{c}^2$. Additionally, it follows from Young's inequality that

$$\begin{aligned}
\Phi &\leqslant \frac{\lambda_0}{2}\hat{\rho}^2 + \frac{1}{2\lambda_0}G^2 - \lambda_0(\hat{c}+\hat{\rho})^2 + \frac{\lambda_0}{2}\hat{c} - \frac{\lambda_0}{2}c_0 I_{N-M} \\
&\leqslant -\lambda_0[(\hat{c}+\hat{\rho})^2 - \frac{1}{2}\hat{\rho}^2 - \frac{1}{2}\hat{c}^2 - \frac{1}{2\lambda_0^2}G^2 + \frac{1}{2}c_0 I_{N-M}] \\
&\leqslant -\lambda_0[\frac{1}{2}(\hat{c}+\hat{\rho})^2 - \frac{1}{2\lambda_0^2}G^2 + \frac{1}{\lambda_0^2}G^2] \\
&= -\frac{1}{2}[\lambda_0(\hat{c}+\hat{\rho})^2 + \frac{1}{\lambda_0}G^2] \\
&\leqslant -(\hat{c}+\hat{\rho})G,
\end{aligned} \tag{3.23}$$

where the constant c_0 is chosen with $c_0 \geqslant \frac{2}{\lambda_0^2}\max_{i=M+1,\cdots,N} g_i^2$. Hence, one can obtain that

$$\dot{V}_0 \leqslant \eta^T[(\hat{c}+\hat{\rho})G \otimes (PA + A^TP - PBB^TP)]\eta = -\eta^T[(\hat{c}+\hat{\rho})G \otimes I_n]\eta \leqslant 0, \tag{3.24}$$

in which (3.14) is used to derive the inequality. Therefore, $V_0(t)$ is bounded as time grows, thus c_i and ρ_i are also bounded. Given that $\dot{c}_i(t) \geqslant 0$, $c_i(t)$ will approach a certain finite value asymptotically. In other words, there is $\dot{c}_i(t) \to 0$ as $t \to \infty$. According to the definition of $\dot{c}_i$ in (3.13), $\lim_{t\to\infty} \dot{c}_i(t) = 0$ is equivalent to $\lim_{t\to\infty} \eta_i(t) = 0$, which indicates $\lim_{t\to\infty} \epsilon_i(t) = 0$ for uninformed followers. ■

Thanks to *Lemma* 3.2, the observer z_i works well to describe or estimate x_0 for each follower i, $i \in \mathbf{I}[1,N]$. Denoting

$$\delta_i = x_i - z_i, \quad i \in \mathbf{I}[1,N], \tag{3.25}$$

the tracking error $e_i \to 0$ is equivalent to $\delta_i \to 0$. In the following, we will show feasible control input to realize $\delta_i \to 0$ as $t \to \infty$, which indicates the achievement of consensus tracking control for the MAS (3.10).

Construct the Lyapunov function for follower i as

$$V_i(\delta_i) = \delta_i^T(t)P\delta_i(t), \quad i \in \mathbf{I}[1,N]. \tag{3.26}$$

It follows from (3.25) that

$$\begin{aligned} \dot{V}_i &= \delta_i^T(PA + A^TP)\delta_i + 2\delta_i^TPBu_i, \quad i \in \mathbf{I}[1,M], \\ \dot{V}_i &= \delta_i^T(PA + A^TP)\delta_i + 2\delta_i^TPBu_i + 2\delta_i^TPBB^TP(c_i+\rho_i)\eta_i, \quad i \in \mathbf{I}[M+1,N]. \end{aligned} \tag{3.27}$$

According to (3.7), the CLF-based QP control input for follower i, $i \in \mathbf{I}[1,M]$ can be outlined as follows:

$$\begin{aligned} u_i^* &= \arg\min_{u_i \in U} \frac{1}{2}u_i^Tu_i \\ \text{s.t.} \quad & 2\delta_i^TPBu_i \leqslant -\delta_i^T(PA + A^TP + cP)\delta_i, \end{aligned} \tag{3.28}$$

and for follower i, $i \in \mathbf{I}[M+1, N]$:

$$
\begin{aligned}
u_i^* &= \arg\min_{u_i \in U} \frac{1}{2} u_i^T u_i \\
\text{s.t.} \quad & 2\delta_i^T P B u_i \leqslant -\delta_i^T (PA + A^T P + cP)\delta_i - 2\delta_i^T P B B^T P (c_i + \rho_i)\eta_i.
\end{aligned} \tag{3.29}
$$

Remark 3.3. *The CLF V_i is built upon δ_i. As the computation of δ_i for each follower depends solely on local information, this method fulfills the distributed control requirement.*

3.2.2 Event-triggering Intermittent Control Mechanism

The proposed CLF-based QP control approach (3.28) (3.29) demonstrates the feasibility of achieving consensus tracking control for MAS (3.10). However, conducting experiments proves more time and energy-consuming than expected due to the need to solve the QP problem frequently to obtain $u_i^*(t)$. To mitigate energy consumption, this section introduces the intermittent event-triggered control strategy to reduce the frequency of QP solving.

Initially, the time axis is divided into working periods $[t_{i,k}^{on}, t_{i,k}^{off})$ and resting periods $[t_{i,k}^{off}, t_{i,k+1}^{on})$, where $k \in \mathbb{N}^+$ for follower i, $i \in \mathbf{I}[1, N]$. Simultaneously, the event-triggered mechanism is employed during the working periods $[t_{i,k}^{on}, t_{i,k}^{off})$. Specifically, compared to (3.8), the control input $u_i(t)$ remains constant as $u_i^*(t_{i,k}^{on})$, obtained from CLF-based QP (3.28) (3.29) at control on instants $t = t_{i,k}^{on}$. Consequently, the QP optimization problem is solved only once during $t \in [t_{i,k}^{on}, t_{i,k}^{off})$. Denoting $u_{i,k}^* = u_i^*(t_{i,k}^{on})$ for brevity, the control input $u_i(t)$ of follower i is described as follows:

$$
u_i(t) = \begin{cases} u_{i,k}^*, & t \in [t_{i,k}^{on}, t_{i,k}^{off}) \\ 0, & t \in [t_{i,k}^{off}, t_{i,k+1}^{on}). \end{cases} \tag{3.30}
$$

It is worth noting that $V_i(t)$ may increase when $t \in [t_{i,k}^{off}, t_{i,k+1}^{on})$. To ensure $V_i(t) \to 0$ as $t \to \infty$, the control on and off instants $t_{i,k}^{on}$ and $t_{i,k}^{off}$, $k \in \mathbb{N}^+$ need to be carefully designed.

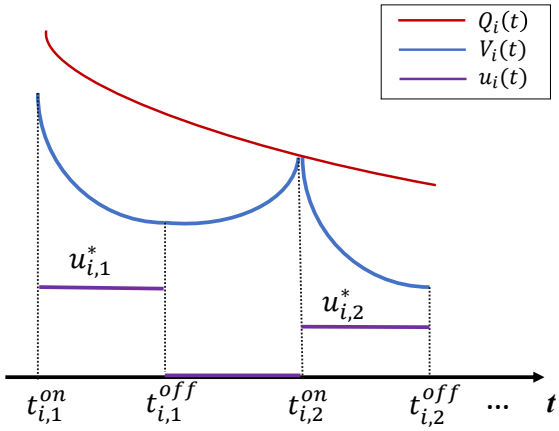

Figure 3.2: The intermittent event-triggered control strategy.

As illustrated in Figure 3.2, another function $Q_i(t)$ is introduced to constrain the increase of $V_i(t)$, acting as a boundary.

Our goal now is to ensure that $Q_i(t) - V_i(t) \geqslant 0$ always holds for $t \geqslant 0$, $i \in \mathbf{I}[1,N]$. Simultaneously, the function $Q_i(t)$ is custom-designed such that $Q_i(t) \to 0$ as $t \to \infty$. Hence, $V_i(t)$ will be bounded by $Q_i(t)$, ensuring that $V_i(t) \to 0$ as $t \to \infty$.

Remark 3.4. *The boundary $Q_i(t)$ serves to limit the growth of $V_i(t)$. As depicted in Figure 3.2, during the resting periods $[t^{off}_{i,k}, t^{on}_{i,k+1})$, $k \in \mathbb{N}^+$, we have $V_i(t) < Q_i(t)$. At $t = t^{on}_{i,k+1}$, it is possible that $V_i(t^{on}_{i,k+1}) = Q_i(t^{on}_{i,k+1})$, signaling the start of the next working period. When $V_i(t^{on}_{i,k+1}) = Q_i(t^{on}_{i,k+1})$, ensuring $\dot{V}_i(t^{on}_{i,k+1}) < \dot{Q}_i(t^{on}_{i,k+1})$ is necessary to guarantee $\lim_{\Delta \to 0^+} V_i(t^{on}_{i,k+1} + \Delta) < \lim_{\Delta \to 0^+} Q_i(t^{on}_{i,k+1} + \Delta)$ for the subsequent working period $[t^{on}_{i,k+1}, t^{off}_{i,k+1})$. One possible approach to designing $Q_i(t)$ is using an exponential function with a rate of $e^{-c't}$, where $c > c' > 0$ and e^{-ct} represents the convergence rate of $V_i(t)$. Generally, although $V_i(t)$ may not be monotonous due to the discontinuous control strategy, its curve always lies below $Q_i(t)$, which monotonously decreases with a rate of $e^{-c't}$.*

Both the event-triggered mechanism and intermittent control share a common objective: maintaining consensus tracking by monitoring certain error conditions and

adjusting controllers accordingly. The underlying principle is that control begins (updating the control input) when errors exceed a certain threshold for achieving consensus tracking and ends (allowing time to rest) when errors decrease too slowly.

Firstly, the k-th intermittent control off instant $t_{i,k}^{off}$ ($k \in \mathbb{N}^+$) for follower i ($i \in \mathbf{I}[1,N]$) is determined using the Lyapunov function $V_i(t)$ as follows:

$$t_{i,k}^{off} = \min\{t > t_{i,k}^{on} | \dot{V}_i \geqslant -\gamma c V_i\}, \tag{3.31}$$

where the discount parameter γ is custom-specific, satisfying $0 < \gamma < 1$. During $t \in [t_{i,k}^{on}, t_{i,k}^{off})$, condition (3.31) implies $\dot{V}_i < -\gamma c V_i$, resulting in V_i having a convergence rate of $e^{-\gamma c t}$. When V_i decreases slower than this threshold, the event is triggered, and the controller is turned off.

Secondly, the k-th intermittent control on instant $t_{i,k}^{on}$ ($k \in \mathbb{N}^+$) for each follower i ($i \in \mathbf{I}[1,N]$) is determined as follows:

$$t_{i,k+1}^{on} = \min\{t > t_{i,k}^{off} | \dot{Q}_i(t) - \dot{V}_i(t) \leqslant -\beta_{i,k}(Q_i(t) - V_i(t))\}, \tag{3.32}$$

where the constant $\beta_{i,k}$ satisfies $\beta_{i,k} > \frac{\dot{V}_i(t_{i,k}^{off}) - \dot{Q}_i(t_{i,k}^{off})}{Q_i(t_{i,k}^{off}) - V_i(t_{i,k}^{off})}$.

Lemma 3.3. *During resting periods* $[t_{i,k}^{off}, t_{i,k+1}^{on})$*, if* $Q_i(t_{i,k}^{off}) > V_i(t_{i,k}^{off})$*, then* $Q_i(t) > V_i(t)$ *holds for* $\forall t \in [t_{i,k}^{off}, t_{i,k+1}^{on})$ *under the triggering function (3.32).*

Proof: According to the conditions $\beta_{i,k} > \frac{\dot{V}_i(t_{i,k}^{off}) - \dot{Q}_i(t_{i,k}^{off})}{Q_i(t_{i,k}^{off}) - V_i(t_{i,k}^{off})}$ and $Q_i(t_{i,k}^{off}) > V_i(t_{i,k}^{off})$, one can obtain that

$$\dot{Q}_i(t_{i,k}^{off}) - \dot{V}_i(t_{i,k}^{off}) > -\beta_{i,k}(Q_i(t_{i,k}^{off}) - V_i(t_{i,k}^{off})). \tag{3.33}$$

In addition, triggering function (3.32) ensures that

$$\dot{Q}_i(t) - \dot{V}_i(t) > -\beta_{i,k}(Q_i(t) - V_i(t)), \quad t \in [t_{i,k}^{off}, t_{i,k+1}^{on}). \tag{3.34}$$

By the Comparison Lemma, (3.33) and (3.34) imply that

$$Q_i(t) - V_i(t) > e^{-\beta_{i,k}(t-t_{i,k}^{off})}(Q_i(t_{i,k}^{off}) - V_i(t_{i,k}^{off})) > 0 \tag{3.35}$$

for $\forall t \in [t_{i,k}^{off}, t_{i,k+1}^{on})$. ■

Lemma 3.4. *Considering the two triggering functions defined in (3.31) and (3.32), their Zeno behaviors can be ruled out.*

Proof: In this proof, we will show that there are two constants $\tau_i > 0$ and $\tau_i^{'} > 0$ for each follower i such that $t_{i,k}^{off} - t_{i,k}^{on} > \tau_i$ and $t_{i,k+1}^{on} - t_{i,k}^{off} > \tau_i^{'}$ hold, $k \in \mathbb{N}^+$, respectively. Hence, the Zeno behavior will not exist for the triggering functions (3.31) or (3.32).

Firstly, for the triggering function (3.31), take the informed followers $i \in \mathbf{I}[1, M]$ as an example. During the working periods $t \in [t_{i,k}^{on}, t_{i,k}^{off})$, $k \in \mathbb{N}^+$, it gives from (3.10), (3.25) and (3.30) that

$$\dot{\delta}_i(t) = A\delta_i(t) + Bu_i(t_{i,k}^{on}) = A\delta_i(t) + B[u_i(t) + \xi_{i,k}(t)], \tag{3.36}$$

where $\xi_{i,k}(t) \triangleq u_i(t_{i,k}^{on}) - u_i(t)$. In the dynamical model of $\dot{\delta}_i(t)$, the term $\xi_{i,k}(t)$ can be seen as the input-to-state disturbance on $u_i(t)$. Consider the triggering function introduced in [73]:

$$t_{i,k} = \min\{t > t_{i,k}^{on} | (\gamma - 1)cV_i(t) + k_1(\|\xi_{i,k}(t)\|) = 0\}, \tag{3.37}$$

where $k_1(\|\xi_{i,k}(t)\|)$ is a $\mathcal{K}$-class function. Thanks to *Theorem 3.1* in [73], there is a minimal inter-event time $\tau_i > 0$ so that

$$t_{i,k} - t_{i,k}^{on} \geqslant \tau_i, \quad k \in \mathbb{N}^+. \tag{3.38}$$

Moreover, the input-to-state stability can be achieved through the satisfactory of the condition $\dot{V}_i(t) \leqslant -cV_i(t) + k_1(\|\xi_{i,k}(t)\|)$, which can be reformulated as follows:

$$\dot{V}_i(t) + \gamma cV_i(t) \leqslant (\gamma - 1)cV_i(t) + k_1(\|\xi_{i,k}(t)\|). \tag{3.39}$$

During $t \in [t_{i,k}^{on}, t_{i,k}^{off})$, the triggering function (3.31) ensures that the left side of (3.39), $\dot{V}_i(t) + \gamma c V_i(t)$, is smaller than 0. But the situation is different for the right side of (3.39). When $t = t_{i,k}^{on}$, one has $\xi_{i,k}(t) = u_i(t_{i,k}^{on}) - u_i(t_{i,k}^{on}) = 0$. Since $k_1(\cdot)$ is a $\mathcal{K}$-class function, there is $k_1(\|\xi_{i,k}(t)\|) = 0$, which results in

$$(\gamma - 1)cV_i(t) + k_1(\|\xi_{i,k}(t)\|) = (\gamma - 1)cV_i(t) < 0. \tag{3.40}$$

However, during $t \in (t_{i,k}^{on}, t_{i,k}^{off})$, since $\|\xi_{i,k}(t)\|$ increases under the event-triggered mechanism and $k_1(\|\xi_{i,k}(t)\|)$ increases from zero, the right side of (3.39), $(\gamma - 1)cV_i(t) + k_1(\|\xi_{i,k}(t)\|)$, will gradually increase and approach zero, which triggers faster than the left side, $\dot{V}_i(t) + \gamma c V_i(t)$. Hence, compared with (3.31) and (3.37), it follows from (3.38) that

$$t_{i,k}^{off} - t_{i,k}^{on} > t_{i,k} - t_{i,k}^{on} \geqslant \tau_i, \quad k \in \mathbb{N}^+, \tag{3.41}$$

which rules out the Zeno behavior of the control off triggering function (3.31). For the uninformed followers $i \in \mathbf{I}[M+1, N]$, the input-to-state disturbance is also $\xi_{i,k}(t) = u_i(t_{i,k}^{on}) - u_i(t)$. The proof is the same as informed followers, so omitted here.

Secondly, we can conclude from *Lemma* 3.3 that $h_i(t) \triangleq Q_i(t) - V_i(t)$ is a continuous function for follower $i \in \mathbf{I}[1, N]$. Given the sign-preserving property of continuous functions, a positive constant $\tau_i^{'}$ exists that

$$t_{i,k+1}^{on} - t_{i,k}^{off} > \tau_i^{'}, \quad k \in \mathbb{N}^+, \tag{3.42}$$

which rules out the Zeno behavior of the control on triggering function (3.32). ■

Based on the above conclusions, the controller (3.30) is feasible for consensus tracking control, as described below.

Theorem 3.1. *Given the general linear MAS (3.10) and QP control input (3.28) (3.29) (3.30), under the triggering functions (3.31) and (3.32), the consensus tracking control*

problem will be solved if $Q_i(t)$ for each follower i, $i \in \boldsymbol{I}[1,N]$ is custom-designed to be continuous and satisfy:

(1) $Q_i(t) \geqslant V_i(t)$ *for* $t \in [t_{i,k}^{on}, t_{i,k}^{off})$, $k \in \mathbb{N}^+$;

(2) $Q_i(t_{i,k}^{off}) > V_i(t_{i,k}^{off})$, $k \in \mathbb{N}^+$;

(3) $\lim_{t\to\infty} Q_i(t) = 0$.

Proof: Although $V_i(t)$ may increase during the resting periods $t \in [t_{i,k}^{off}, t_{i,k+1}^{on})$, the triggering function (3.32) and *Lemma* 3.3 render $Q_i(t) > V_i(t)$ when $t \in [t_{i,k}^{off}, t_{i,k+1}^{on})$. Combined with the condition $Q_i(t) \geqslant V_i(t)$, $t \in [t_{i,k}^{on}, t_{i,k}^{off})$, one has $Q_i(t) \geqslant V_i(t)$ for $t \geqslant 0$. Therefore, $\lim_{t\to\infty} V_i(t) = 0$ is followed by $\lim_{t\to\infty} Q_i(t) = 0$, which indicates $\lim_{t\to\infty} \delta_i(t) = 0$ of follower i, $i \in \mathbf{I}[1,N]$. Thanks to the conclusion in *Lemma* 3.2, there is $\lim_{t\to\infty} e_i(t) = 0$ for follower i, $i \in \mathbf{I}[1,N]$. ■

Remark 3.5. *In fact, meeting the condition $Q_i(t) \geqslant V_i(t)$ for $t \in [t_{i,k}^{on}, t_{i,k}^{off})$ is straightforward. If $Q_i(t_{i,k}^{on}) > V_i(t_{i,k}^{on})$, thanks to the continuity of $Q_i(t)$ and $V_i(t)$, there exists a small $\tilde{\tau}_i > 0$ such that $Q_i(t) \geqslant V_i(t)$ when $t \in [t_{i,k}^{on}, t_{i,k}^{on} + \tilde{\tau}_i)$. If $Q_i(t_{i,k}^{on}) = V_i(t_{i,k}^{on})$, as mentioned in Remark 3.4, the condition can still be satisfied by appropriately designing the convergence rate of $Q_i(t)$. Furthermore, the exact expression of $Q_i(t)$ for $t \in [t_{i,k}^{on}, t_{i,k}^{off})$ is not crucial since it is not required in triggering function (3.31). What matters is the continuity of $Q_i(t)$ and the condition in Lemma 3.3, which ensures $Q_i(t) \geqslant V_i(t)$ for $t \geqslant 0$.*

Remark 3.6. *The QP problems* (3.28) *and* (3.29) *considered in the controller design include linear inequality constraints, along with box constraints. Although this QP structure admit a unique solution due to the strict convexity of the objective function and the convexity of the feasible set, obtaining an explicit (closed-form) solution is generally not straightforward. In particular, finding an explicit expression for the optimizer requires identifying the active set of constraints at the solution, which depends on the problem data in the constraints. Only when the set of active constraints is known in advance*

(e.g., remains constant), the optimal solution can be expressed explicitly as a projection of the origin onto the corresponding affine subspace. Otherwise, the solution needs to be computed numerically using standard QP solvers. Therefore, in this thesis, the QP solution is obtained numerically at each control step, and a general closed-form expression is not pursued.

3.3 Uncertain Systems

In this section, we will extend the CLF-based QP framework in uncertain MASs to enhance the robustness of the proposed control methods.

Consider the dynamics of follower i given by:

$$\dot{x}_i(t) = Ax_i(t) + Bu_i(t) + w_i(x_i(t)), \quad i \in \mathbf{I}[1, N] \tag{3.43}$$

where $w_i(x_i(t)) \in \mathbb{R}^n$ represents the system uncertainty, and the other notations are consistent with those defined in MAS (3.10).

3.3.1 GP-CLF-based QP Controller Design

For the Lyapunov function in (3.26), its derivative along the dynamics (3.43) is obtained as

$$\begin{aligned} \dot{V}_i &= \delta_i^T (PA + A^T P)\delta_i + 2\delta_i^T PBu_i + 2\delta_i^T Pw_i, i \in \mathbf{I}[1, M], \\ \dot{V}_i &= \delta_i^T (PA + A^T P)\delta_i + 2\delta_i^T PBu_i + 2\delta_i^T Pw_i \\ &\quad + 2\delta_i^T PBB^T P(c_i + \rho_i)\eta_i, i \in \mathbf{I}[M+1, N]. \end{aligned} \tag{3.44}$$

Consequently, the CLF-based QP controller for follower i is

$$
\begin{aligned}
u_i^* = &\arg\min_{u_i \in U} \frac{1}{2} u_i^T u_i \\
\text{s.t.} \quad & 2\delta_i^T P B u_i \leqslant -\delta_i^T (PA + A^T P + cP)\delta_i - 2\delta_i^T P w_i, i \in \mathbf{I}[1, M] \\
& 2\delta_i^T P B u_i \leqslant -\delta_i^T (PA + A^T P + cP)\delta_i - 2\delta_i^T P w_i \\
& \qquad - 2\delta_i^T P B B^T P (c_i + \rho_i)\eta_i, i \in \mathbf{I}[M+1, N].
\end{aligned} \tag{3.45}
$$

However, the unknown uncertainty w_i cannot be directly utilized in controller design in practice. Without requiring the upper bound of w_i, the GP serves as a useful tool for training an estimated model in an online manner.

In the QP problem (3.45), the term $2\delta_i^T P w_i \in \mathbb{R}$ in the CLF constraint needs to be addressed, which can be modeled using GP regression. For each follower i, $i \in \mathbf{I}[1, N]$, consider the dataset $\mathscr{D}_i = \{\theta_{i,l}, y_{i,l}\}_{l=1}^s$ with s samples, where each sample (θ_i, y_i) is defined as $\theta_i = [x_i^T, \delta_i^T]^T \in \mathbb{R}^{2n}$ and $y_i(\theta_i) = 2\delta_i^T P(\dot{x}_i - Ax_i - Bu_i) \in \mathbb{R}$. Using this dataset $\mathscr{D}_i$, a one-dimensional GP model can be obtained for each follower i, which provides the mean and variance functions for the term $2\delta_i^T P w_i$ according to (3.9), denoted as μ_i and σ_i^2, respectively. It is worth noting that computational capability is usually finite in real applications, naturally limiting the number of samples s.

According to *Theorem 6* in [163], the prediction error from the GP model is bounded for each follower in a probabilistic sense, which can be formulated as follows:

$$
\mathbb{P}\{|\mu_i - 2\delta_i^T P w_i| \leqslant \xi_i \sigma_i\} \geqslant \varpi, \tag{3.46}
$$

where the probability $0 < \varpi < 1$ is related to the value of the constant $\xi_i > 0$. In order to achieve a high probability, the constant ξ_i is chosen as

$$
\xi_i \geqslant \sqrt{2\|y_i\| + 300\varrho_i \ln^3(\frac{s+1}{1-\varpi})} \tag{3.47}
$$

under the dataset $\mathscr{D}_i$, where ϱ_i is the maximum mutual information among the samples[1].

[1]Here, the lower bound of ξ_i is used for theoretical analysis. In practice, $\xi_i = 1.96$ can be chosen to achieve a 95% confidence level.

For ease of writing, denote

$$\hat{\dot{V}}_i = \delta_i^T (PA + A^T P)\delta_i + 2\delta_i^T PBu_i + \mu_i + \xi_i \sigma_i \tag{3.48}$$

for $i \in \mathbf{I}[1, M]$, and

$$\hat{\dot{V}}_i = \delta_i^T (PA + A^T P)\delta_i + 2\delta_i^T PBu_i + 2\delta_i^T PBB^T P(c_i + \rho_i)\eta_i + \mu_i + \xi_i \sigma_i \tag{3.49}$$

for $i \in \mathbf{I}[M+1, N]$. The GP-CLF-based QP control protocol for follower i is expressed as follows:

$$\begin{aligned} u_i^* = &\arg\min_{u_i \in U} \frac{1}{2} u_i^T u_i \\ \text{s.t.} \quad &\hat{\dot{V}}_i \leqslant -cV_i, \quad i \in \mathbf{I}[1, N]. \end{aligned} \tag{3.50}$$

Remark 3.7. *Typically, unknown uncertainties are managed using their bounds in the literature, such as in [164][121]. In contrast, our work removes this requirement by estimating uncertainties via training GP models. Unlike other works that use multi-dimensional GPs for uncertainty estimation [165][142], we employ one-dimensional GPs to estimate scalar terms in the CLF condition, thereby reducing the number of necessary GP models.*

3.3.2 Event-triggered Model and Controller Update

Note that GP models for system uncertainty require updates with new training data samples. Our object is to employ an online learning approach to collect new samples when necessary, which is achieved through an event-triggered mechanism. Additionally, the GP-CLF-based QP problem (3.50) is solved accordingly when the GP models are updated. This strategy also ensures that the QP problem is solved at switching time instants to minimize computational resources.

In previous works, such as [166], a time-triggered approach is utilized, where training samples are collected at $t_{k+1} = t_k + \Delta t$ with a fixed time interval $\Delta t > 0$. This method

presents two drawbacks. Firstly, the collection of training data may exceed what is necessary, resulting in a higher-than-expected frequency of GP model updates. Secondly, the accuracy of the uncertainty estimation μ_i of w_i is unknown, potentially affecting the unexpected changes in the Lyapunov function. To address these issues and enhance data efficiency, we consider an event-triggered approach for adding new training samples for GP model updates, and consequently, QP solving. The core idea involves monitoring the derivative of the Lyapunov function to ensure its non-negativity. Given that the exact value of $\dot{V}_i$ is inaccessible, we design the triggering function for follower i, $i \in \mathbf{I}[1,N]$, using the estimated value $\hat{\dot{V}}_i$ as follows:

$$t_{i,k+1} = \min\{t > t_{i,k} | \hat{\dot{V}}_i \geqslant 0\}, \quad k \in \mathbb{N}^+. \tag{3.51}$$

Consider the following controller for follower i, $i \in \mathbf{I}[1,N]$:

$$u_i(t) = u_{i,k}^*, \quad t \in [t_{i,k}, t_{i,k+1}), \tag{3.52}$$

one can draw the following conclusion.

Theorem 3.2. *Given the uncertain MAS (3.43), under the QP controller (3.48)(3.49)(3.50)(3.52) and triggering function (3.51), if taking* $\xi_i \geqslant \sqrt{2\|y_i\| + 300\varrho_i \ln^3(\frac{s+1}{1-\varpi})}$, *the follower* i *can achieve consensus tracking control with a probability of at least* ϖ.

Proof: Firstly, we will show the feasibility of the GP-CLF-based QP controller (3.50). In order to estimate the unknown term $2\delta_i^T P w_i$, the one-dimensional GP regression model is used. Thanks to *Theorem 6* in [163], taking an appropriate value of ξ_i with the condition

$$\xi_i \geqslant \sqrt{2\|y_i\| + 300\varrho_i \ln^3(\frac{s+1}{1-\varpi})} \tag{3.53}$$

ensures the bound of the GP model error with a probability of at least ϖ. Hence, there is

$$\begin{aligned} & \mathbb{P}\{|\mu_i - 2\delta_i^T P w_i| \leqslant \xi_i \sigma_i\} \geqslant \varpi \\ \Longrightarrow \quad & \mathbb{P}\{2\delta_i^T P w_i \leqslant \mu_i + \xi_i \sigma_i\} \geqslant \varpi, \end{aligned} \tag{3.54}$$

which indicates $\dot{V}_i \leqslant \hat{\dot{V}}_i$ with a probability of at least ϖ. Under the controller u_i^* from (3.50), the CLF condition $\hat{\dot{V}}_i \leqslant -cV_i$ is satisfied. Hence, $\dot{V}_i \leqslant -cV_i$ is achieved with a high probability, which indicates the convergence of consensus tracking errors in a probabilistic sense. Note that these results hold for any time $t > 0$, since t_k has not been specified so far.

Secondly, the triggering function (3.51) works as follows. Under the QP controller $u_{i,k}^*$ solved at $t = t_{i,k}$, there is $\hat{\dot{V}}_i \leqslant -cV_i$ at $t = t_{i,k}$. As time grows, $\hat{\dot{V}}_i$ increases from a negative value to zero. And the function (3.51) triggers when $\hat{\dot{V}}_i$ is zero. Overall speaking, $\hat{\dot{V}}_i \leqslant 0$ holds during $t \in [t_{i,k}, t_{i,k+1})$. Hence, there is $\dot{V}_i \leqslant \hat{\dot{V}}_i \leqslant 0$ with a high probability. Additionally, since $\hat{\dot{V}}_i$ is a continuous function during the time period $[t_{i,k}, t_{i,k+1})$, thanks to the sign-preserving property, there exists a positive constant $\hat{\tau}_i > 0$ such that $t_{i,k+1} - t_{i,k} > \hat{\tau}_i$, $k \in \mathbb{N}^+$, which excludes the Zeno behavior of the triggering function (3.51). ■

Remark 3.8. *The computational resources are primarily concerned with two aspects. The first is the training of the GP model, which has a complexity of $O(N^3)$ relative to the input data dimension or $O(N^2)$ relative to the number of samples [151]. The second is solving the QP problem. Although an exact computational complexity for QP solving is not available, it can be estimated in terms of time. For instance, using the $quadprog(\cdot)$ function in MATLAB, solving a constrained QP problem typically takes approximately 0.001 seconds.*

Remark 3.9. *Compared to the content in Section III, the intermittent control strategy is not applied to uncertain MASs. When replacing $\dot{V}_i$ with its upper bound $\hat{\dot{V}}_i$, the original results for the intermittent event-triggering functions (3.31) and (3.32) still hold for*

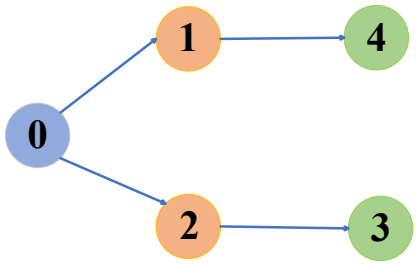

Figure 3.3: The communication topology of MASs.

uncertain MASs in a probabilistic sense. The proof follows a similar approach as in Theorem 3.2. In fact, the inherent nature of the intermittent control is a trade-off between computational complexity and convergence time. For uncertain MASs, considering the additional computation required for GP model training, we eliminate the control off period of intermittent control to reduce the frequency of GP model updates. Consequently, the triggering function (3.51) is designed to ensure a continuous decrease in the Lyapunov function.

3.4 Numerical Simulation

This section presents two numerical examples to illustrate the feasibility of the theoretical conclusions.

Example 3-1: Consider the general linear MAS (3.10) with one leader and four followers, and the communication topology is in Figure 3.3. The system matrices are

$$A = \begin{bmatrix} 0 & 1 & 0 \\ 0 & 0 & 1 \\ 0 & 0 & 0 \end{bmatrix} \quad \text{and} \quad B = \begin{bmatrix} 0 \\ 0 \\ 1 \end{bmatrix}.$$

The solution to the ARE (3.14) is

$$P = \begin{bmatrix} 2.4142 & 2.4142 & 1 \\ 2.4142 & 4.8284 & 2.4142 \\ 1 & 2.4142 & 2.4142 \end{bmatrix}.$$

In this experiment, choose the CLF parameter $c = 0.2$ and the discount parameter $\gamma = 0.5$. In the triggering function (3.32), the boundary $Q_i(t)$ for follower i ($i = 1,2,3,4$) is custom-designed as an exponential function $\dot{Q}_i(t) = -0.2Q_i(t)$. The initial states of all agents can be random numbers. In this simulation, they are

$$x_0(0) = [0.3433; 0.1485; 0.5752],$$

$$x_1(0) = [0.9586; 0.6440; 0.0486],$$

$$x_2(0) = [0.8403; 0.4380; 0.1741],$$

$$x_3(0) = [0.7626; 0.7290; 0.2798],$$

$$x_4(0) = [0.6860; 0.6970; 0.4240].$$

For the uninformed followers $i = 3,4$, set $c_3(0) = 1.2$ and $c_4(0) = 1.2$, and the initial states in (3.13) are randomly given as

$$z_3(0) = [0.6551; 0.1626; 0.1190],$$

$$z_4(0) = [0.3404; 0.5853; 0.2238].$$

The initial value of $Q_i(t)$ is $Q_i(0) = V_i(0) + 0.1$. Take the constant $\beta_{i,k} = 1.2 \times \frac{\dot{V}_i(t_{i,k}^{off}) - \dot{Q}_i(t_{i,k}^{off})}{Q_i(t_{i,k}^{off}) - V_i(t_{i,k}^{off})}$ for follower i, $i = 1,2,3,4$.

As shown in Figure 3.4, for uninformed follower i, $i = 3,4$, their observation errors of the leader's state information $\epsilon_i(t) = z_i(t) - x_0(t)$ converge to zero asymptotically, and the coupling gains $c_i(t)$ approaches fixed values ultimately. Figure 3.5 shows the trajectories of two kinds of errors for each follower, where (a) indicates the convergence of error $\delta_i(t) = x_i(t) - z_i(t)$ and (b) implies the realization of consensus tracking control objective.

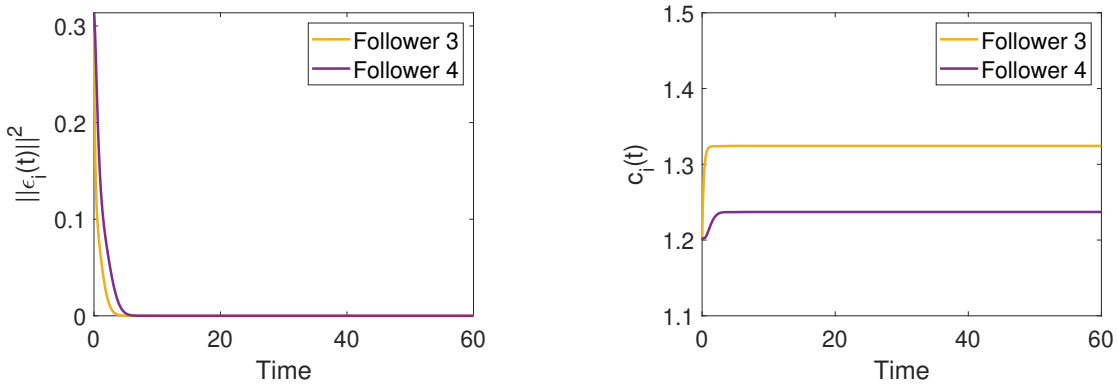

(a) (b)

Figure 3.4: (a) The observation error $\epsilon_i(t) = z_i(t) - x_0(t)$; (b) The coupling gain $c_i(t)$ in the observer (3.13) of uninformed follower i, $i = 3, 4$.

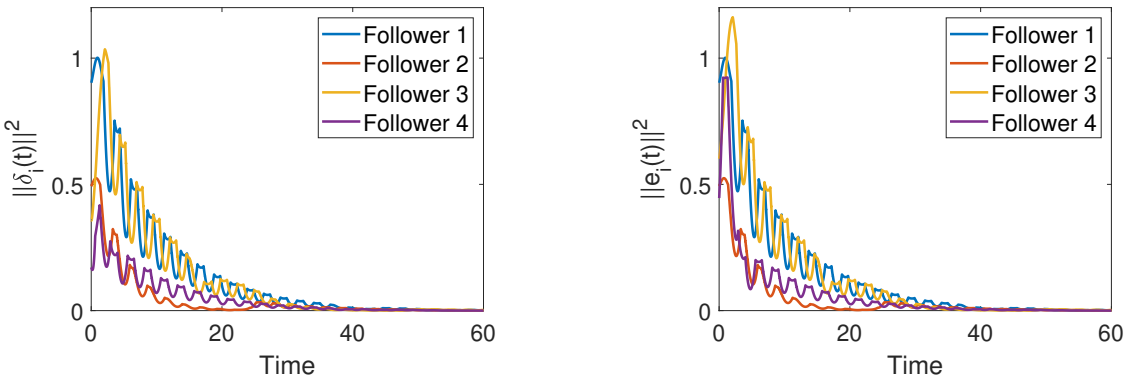

(a) (b)

Figure 3.5: (a) The error $\delta_i(t) = x_i(t) - z_i(t)$; (b) The tracking error $e_i(t) = x_i(t) - x_0(t)$ of follower i, $i = 1, 2, 3, 4$.

In Figure 3.6, the CLF $V_i(t)$ decreases exponentially with the QP controller (3.30) during working periods, and it ultimately goes to zero since the boundary $Q_i(t)$ is custom-designed to approach zero. It also shows that $Q_i(t) \geqslant V_i(t)$ always holds during the whole process. Figure 3.7 depicts the triggering instants of all followers, where (a) shows the case of control off triggering function (3.31) and (b) is for control on triggering function (3.32).

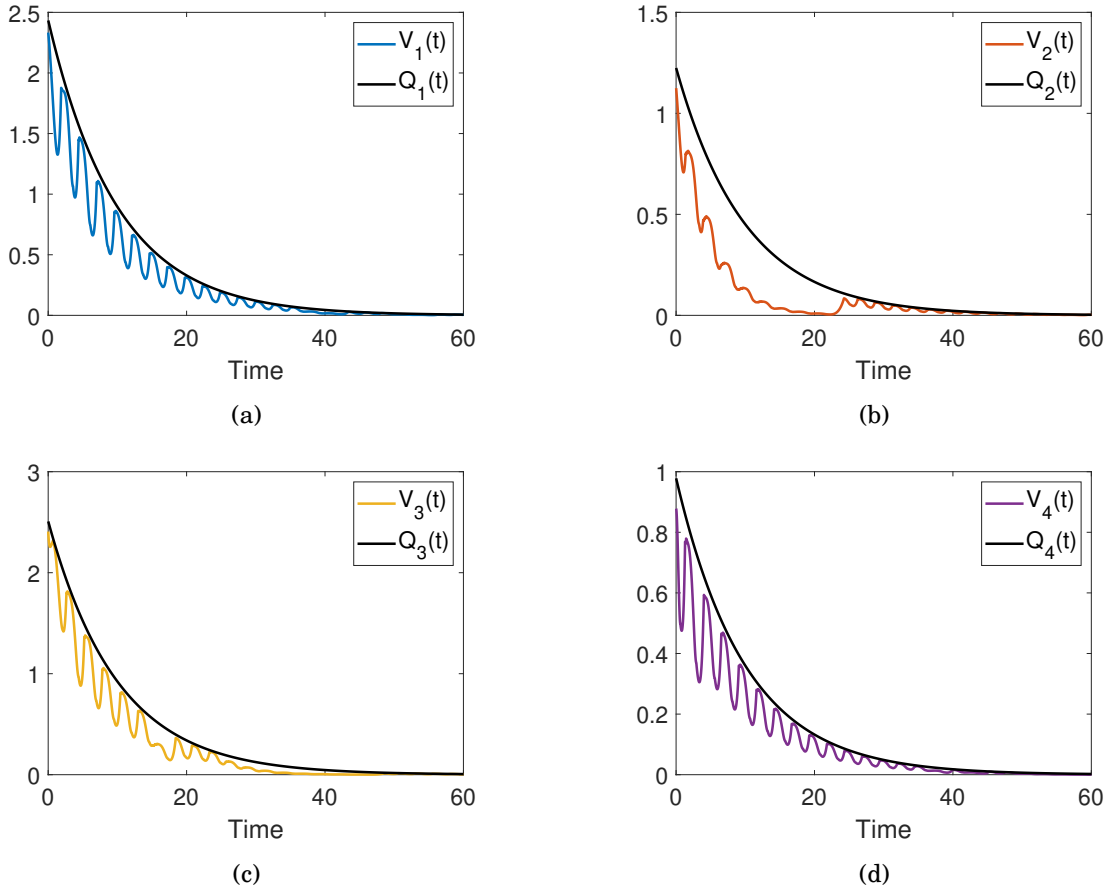

Figure 3.6: The trajectories of the Lyapunov function $V_i(t)$ for (a) Follower 1; (b) Follower 2; (c) Follower 3; (d) Follower 4.

Example 3-2: Consider the uncertain MAS (3.43) where the system uncertainty is $w_i(t) = 0.5\sin(x_i(t))$, $i = 1,2,3,4$. According to (3.9), the GP models are trained for uncertain terms $2\delta_i^T P w_i$ in the CLF constraints (3.50). The parameter ξ_i is set as 3 for

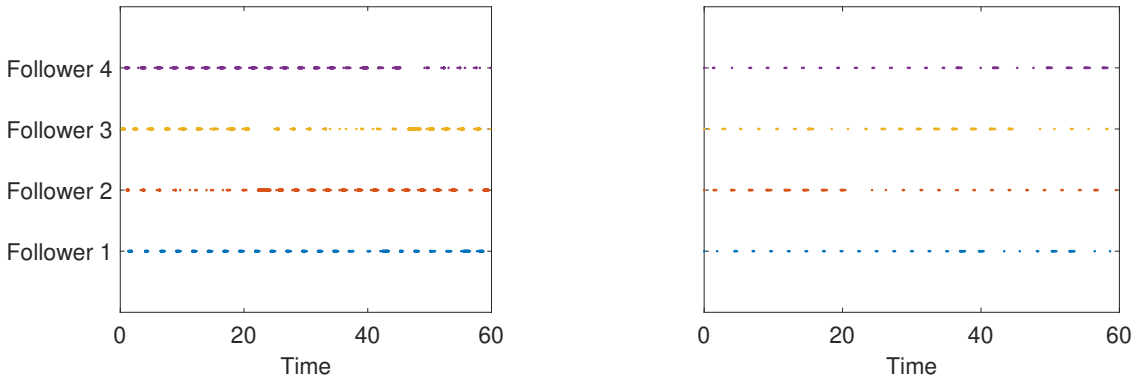

Figure 3.7: The triggering instants for (a) triggering function (3.31); (b) triggering function (3.32).

each follower to ensure a more than 95% confidence level. The other parameters and initial values are the same as those in *Example 3-1*.

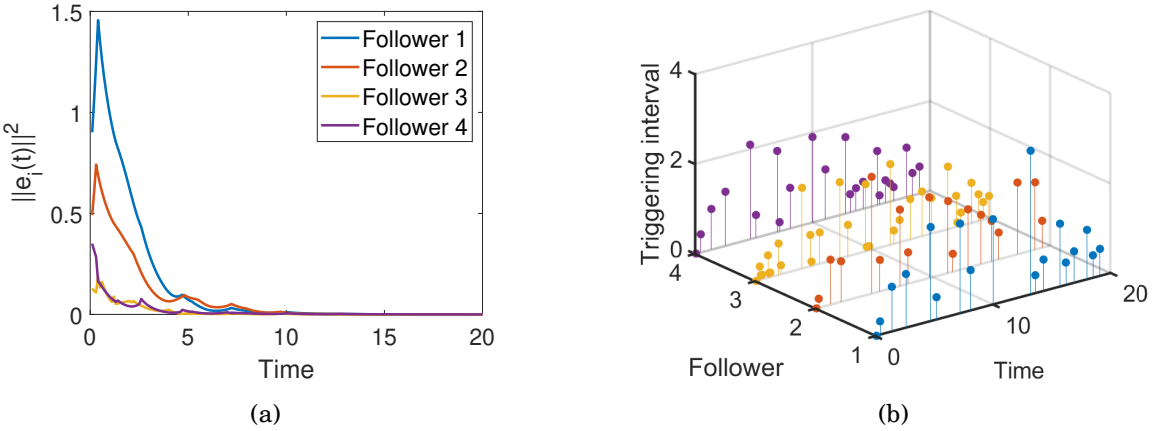

Figure 3.8: (a) The tracking error $e_i(t) = x_i(t) - x_0(t)$; (b) The triggering instants of follower i, $i = 1,2,3,4$.

Under the GP-CLF-based QP controller (3.50) and triggering function (3.51), as shown in Figure 3.8 (a), the consensus tracking control is realized for each follower. Figure 3.8 (b) shows the triggering instants of each follower. Taking Follower 4 as an example, the event triggers 23 times during this process, indicating the number of updates for the QP

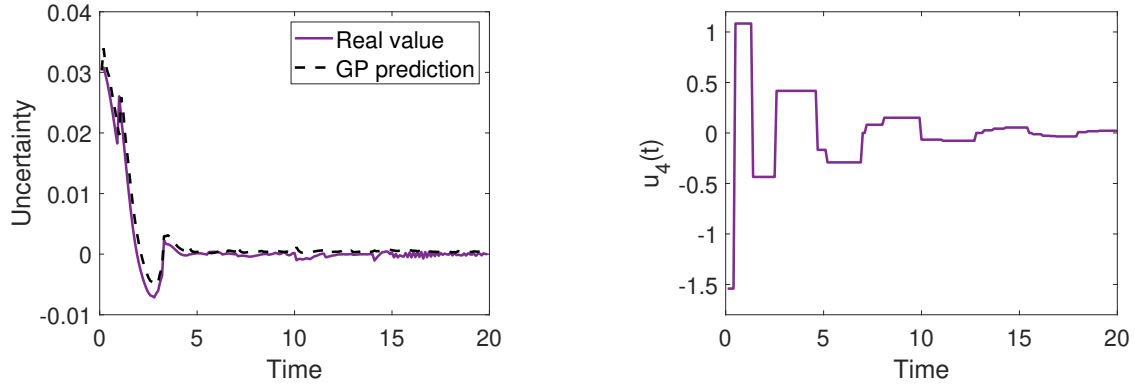

(a) (b)

Figure 3.9: (a) The trajectory of the uncertain term $2\delta_4^T P w_4$ and its GP prediction $\mu_4 + \xi_4 \sigma_4$; (b) The control input $u_4(t)$ of Follower 4.

controller u_4^* and training dataset $\mathscr{D}_4$.

In Figure 3.9 (a), the comparison is made between the actual value of the uncertain term $2\delta_4^T P w_4$ and its predicted value from the GP model: $\mu_4 + \xi_4 \sigma_4$, demonstrating that $\dot{V}_i \leqslant \hat{\dot{V}}_i$ with high probability. Additionally, Figure 3.9 (b) depicts the controller updates for Follower 4.

3.5 Conclusion

In summary, this chapter has presented a QP-based control framework for tracking control in MASs, where CLF constraints ensure stability. Discontinuous control strategies were introduced to reduce computational cost and enhance energy efficiency. Furthermore, to address system uncertainties, GP models were incorporated into the CLF constraints, enabling robust control under unknown dynamics. The effectiveness of the proposed methods was verified through simulation results, confirming both theoretical feasibility and practical applicability.

It is worth noting that although this chapter primarily focuses on stability, the design

of event-triggered mechanism, such as the triggering function (3.32), implicitly reflects a generalized notion of safety. Specifically, allowing $V_i(t)$ to increase within a bounded range constrained by $Q_i(t)$ can be interpreted as imposing an upper bound on the rate of change of the Lyapunov function. In this sense, the triggering condition (3.32) ensures that the system remains within a "safe" envelope of energy growth, whose construction is inspired by the idea of barrier function.

This conceptual similarity motivates the use of CBF for enforcing more explicit safety constraints, such as extending the CLF-based QP framework to incorporate CBF conditions for safe tasks. Accordingly, in the next chapter, we shift our focus from stability to safety, i.e., collision avoidance among agents. Additionally, we generalize the control objective from consensus to formation control, enabling agents to maintain desired formation shapes under safety constraints.

CHAPTER 4

SAFETY UNDER CBF-BASED QP APPROACH

In the formation control problem of MASs, collision avoidance is an important safety requirement. One effective approach to ensure safety involves combining CBFs with QP, where nominal control inputs are incorporated into QPs to achieve desired control objectives. Another approach is to use both CLF and CBF constraints in QP formulations, which guide the realization of formation control objective and safety objective, respectively. In this section, we will firstly construct the CBF-based QP control input for deterministic MASs to see the usage of CBF approach, then we formulate the GP-CLF-CBF-based QP control method for uncertain MASs.

This chapter is based on the academic paper "Safe Formation Control of Uncertain Multiagent Systems From a Bayesian Perspective," in IEEE Transactions on Automatic Control, 2025. DOI: 10.1109/TAC.2024.3470928.

4.1 Background and Preliminaries

4.1.1 Background

In addition to ensuring system stability, the physical safety of MASs has also emerged as an important concern in practical applications. Issues such as obstacle avoidance and collision avoidance are essential for the deployment of MASs. To address these safety challenges, CBFs have been introduced as a powerful framework and gained increasing attention in past several years [167, 168]. As demonstrated in the previous chapter, the CLF-based QP approach provides a unified and flexible control framework. This QP structure naturally lends itself to the incorporation of CBF conditions, whose conceptual foundations closely mirror those of CLFs. Given their mathematical similarities and complementary objectives, it is efficient to integrate CBF constraints into the existing QP framework to achieve both stability and safety in a unified optimization formulation [169].

However, direct application of pairwise CBF constraints for all agent pairs presents one major challenge: it contradicts the requirement of distributed control, as each agent would require full state information of all the other agents to construct complete pairwise constraints. To address this issue, the notion of nearby area was designed for each agent [91], under which only the most relevant inter-agent interactions are considered in the QP formulation. This approach not only aligns with distributed control requirement but also reduces the number of CBF constraints in the QP framework. In addition, this chapter explores uncertainty modeling within the CBF framework, extending the ideas presented in the previous chapter. Here, we examine whether GP models can similarly be used to approximate unknown terms in the CBF constraints. This allows the controller to account for external disturbances, thereby enhancing the robustness of safety guarantees in a data-driven way.

4.1.2 Safety and CBF

Consider a closed set $\mathscr{C}$ defined as follows

$$\begin{aligned} \mathscr{C} &= \{x \in X | h(x) \geqslant 0\}, \\ \partial\mathscr{C} &= \{x \in X | h(x) = 0\}, \\ \text{Int}(\mathscr{C}) &= \{x \in X | h(x) > 0\}, \end{aligned} \tag{4.1}$$

where $h : \mathbb{R}^n \to \mathbb{R}$ is a scalar function, and $\partial\mathscr{C}$ and $\text{Int}(\mathscr{C})$ are the boundary and interior of set $\mathscr{C}$, respectively. The notion of *safety* with respect to $\mathscr{C}$ is given as follows.

Definition 4.1. [115] If for any $x_0 \in \mathscr{C}$ and $t \geqslant t_0$, one has $x(t) \in \mathscr{C}$ along system (3.1), then $\mathscr{C}$ is forward invariant. Meanwhile, the ACS (3.1) is said to be *safe*.

One can see from Definition 4.1 that the safety of the ACSs could be verified through the forward invariance of the set $\mathscr{C}$. For the subsequent discussions, the definition of a barrier function will be given in advance.

Definition 4.2. [76] For a continuously differentiable function $h(x) : \mathbb{R}^n \to \mathbb{R}$, it is a (zeroing) barrier function if for $\forall x \in \mathscr{C}$, there is

$$\dot{h}(x) \geqslant -\bar{\alpha}(h(x)) \tag{4.2}$$

where $\bar{\alpha}(\cdot)$ is an extended $\mathscr{K}$-class function.

Remark 4.1. *Another kind of barrier function $B(x)$ is called the reciprocal barrier function if $\dot{B} \leqslant 0$ or $\dot{B} \leqslant \frac{\gamma}{B}, \gamma > 0$ [113]. See [115] for more details about the relationship and differences among the zeroing barrier function, reciprocal barrier function and forward invariance.*

Here comes the question. How to find an appropriate control input $u(t)$ to ensure the forward invariance of set $\mathscr{C}$, i.e., the safety of system (3.1). Similar as the definition of

CLF for system stability, the notion of CBF was proposed by Peter Wieland and Frank Allgower as follows.

Definition 4.3. [11] Considering the ACS (3.1) and the set $\mathscr{C}$ (4.1), a continuously differentiable function $h(x):\mathbb{R}^n \to \mathbb{R}$ is a valid CBF if there exists a control input $u \in U$ such that for any $x_0 \in \mathscr{C}$ and $\forall t \geqslant t_0$, there is

$$\sup_{u\in U}[L_f h(x) + L_g h(x)u + \bar{\alpha}(h(x))] \geqslant 0 \tag{4.3}$$

where $\bar{\alpha}(\cdot)$ is an extended $\mathcal{K}$-class function, and $L_f h(x) = \frac{\partial h(x)}{\partial x} f(x)$ and $L_g h(x) = \frac{\partial h(x)}{\partial x} g(x)$ denote the partial derivative of $h(x)$ along system (3.1), respectively.

Remark 4.2. *Note that any control input u satisfying (4.3) could ensure the safety of the ACS* (3.1)*. Additionally, a special case of function $\bar{\alpha}(h(x))$ could be the linear form $\bar{\alpha}(h(x)) = \alpha h(x)$ with α being a positive constant.*

Gurriet et al. proposed the following formulation to seek a safe controller u^* near a (potentially) unsafe controller u^{nom} with minimum cost [170]:

$$\begin{aligned} u^*(x) = \arg\min_{u\in U} \frac{1}{2}(u-u^{nom})^T(u-u^{nom}) \\ \text{s.t.} \quad L_f h(x) + L_g h(x)u + \alpha h(x) \geqslant 0. \end{aligned} \tag{4.4}$$

The solution to the QP (4.4) is the nearest controller around u^{nom} to maintain the system safety [171]. Consider the situation where the desired controller u^{nom} is pre-designed to ensure stability such as the state-feedback controller, but violates the safety requirement. Since safety is the *hard* condition, the CBF constraint is reserved in the QP formulation. At this moment, the system stability has been described by u^{nom} and embedded in the cost function. Taking the general linear systems as an example, u^{nom} can be the state-feedback controller $u^{nom} = -Kx$ to ensure system stability. In the context of MASs, the nominal control input u^{nom} can be designed in a distributed manner based on relative information between neighboring agents. A common approach is to

construct u^{nom} from consensus-based or formation control laws that rely on aggregate measurement errors, such as differences in agent states or tracking errors with respect to reference trajectories. For instance, a typical distributed state-feedback control law for agent i may take the form $u_i^{nom} = -\sum_{j\neq i} a_{ij}(x_i - x_j)$, where x_i and x_j denote the states of agent i and its neighbor j. This control input drives the agents toward a coordinated behavior (e.g., consensus or formation) and ensures stability in the absence of constraints. By integrating this distributed u_i^{nom} into the QP framework, the final control input remains close to the desired cooperative behavior while satisfying safety constraints in a minimally invasive fashion.

4.1.3 CLF-CBF-based QP Formulation

When both stability and safety objectives are considered, different from QP formulation (4.4), anther natural approach is to combine the CLF constraint and CBF constraint in the QP formulation at the same time, which is shown as

$$
\begin{aligned}
& u^*(x) = \arg\min_{u\in U} \frac{1}{2} u^T H(x) u \\
\text{s.t.} \quad & L_f V(x) + L_g V(x) u + cV(x) \leqslant 0 \\
& L_f h(x) + L_g h(x) u + \alpha h(x) \geqslant 0,
\end{aligned}
\tag{4.5}
$$

where $H(x) : \mathbb{R}^n \to \mathbb{R}^{m\times m}$ is a positive definite matrix.

However, it is worth noting how to determine if there exists a solution u^* to the CLF-CBF-based QP (4.5). The two constraints might be conflicting such that there is no solution to the QP problem. Thus, we need to select the more important one from the two control objectives. Ames et al. mediated the specifications in [115]. Safety may be a necessary requirement in systems, which should be regarded as a *hard* constraint. While stability could be a little relaxed as a *soft* constraint. In this case, the QP problem (4.5) is

extended to the following form

$$\begin{aligned} \mathbf{u}^*(x) = \underset{\mathbf{u}=(u,\delta)}{\arg\min} \frac{1}{2}\mathbf{u}^T H(x)\mathbf{u} + F(x)^T\mathbf{u} \\ \text{s.t.} \quad L_f V(x) + L_g V(x)u + cV(x) \leqslant \delta \\ L_f h(x) + L_g h(x)u + \alpha h(x) \geqslant 0 \end{aligned} \tag{4.6}$$

where $\mathbf{u} \in \mathbb{R}^{m+1}$, $H(x) \in \mathbb{R}^{(m+1)\times(m+1)}$, $F(x) \in \mathbb{R}^{m+1}$ and δ is a positive constant. The parameter δ indicates that safety performance comes prior to the stability, under which the existence of the solution to the QP (4.6) is given as follows.

Lemma 4.1. *[115] For the ACS* (3.1) *and QP problem (4.6), assuming that functions f, g, H, F, and the gradients of CLF $V(x)$ and CBF $h(x)$ are all locally Lipschitz, if $L_g V(x) \neq 0$ and $L_g h(x) \neq 0$ (i.e., relative degree one) hold for any $x \in \text{Int}(\mathscr{C})$, then the CLF-CBF-based QP problem (4.6) has a locally Lipschitz continuous and unique solution $\mathbf{u}^*$.*

In the following sections, we will utilize the CBF-based QP control (4.4) or CLF-CBF-based QP control (4.6) to study the safe formation control of MASs.

4.2 Deterministic Systems

To achieve the desired control objectives of MASs, various methods have been proposed in the open literature, which are denoted as the nominal control inputs u^{nom} in this section. However, in certain circumstances, ensuring system safety may take precedence over control objectives if there is a conflict. In this section, we will discuss collision avoidance as a safety requirement in MASs.

Consider a MAS composed of N agents, each with position $x_i \in \mathbb{R}^n$, velocity $v_i \in \mathbb{R}^n$, and control input $u_i \in \mathbb{R}^n$. The dynamics of agent i, $i \in \mathbf{I}[1,N]$ is described as

$$\begin{cases} \dot{x}_i = v_i \\ \dot{v}_i = u_i. \end{cases} \tag{4.7}$$

In practical applications, the velocity and acceleration of agents are often limited by upper bounds. Assume that $\|v_i(t)\| \leqslant b_v$ and $\|u_i(t)\| \leqslant b_u$ for $\forall i \in \mathbf{I}[1,N]$ and $\forall t \geqslant t_0$, where b_v and b_u are positive constants. Before moving on, it is crucial to identify the safe objective during the control process.

Collision avoidance is considered a safety requirement for the MAS (4.7). Specifically, any two agents should maintain a safe distance $D_{safe} > 0$ throughout the control process. Denote

$$\begin{aligned} \Delta x_{ij} &= x_i - x_j, \\ \Delta v_{ij} &= v_i - v_j \end{aligned} \tag{4.8}$$

as the relative position and relative velocity between agents i and j, respectively. A safe system means that $\|\Delta x_{ij}\| \geqslant D_{safe}$ for $\forall t \geqslant t_0$.

4.2.1 CBF-based QP Controller Design

A valid CBF to ensure the safety between agents i and j has been introduced in [91], which is given as follows:

$$h_{ij}(t) = \sqrt{2b_u(\|\Delta x_{ij}\| - D_{safe})} + \frac{\Delta x_{ij}^T}{\|\Delta x_{ij}\|}\Delta v_{ij}. \tag{4.9}$$

According to Section 4.1.2, the control input u_i of agent i coming from the set (4.3) can ensure the safety of MAS (4.7). In addition, recall that there is a nominal control input u_i^{nom} to accomplish desired control objectives, which however may result in collisions among agents. In this situation, we propose to modify u_i^{nom} in a minimally invasive way by using the CBF-based QP problem. Hence, when all the CBF constraints of agent pair (i,j), $i,j \in \mathbf{I}[1,N], i \neq j$ are assembled together to avoid collisions, the safe QP controller $\bar{u} = [u_1^T, \cdots, u_N^T]^T$ could be calculated as follows:

$$\begin{aligned} \bar{u}^* &= \arg\min_{\bar{u}} \sum_{i=1}^{N} \frac{1}{2}\|u_i - u_i^{nom}\|^2 \\ \text{s.t.} \quad & L_f h_{ij} + L_g h_{ij}\bar{u} + \alpha h_{ij} \geqslant 0, \quad \forall i,j \in \mathbf{I}[1,N], i \neq j. \end{aligned} \tag{4.10}$$

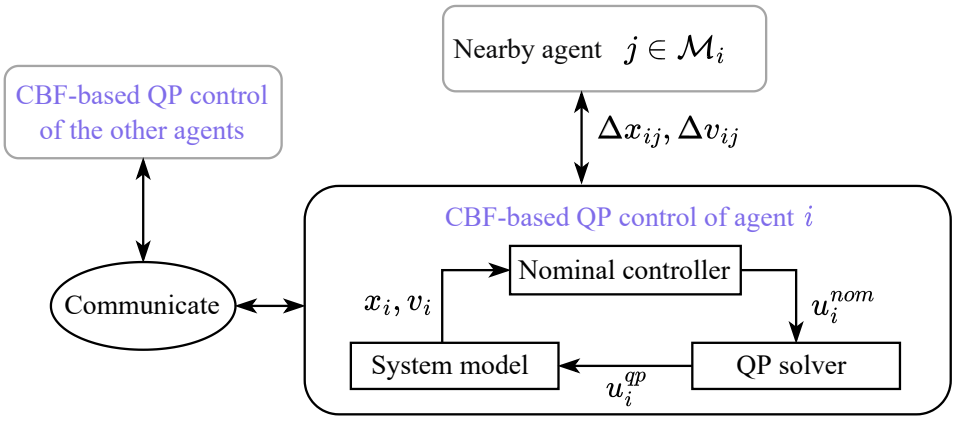

Figure 4.1: An overview of decentralized CBF-based QP control method of MASs.

4.2.2 Decentralized Approach

We begin with the derivative of CBF (4.9) along the MAS (4.7). The CBF constraint is given by $L_f h_{ij} + L_g h_{ij} \bar{u} + \alpha h_{ij} \geqslant 0$, whose concrete form is shown as follows:

$$\begin{aligned} -\Delta x_{ij}^T u_i - \Delta x_{ji}^T u_j \leqslant & \alpha h_{ij} \|\Delta x_{ij}\| - \frac{(\Delta v_{ij}^T \Delta x_{ij})^2}{\|\Delta x_{ij}\|^2} \\ & + \|\Delta v_{ij}\|^2 + \frac{b_u \Delta v_{ij}^T \Delta x_{ij}}{\sqrt{2 b_u (\|\Delta x_{ij}\| - D_{safe})}} \triangleq b_{ij}. \end{aligned} \tag{4.11}$$

One can see from (4.11) that the control protocol (4.10) is centralized due to the following two reasons:

- The control inputs of agent i and j (i.e., u_i and u_j) are coupled with each other.
- To avoid collisions of agent i, the relative position and velocity of all the other agents are required.

To address the first point, thanks to the completely symmetric form of agents pair (i, j), the condition (4.11) can be satisfied through satisfying that

$$-\Delta x_{ij}^T u_i \leqslant \frac{1}{2} b_{ij} \quad \text{and} \quad -\Delta x_{ji}^T u_j \leqslant \frac{1}{2} b_{ji}, \tag{4.12}$$

which depends on the relative information between agents i and j. For the second point, the CBF constraints in the QP (4.10) can be reduced by only considering collision avoidance of 'nearby' agents [91]. Specifically, an agent will not collide with others that are far away in a finite time, so only a group of agents denoted as $\mathscr{M}_i$ need to be considered for agent i to avoid a collision. We define the distance

$$D_{near} = D_{safe} + \frac{1}{2b_u}(\frac{3b_u}{\alpha} + 2b_v)^2 \tag{4.13}$$

as the cutoff radius for determining which agents are considered nearby. Consider the following set:

$$\mathscr{M}_i = \{j \in \mathbf{I}[1,N] | \|\Delta x_{ij}\| \leqslant D_{near}, j \neq i\}, \quad i \in \mathbf{I}[1,N]. \tag{4.14}$$

Lemma 4.2. *A collision will not occur between agent i and agent j where $j \notin \mathscr{M}_i$ in the near future, regardless of the control input u_i.*

Proof: This proof is similar to that of *Theorem III.2* in [91]. Specifically, according to the definition of $\mathscr{M}_i$ in (4.14), for agent i and agent j ($j \notin \mathscr{M}_i$), there is

$$\|\Delta x_{ij}\| > D_{near}, \quad j \notin \mathscr{M}_i. \tag{4.15}$$

Denoting $D_{ij} \triangleq \|\Delta x_{ij}\|$, it gives

$$\dot{D}_{ij} = \|\Delta \dot{x}_{ij}\| = \frac{\Delta x_{ij}^T}{\|\Delta x_{ij}\|}\Delta v_{ij}. \tag{4.16}$$

Additionally, the CBF (4.9) can be rewritten as

$$h_{ij} = \sqrt{2b_u(D_{ij} - D_{safe})} + \dot{D}_{ij}, \tag{4.17}$$

which yields

$$\dot{h}_{ij} = \frac{b_u}{\sqrt{2b_u(D_{ij} - D_{safe})}}\dot{D}_{ij} + \ddot{D}_{ij}. \tag{4.18}$$

Given the velocity and acceleration limits of each agent are b_v and b_u, respectively, it follows that

$$\dot{D}_{ij} \geqslant -2b_v \quad \text{and} \quad \ddot{D}_{ij} \geqslant -2b_u. \tag{4.19}$$

Combined with the definition in (4.14), one has

$$h_{ij} > \frac{3b_u}{\alpha} + 2b_v - 2b_v = \frac{3b_u}{\alpha}. \tag{4.20}$$

Hence,

$$\dot{h}_{ij} \geqslant -\frac{2b_u b_v}{\sqrt{2b_u(D_{ij}-D_{safe})}} - 2b_u > -\frac{2b_u b_v}{2b_v} - 2b_u = -3b_u > -\alpha h_{ij}. \tag{4.21}$$

That is to say, safety between agent i and j ($j \notin \mathscr{M}_i$) is always ensured within a short time frame, regardless of the control input. ■

According to the above analysis, the CBF-based QP controller of agent i ($i \in \mathbf{I}[1,N]$) is given as follows:

$$\begin{aligned} u_i^* = &\arg\min_{u_i \in U} \frac{1}{2}(u_i - u_i^{nom})^T(u_i - u_i^{nom}) \\ \text{s.t.} \quad &-\Delta x_{ij}^T u_i \leqslant \frac{1}{2} b_{ij}, \quad j \in \mathscr{M}_i, \end{aligned} \tag{4.22}$$

where U is the set $[-b_u, b_u]$. An overview of the proposed CBF-based QP control method can be found from Figure 4.1.

Theorem 4.1. *The collision avoidance of MAS* (4.7) *can be realized under the control input* u_i^* *solved from the CBF-based QP problem* (4.22)*.*

Proof: This conclusion can be easily obtained from (4.4) and *Lemma 4.2*. ■

Remark 4.3. *In the CBF-based QP control framework* (4.22)*, the number of CBF constraint for each agent is reduced by designing the neighbor set* $\mathscr{M}_i$*. One can adjust the value of* α *to make the neighboring agents remain within sensing range.*

4.3 Uncertain Systems

In this section, we will study the safe formation control of uncertain MASs. Different from the previous section, we adopt another approach: CLF-CBF-based QP control method as introduced in Section 4.1.3, to achieve formation through CLF condition and guarantee collision avoidance through CBF conditions. The original CLF-CBF-based QP control framework is shown below:

$$\begin{aligned} u^*, \delta^* = & \operatorname{argmin}_{(u;\delta)\in\mathbb{R}^{m+1}} \frac{1}{2} u^T H(x) u + w p^2 \\ \text{s.t.} \quad & L_f V(x) + L_g V(x) u + c V(x) \leqslant \delta \\ & L_f h(x) + L_g h(x) u + \alpha h(x) \geqslant 0, \end{aligned} \tag{4.23}$$

where $H(x) \in \mathbb{R}^{m\times m}$ is a positive definite matrix, δ is a relaxation parameter indicating the priority of the safety objective, and $w > 0$ is a penalty parameter on variable δ.

The dynamics of uncertain MAS is described as follows:

$$\begin{cases} \dot{x}_i = v_i \\ \dot{v}_i = u_i + d_i, \end{cases} \tag{4.24}$$

where $x_i \in \mathbb{R}^n$, $v_i \in \mathbb{R}^n$ and $u_i \in \mathbb{R}^n$ denote the position, velocity and control input of agent i, $i \in \mathbf{I}[1,N]$, respectively. The uncertainty $d_i \in \mathbb{R}^n$ is unknown. In addition, the motion reference information of the agents is provided with a virtual leader indexed by 0, whose position is denoted as $x_0 \in \mathbb{R}^n$, and velocity is bounded with a positive constant b_l. In other words, $\|v_0(t)\| \leqslant b_l$ for $\forall t \geqslant t_0$.

Denote $a_{i0} = 1$ if agent i is accessible to the virtual leader 0, and $a_{i0} = 0$ otherwise. The communication topology of the virtual leader and the N agents is described as $\bar{\mathcal{G}}$ whose node set is $\bar{\mathcal{V}} = \mathcal{V} \cup \{0\}$. The topology $\bar{\mathcal{G}}$ has a spanning tree if there is a root node from which a path exists to all the other nodes.

Assumption 4.1. *The topology $\bar{\mathcal{G}}$ is directed and has a spanning tree where the virtual leader works as the root node.*

Denote $\mathscr{A}_0 = \text{diag}\{a_{10}, \cdots, a_{N0}\}$ and $\bar{\mathscr{L}} = \mathscr{L} + \mathscr{A}_0$. It follows from Assumption 4.1 that $\bar{\mathscr{L}}$ is a positive definite matrix [172]. The purpose of this work is to obtain the optimal control input u_i^* for agent i, which can realize the following objectives.

- Formation control objective is achieved if there is

$$\lim_{t\to\infty}[x_i(t) - x_0(t) - s_i] = 0, \quad i \in \mathbf{I}[1,N], \tag{4.25}$$

  where $s = [s_1^T, \cdots, s_N^T]^T \in \mathbb{R}^{nN}$ is a constant vector to describe the desired formation information.

- Collision avoidance objective is achieved if any two agents keep a safe distance D_{safe} all the time. In other words, for any agent pair $(i,j), i,j \in \mathbf{I}[1,N]$, there is

$$\|x_i - x_j\| \geqslant D_{safe} > 0, \quad i \neq j. \tag{4.26}$$

4.3.1 CLF Condition Design

It is worth noting that the leader's information x_0 is not accessible to all the agents. In order to construct a distributed CLF for each agent, firstly we consider the following desired dynamics for agent i, $i \in \mathbf{I}[1,N]$:

$$\begin{aligned}\dot{x}_i = &-\gamma_1[\textstyle\sum_{j=1}^N a_{ij}((x_i - s_i) - (x_j - s_j)) + a_{i0}(x_i - x_0 - s_i)] \\ &-\gamma_2 \text{sgn}[\textstyle\sum_{j=1}^N a_{ij}((x_i - s_i) - (x_j - s_j)) + a_{i0}(x_i - x_0 - s_i)],\end{aligned} \tag{4.27}$$

where sgn$[\cdot]$ is the sign function and γ_1, γ_2 are positive constants to be designed later.

Denoting the formation tracking error as

$$e_i = x_i - x_0 - s_i, \tag{4.28}$$

the following conclusion is obtained.

Lemma 4.3. *Based on Assumption 4.1 and the dynamics* (4.27)*, the formation tracking error* e_i *of agent* i ($i \in \boldsymbol{I}[1,N]$) *approaches to zero asymptotically if taking* $\gamma_1 > 0$ *and* $\gamma_2 > b_l$.

Proof: According to the dynamics (4.27), the derivative of e_i is given as

$$\dot{e}_i = -\gamma_1[\sum_{j=1}^{N} a_{ij}(e_i - e_j) + a_{i0}e_i] - \gamma_2[\sum_{j=1}^{N} a_{ij}(e_i - e_j) + a_{i0}e_i] - v_0. \tag{4.29}$$

Denoting

$$e = [e_1^T, \cdots, e_N^T]^T \in \mathbb{R}^{nN}, \tag{4.30}$$

it follows that

$$\dot{e} = -\gamma_1(\bar{\mathscr{L}} \otimes I_n)e - \gamma_2 \mathrm{sgn}[(\bar{\mathscr{L}} \otimes I_n)e] - 1_N \otimes v_0. \tag{4.31}$$

Considering the Lyapunov function

$$V = \frac{1}{2} e^T(\bar{\mathscr{L}}^T \otimes I_n)e, \tag{4.32}$$

its derivative is calculated as follows:

$$\begin{aligned} \dot{V} &= e^T(\bar{\mathscr{L}}^T \otimes I_n)[-\gamma_1(\bar{\mathscr{L}} \otimes I_n)e - \gamma_2 \mathrm{sgn}[(\bar{\mathscr{L}} \otimes I_n)e] - 1_N \otimes v_0] \\ &= -\gamma_1 e^T(\bar{\mathscr{L}}^T\bar{\mathscr{L}} \otimes I_n)e - \gamma_2 \|(\bar{\mathscr{L}} \otimes I_n)e\|_1 - e^T(\bar{\mathscr{L}}^T \otimes I_n)(1_N \otimes v_0) \\ &\leqslant -\gamma_1 e^T(\bar{\mathscr{L}}^T\bar{\mathscr{L}} \otimes I_n)e - \gamma_2 \|(\bar{\mathscr{L}} \otimes I_n)e\|_\infty + b_l \|(\bar{\mathscr{L}} \otimes I_n)e\|_\infty. \end{aligned} \tag{4.33}$$

By taking $\gamma_1 > 0$ and $\gamma_2 > b_l$, one has $\dot{V} \leqslant 0$, indicating the convergence of V and hence the convergence of e and e_i. ■

Thanks to *Lemma 4.3*, the formation control objective can be achieved under the dynamics (4.27). In other words, the velocity of agent i is desired to be

$$\begin{aligned} \hat{v}_i \triangleq &-\gamma_1[\sum_{j=1}^{N} a_{ij}((x_i - s_i) - (x_j - s_j)) + a_{i0}(x_i - x_0 - s_i)] \\ &-\gamma_2 \mathrm{sgn}[\sum_{j=1}^{N} a_{ij}((x_i - s_i) - (x_j - s_j)) + a_{i0}(x_i - x_0 - s_i)]. \end{aligned} \tag{4.34}$$

Hence, the formation control problem can be transformed to find appropriate control input u_i that makes $v_i \to \hat{v}_i$. Denoting $\epsilon_i = v_i - \hat{v}_i$, the Lyapunov function for agent i is considered as

$$V_i = \frac{1}{2}\epsilon_i^T \epsilon_i, \quad i \in \mathbf{I}[1,N]. \tag{4.35}$$

Obviously, ϵ_i will converge to zero exponentially if V_i exponentially converges, which can be ensured by the CLF condition $\dot{V}_i + cV_i \leqslant 0$. Based on (4.24) and (4.27), the CLF condition of agent i, $i \in \mathbf{I}[1,N]$ can be found as follows:

$$\epsilon_i^T u_i + \epsilon_i^T d_i \leqslant -cV_i - \Delta_i^{clf}, \tag{4.36}$$

where $\Delta_i^{clf} \triangleq -\epsilon_i^T \dot{\hat{v}}_i$ is a constant for agent i, $i \in \mathbf{I}[1,N]$.

4.3.2 CBF Condition Design

The collision avoidance of MASs has been studied in the previous Section 4.2. In this uncertain case, the CBF expression h_{ij} defined in (4.9) and the nearby agents defined by set (4.14) remain consistent. Then, the CBF condition for agent pair (i,j) along the uncertain MAS (4.24) is given as follows:

$$\begin{aligned} \dot{h}_{ij} = &\frac{1}{\|\Delta x_{ij}\|}[\Delta x_{ij}^T(u_i + d_i) + \Delta x_{ji}^T(u_j + d_j) - \frac{(\Delta v_{ij}^T \Delta x_{ij})^2}{\|\Delta x_{ij}\|^2} \\ &+ \|\Delta v_{ij}\|^2 + \frac{b_u \Delta v_{ij}^T \Delta x_{ij}}{\sqrt{2b_u(\|\Delta x_{ij}\| - D_{safe})}}] \geqslant -\alpha h_{ij}. \end{aligned} \tag{4.37}$$

Considering the completely symmetric form of (4.37) and denoting

$$\Delta_{ij}^{cbf} \triangleq -\frac{(\Delta v_{ij}^T \Delta x_{ij})^2}{\|\Delta x_{ij}\|^2} + \|\Delta v_{ij}\|^2 + \frac{b_u \Delta v_{ij}^T \Delta x_{ij}}{\sqrt{2b_u(\|\Delta x_{ij}\| - D_{safe})}}, \tag{4.38}$$

the CBF condition for agent i ($i \in \mathbf{I}[1,N]$) can be written as follows:

$$-\Delta x_{ij}^T u_i - \Delta x_{ij}^T d_i \leqslant \frac{\alpha}{2} h_{ij} \|\Delta x_{ij}\| + \frac{1}{2}\Delta_{ij}^{cbf}, \quad j \neq i. \tag{4.39}$$

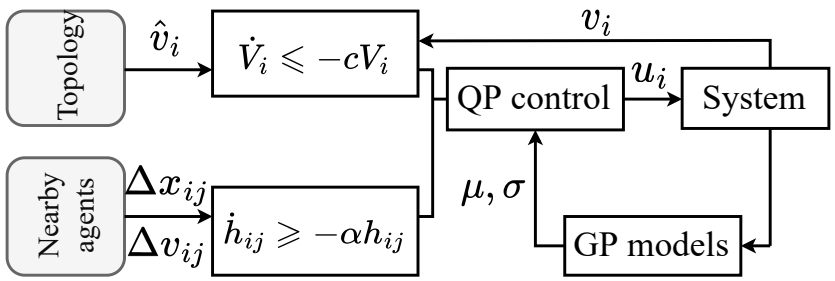

Figure 4.2: An overview of GP-CLF-CBF-based QP control method of uncertain MASs.

Thanks to Lemma 4.2, one can update the CBF condition (4.39) for agent i ($i \in \mathbf{I}[1,N]$) as follows, where only its nearby agents in set $\mathscr{M}_i$ are required to be considered:

$$-\Delta x_{ij}^T u_i - \Delta x_{ij}^T d_i \leqslant \frac{\alpha}{2} h_{ij} \|\Delta x_{ij}\| + \frac{1}{2}\Delta_{ij}^{cbf}, \quad j \in \mathscr{M}_i. \tag{4.40}$$

The CLF condition (4.36) and CBF condition (4.40) provide the feasible controller selection to achieve both control and safety objectives for the MAS (4.24). In addition, the uncertainty d_i will be addressed by GPs in the subsequent section.

4.3.3 GP-CLF-CBF-based QP Controller Design

According to the QP control approach (4.23) and the conditions (4.36) (4.40), the optimal controller u_i^* for agent i ($i \in \mathbf{I}[1,N]$) is obtained by solving the following QP problem:

$$\begin{aligned} u_i^* &= \text{argmin}_{u_i \in U} \frac{1}{2} u_i^T H u_i + w p_i^2 \\ \text{s.t.} \quad & \epsilon_i^T u_i + \epsilon_i^T d_i \leqslant -cV_i - \Delta_i^{clf} + \delta_i \\ & -\Delta x_{ij}^T u_i - \Delta x_{ij}^T d_i \leqslant \frac{\alpha}{2} h_{ij} \|\Delta x_{ij}\| + \frac{1}{2}\Delta_{ij}^{cbf}, \quad j \in \mathscr{M}_i. \end{aligned} \tag{4.41}$$

Due to the uncertainty d_i, the terms $\epsilon_i^T d_i$ and $\Delta x_{ij}^T d_i$ need to be estimated via GP models, as introduced in Section 2.3.2. An overview of the GP-CLF-CBF-based QP control method can be found from Figure 4.2.

Taking the CLF constraint of agent i ($i \in \mathbf{I}[1,N]$) as an example, for the unknown term $\epsilon_i^T d_i \in \mathbb{R}$, the training sampled data of agent i is denoted as

$$\begin{aligned} &\text{Input}: \quad \theta_i = [v_i^T, \hat{v}_i^T]^T \in \mathbb{R}^{2n}, \\ &\text{Output}: \quad y_i(\theta_i) = (v_i - \hat{v}_i)^T(\dot{v}_i - u_i) + \eta_0 \in \mathbb{R}, \end{aligned} \tag{4.42}$$

where $\eta_0 \sim \mathcal{N}(0, \sigma_0^2)$ is a Gaussian noise. Hence the training dataset with q samples is given as $\mathscr{D}_i = \{\theta_{i,k}, y_{i,k}\}_{k=1}^q$, with which a GP model can be trained to derive the posterior information of other observable states. That is to say, for the test input θ_i, the trained GP model gives its

$$\begin{aligned} &\text{Mean}: \quad \mu_i[\epsilon_i^T d_i | \theta_i, \mathscr{D}_i], \\ &\text{Variance}: \quad \sigma_i^2[\epsilon_i^T d_i | \theta_i, \mathscr{D}_i] \end{aligned} \tag{4.43}$$

of the unknown term $\epsilon_i^T d_i$ according to (3.9).

The situation is similar for the CBF constraint of agent i ($i \in \mathbf{I}[1,N]$). The term $\Delta x_{ij}^T d_i$ can be modeled by GP for the agent pair (i,j), $j \in \mathscr{M}_i$. The sampled data is denoted as

$$\begin{aligned} &\text{Input}: \quad \theta_{ij} = [x_i^T, v_i^T, x_j^T]^T \in \mathbb{R}^{3n}, \\ &\text{Output}: \quad y_{ij}(\theta_{ij}) = (x_i - x_j)^T(\dot{v}_i - u_i) + \eta_0 \in \mathbb{R}. \end{aligned} \tag{4.44}$$

The training dataset is $\mathscr{D}_{ij} = \{\theta_{ij,k}, y_{ij,k}\}_{k=1}^q$, and the posterior information of $\Delta x_{ij}^T d_i$ according to (3.9) is provided with the

$$\begin{aligned} &\text{Mean}: \quad \mu_{ij}[\Delta x_{ij}^T d_i | \theta_{ij}, \mathscr{D}_{ij}], \\ &\text{Variance}: \quad \sigma_{ij}^2[\Delta x_{ij}^T d_i | \theta_{ij}, \mathscr{D}_{ij}]. \end{aligned} \tag{4.45}$$

Assumption 4.2. *The kernel function $k(\cdot,\cdot)$ should satisfy that there is a bounded reproducing kernel Hilbert space norm for functions y_i and y_{ij} on a compact set* [1]. *That is, $\|y_i\|_k < \infty$ and $\|y_{ij}\|_k < \infty$ hold for $\forall i, j \in \boldsymbol{I}[1,N], i \neq j$.*

[1] See [173] for details on reproducing kernel Hilbert space norm. This assumption on kernel function can be satisfied with the help of universal kernels in *Lemma 4.55* of [174].

For simplicity of writing, we give the following abbreviated notations:

$$\begin{aligned}
\mu_i &= \mu_i[\epsilon_i^T d_i|\theta_i,\mathscr{D}_i],\\
\sigma_i &= \sigma_i[\epsilon_i^T d_i|\theta_i,\mathscr{D}_i],\\
\mu_{ij} &= \mu_{ij}[\Delta x_{ij}^T d_i|\theta_{ij},\mathscr{D}_{ij}],\\
\sigma_{ij} &= \sigma_{ij}[\Delta x_{ij}^T d_i|\theta_{ij},\mathscr{D}_{ij}].
\end{aligned} \tag{4.46}$$

The GP model error of $\epsilon_i^T d_i$ for agent i is given below:

$$\mathbb{P}\{|\mu_i - \epsilon_i^T d_i| \leqslant \beta_i \sigma_i\} \geqslant 1-\varpi, \tag{4.47}$$

where $1-\varpi \in (0,1)$ represents the probability and constant $\beta_i > 0$ is to be designed later.

Similarly, the GP model error of $\Delta x_{ij}^T d_i$ for agent pair (i,j) is given as follows:

$$\mathbb{P}\{|\mu_{ij} - \Delta x_{ij}^T d_i| \leqslant \beta_{ij} \sigma_{ij}\} \geqslant 1-\varpi, \tag{4.48}$$

where constant $\beta_{ij} > 0$ is to be designed later. Thanks to (4.47) and (4.48), the QP controller (4.41) can be reformulated as

$$\begin{aligned}
u_i^* = \operatorname{argmin}_{u_i \in U} &\frac{1}{2} u_i^T H u_i + w p_i^2\\
\text{s.t.} \quad & \epsilon_i^T u_i \leqslant -(\mu_i + \beta_i \sigma_i) - cV_i - \Delta_i^{clf} + \delta_i\\
& -\Delta x_{ij}^T u_i \leqslant \mu_{ij} - \beta_{ij}\sigma_{ij} + \frac{\alpha}{2} h_{ij} \|\Delta x_{ij}\| + \frac{1}{2}\Delta_{ij}^{cbf}, \quad j \in \mathscr{M}_i.
\end{aligned} \tag{4.49}$$

Theorem 4.2. *Under the QP controller* (4.49)*, taking constant* β_{ij} *with*

$$\beta_{ij} \geqslant \sqrt{2\|y_{ij}\|_k^2 + 300\xi_{ij}\ln^3(\frac{q+1}{\varpi})} \tag{4.50}$$

and

$$\xi_{ij} = \max_{\theta_{ij},\theta'_{ij} \in \{\theta_{ij,1},\cdots,\theta_{ij,q}\}} \frac{1}{2}\log|I + \sigma_0^{-2}\mathrm{K}(\theta_{ij},\theta'_{ij})|, \tag{4.51}$$

if the initial states satisfy $\|x_i(t_0) - x_j(t_0)\| > D_{safe}$ *for agent pair* (i,j)*,* $i,j \in \boldsymbol{I}[1,N]$*,* $i \neq j$*, then the collision avoidance is guaranteed for agent pair* (i,j) *with a probability of* $(1-\varpi)^2$ *at least.*

Proof: The conclusion is a benefit from *Lemma 1* in [175] where the one dimensional case is considered. Thanks to the conditional independence assumption of training samples among different agents, the constants β_{ij} and ξ_{ij} are related with the training dataset $\mathscr{D}_{ij}$. Moreover, the GP model error of $\Delta x_{ij}^T d_i$ is bounded with a probability of $1-\varpi$ at least, shown as

$$\mathbb{P}\{|\mu_{ij} - \Delta x_{ij}^T d_i| \leqslant \beta_{ij}\sigma_{ij}\} \geqslant 1-\varpi. \tag{4.52}$$

Hence, there is

$$\mathbb{P}\{\Delta x_{ij}^T d_i \geqslant \mu_{ij} - \beta_{ij}\sigma_{ij}\} \geqslant 1-\varpi. \tag{4.53}$$

The CBF condition (4.40) of agent i can be rewritten as follows:

$$-\Delta x_{ij}^T u_i \leqslant \mu_{ij} - \beta_{ij}\sigma_{ij} + \frac{\alpha}{2}h_{ij}\|\Delta x_{ij}\| + \frac{1}{2}\Delta_{ij}^{cbf}, \quad j \in \mathscr{M}_i. \tag{4.54}$$

In addition, thanks to Lemma 4.2, the agent i will not collide with any other agent j, $j \notin \mathscr{M}_i$. Therefore, when considering any agent pair (i,j), $i,j = \mathbf{I}[1,N]$, $i \neq j$, the two agents will remain within a safe distance under the QP controller (4.49). ■

Moreover, in (4.47), the constant β_i is selected with the condition:

$$\beta_i \geqslant \sqrt{2\|y_i\|_k^2 + 300\xi_i \ln^3(\frac{q+1}{\varpi})} \tag{4.55}$$

and

$$\xi_i = \max_{\theta_i, \theta_i' \in \{\theta_{i,1}, \cdots, \theta_{i,q}\}} \frac{1}{2}\log|I + \sigma_0^{-2}\mathrm{K}(\theta_i, \theta_i')|. \tag{4.56}$$

Based on the above conclusions, the proposed GP-CLF-CBF-based QP controller (4.49) can drive the formation control objective of uncertain MAS (4.24) while maintaining safety objective, which is described as follows.

Theorem 4.3. *If taking an appropriate value of α that makes the QP problem* (4.49) *solvable and $\delta_i^* \to 0$ satisfied, then the agent i ($i \in \boldsymbol{I}[1,N]$) can achieve the formation control under the QP controller u_i^* with a probability of $1-\varpi$ at least.*

Proof: Similar to the *Proof of Theorem 4.2*, under the constants β_i and ξ_i defined in (4.55), the GP model error of $\epsilon_i^T d_i$ is bounded with a probability of $1-\varpi$ at least, shown as

$$\mathbb{P}\{\epsilon_i^T d_i \leqslant \mu_i + \beta_i \sigma_i\} \geqslant 1-\varpi. \tag{4.57}$$

Hence, the CLF condition (4.36) of agent i can be rewritten as follows:

$$\epsilon_i^T u_i \leqslant -(\mu_i + \beta_i \sigma_i) - cV_i - \Delta_i^{clf} + \delta_i. \tag{4.58}$$

If taking appropriate value of α that makes $\delta_i^* \to 0$, then the convergence of the Lyapunov function V_i can be obtained under the QP controller u_i^* in (4.49). In other words, there is $v_i \to \hat{v}_i$ as $t \to \infty$. Combined with *Lemma 4.3*, one has $e_i = x_i - x_0 - s_i \to 0$, indicating the realization of the formation tracking control for agent i, $i \in \mathbf{I}[1,N]$. ■

Remark 4.4. *Compared with the conclusions in [142] where GPs estimate the uncertain vector $d_i \in \mathbb{R}^n$, this work directly models the scalar terms $\epsilon_i^T d_i \in \mathbb{R}$ and $\Delta x_{ij}^T d_i \in \mathbb{R}$ in the QP constraints instead. The main difference lies in the dimension of GP models. For the former case, n GP models are needed for each dimension of d_i to construct the QP control method. For the latter case, at most N GP models are required. Given the computational consumption in modeling, the former case is suitable for control problems with fewer agents, and the latter is more suited for high-dimensional control problems.*

If the GP model is used to estimate the uncertainty $d_i = [d_i^{(1)}, \cdots, d_i^{(n)}]^T \in \mathbb{R}^n$, consider the training dataset as $\bar{\mathscr{D}}_i = \{\bar{\theta}_{i,k}, \bar{y}_{i,k}\}_{k=1}^q$ with

$$\begin{aligned} \bar{\theta}_i &= [x_i^T, v_i^T]^T \in \mathbb{R}^{2n}, \\ \bar{y}_i(\bar{\theta}_i) &= (v_i - u_i) + \eta_0 \in \mathbb{R}^n. \end{aligned} \tag{4.59}$$

According to (3.9), the posterior mean and standard derivative for d_i are given as

$$\begin{aligned} \bar{\mu}_i &= [\bar{\mu}_i^{(1)}, \cdots, \bar{\mu}_i^{(n)}]^T \in \mathbb{R}^n, \\ \bar{\sigma}_i &= [\bar{\sigma}_i^{(1)}, \cdots, \bar{\sigma}_i^{(n)}]^T \in \mathbb{R}^n, \end{aligned} \tag{4.60}$$

respectively.

Corollary 4.1. *If* $||x_i(t_0)-x_j(t_0)|| > D_{safe}$ *is satisfied and an appropriate value of* α *is selected, then the collision avoidance for agent pair* (i,j) *can be ensured with a probability of* $(1-\varpi)^{2n}$ *at least under the following QP controller:*

$$
\begin{aligned}
& u_i^* = \mathrm{argmin}_{u_i\in U}\frac{1}{2}u_i^T H u_i + w p_i^2 \\
& s.t. \quad \epsilon_i^T u_i \leqslant -(\epsilon_i^T\bar{\mu}_i + \bar{\beta}_i|\epsilon_i|^T\bar{\sigma}_i) - cV_i - \Delta_i^{clf} + \delta_i \\
& -\Delta x_{ij}^T u_i \leqslant \Delta x_{ij}^T\bar{\mu}_{ij} - \bar{\beta}_i\|\Delta x_{ij}\|^T\bar{\sigma}_i + \frac{\alpha}{2}h_{ij}\|\Delta x_{ij}\| + \frac{1}{2}\Delta_{ij}^{cbf}, j\in\mathscr{M}_i,
\end{aligned}
\tag{4.61}
$$

where

$$
\bar{\beta}_i \geqslant \max_{l=1,\cdots,n}\sqrt{2\|\bar{y}_i^{(l)}\|_k^2 + 300\bar{\xi}_i^{(l)}\ln^3(\frac{q+1}{1-(1-\varpi)^{\frac{1}{n}}})}
\tag{4.62}
$$

and

$$
\bar{\xi}_i^{(l)} = \max_{\bar{\theta}_i,\bar{\theta}_i'\in\{\bar{\theta}_{i,1},\cdots,\bar{\theta}_{i,q}\}}\frac{1}{2}\log|I + (\bar{\sigma}_i^{(l)})^{-2}\mathrm{K}(\bar{\theta}_i,\bar{\theta}_i')|.
\tag{4.63}
$$

Besides, the formation control of uncertain MAS (4.24) can be realized with a probability of $(1-\varpi)^n$ *at least.*

Proof: The proof is similar to that of Theorem 4.2 or Theorem 4.3, so omitted here for space limitation. ■

Remark 4.5. *The proposed control method can also be applied to other cooperative control scenarios of uncertain MASs, such as containment control and destination achieving control. The primary difference lies in the design of the corresponding control Lyapunov functions.*

4.4 Numerical Simulation

Example 4-1: This experiment tests the feasibility of the proposed CBF-based QP control method (4.22) for deterministic MAS (4.7) with four agents.

The control objective is to guide each agent from its initial position $x_i(0) \in \mathbb{R}^2$ to its destination $P_i \in \mathbb{R}^2$ while ensuring collision avoidance. Specifically, we aim to achieve:

$$x_i(t) \to P_i, \quad \text{and} \quad v_i(t) \to \mathbf{0}_2, \quad \text{as} \quad t \to \infty.$$

Denote the state tracking error of agent i $(i = 1,2,3,4)$ as follows:

$$\bar{e}_i(t) = \begin{bmatrix} x_i(t) - P_i \\ v_i \end{bmatrix} \in \mathbb{R}^4.$$

The nominal controller for agent i is given as

$$u_i^{nom}(t) = -k_{i1}(x_i - P_i) - k_{i2} v_i,$$

where k_{i1} and k_{i2} are positive gain parameters. In this example, the control gains are $k_{11} = 1.0$, $k_{12} = 1.0$, $k_{21} = 0.5$, $k_{22} = 1.0$, $k_{31} = 1.0$, $k_{32} = 0.5$, $k_{41} = 1.0$, $k_{12} = 2.0$.

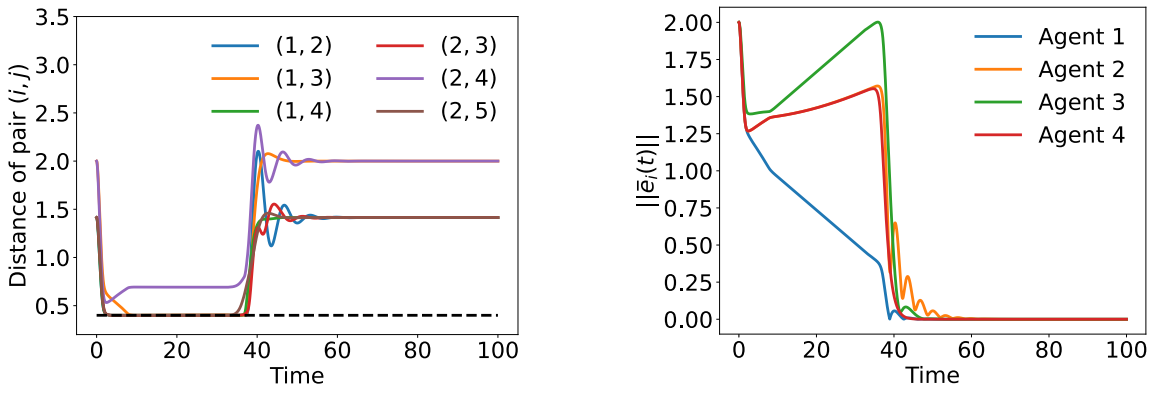

(a) (b)

Figure 4.3: (a) The distance of each pair of agents (i,j); (b) The state tracking error $\|\bar{e}_i(t)\|$ of agent i, $i = 1,2,3,4$.

If there is a risk of collision with nearby agents $j \in \mathcal{M}_i$, the CBF-based QP controller u_i^{qp} obtained from (4.22) is applied. Therefore, the control input of agent i, $i = 1,2,3,4$ is designed as follows:

$$u_i(t) = \begin{cases} u_i^{nom}(t), & \text{if} \quad \mathcal{M}_i = Null \\ u_i^{qp}(t), & \text{if} \quad \mathcal{M}_i \neq Null. \end{cases}$$

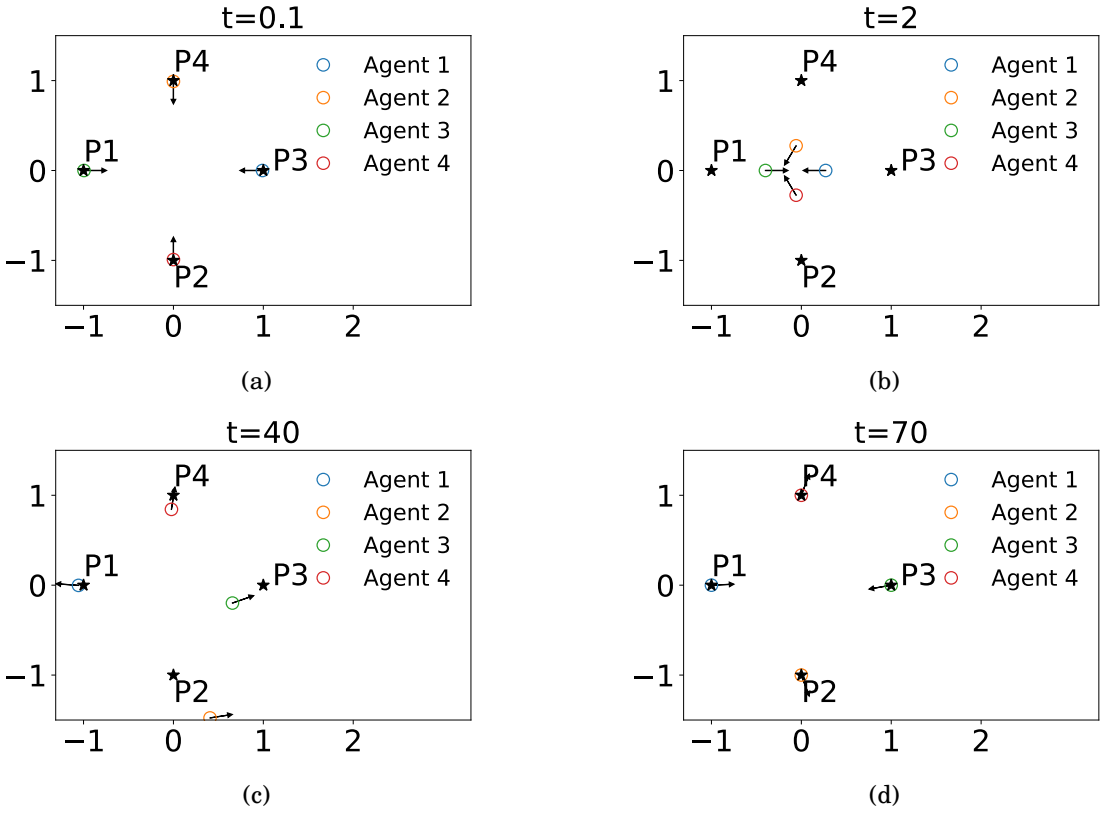

Figure 4.4: The position of each agent at time instant (a) $t = 0.1$; (b) $t = 2$; (c) $t = 40$; (d) $t = 70$.

The initial positions and destination positions of the four agents are specified as follows:

$$[x_1(0), x_2(0), x_3(0), x_4(0)] = [(1,0),(0,1),(-1,0),(0,-1)],$$

$$[P_1, P_2, P_3, P_4] = [(-1,0),(0,-1),(1,0),(0,1)].$$

The initial velocity of each agent is set as zero. Let $b_v = 4.0$ and $b_u = 4$. The safe distance between two agents is $D_{safe} = 0.4$. The CBF parameter $\alpha = 1.0$.

Figure 4.3 (a) shows the distance among agents, indicating the success of collision avoidance. Note that the black dotted line is the safe boundary $D_{safe} = 0.4$. Figure 4.3 (b) depicts the error of each agent, which implies the destination achievement. Moreover, we show the positions of agents in Figure 4.4, where one can see from the final subplot that each agent can reach its destination along time.

Example 4-2: This numerical experiment considers the formation tracking control of uncertain MAS (4.24) with the proposed GP-CLF-CBF-based QP control method (4.41). The communication topology of MAS is shown in Figure 3.3.

Consider $N = 4$ agents whose uncertainty are set as

$$d_i = 0.1\sin(v_i), \quad i = 1,2,3,4.$$

The velocity and acceleration bounds of agents are $b_v = 4$ and $b_u = 4$, respectively. Set the safe distance between any two agents as $D_{safe} = 0.4$. The initial position of agents is

$$x(t_0) = ([1,0],[-1,0],[0,1],[0,-1]),$$

and the formation information is

$$s = ([-1,-1],[-1,1],[-2,-1],[-2,1]).$$

The initial velocity of each agent is zero, and the motion reference information is provided with

$$x_0(t) = 5\sin(\frac{t}{4})$$

whose bound is $b_l = 5$. In (4.27), let $\gamma_1 = 2$ and $\gamma_2 = 6$. Select the hyperparameters $c = 1.0$ and $\alpha = 1.0$. The GP models are updated per $0.1s$, and the parameters β_i and β_{ij} are adopted as 3 to achieve more than 95% confidence level [163]. Take w with a relatively large value, such as $w = 100$, in order to obtain as small δ_i as possible.

Figure 4.5 (a) depicts the formation tracking error of each agent, indicating the achievement of the formation control objective, where (b) shows the positions of each agent at time instant $t = 20$. The distance of each agent pair can be found from Figure 4.6 (a), indicating the success of collision avoidance. Taking the agent pair $(2,3)$ as an example, in Figure 4.6 (b), the solid line represents the actual value of uncertainty $\Delta x_{23}^T d_2$, while the dotted lines indicate the predicted values from the GP models, with

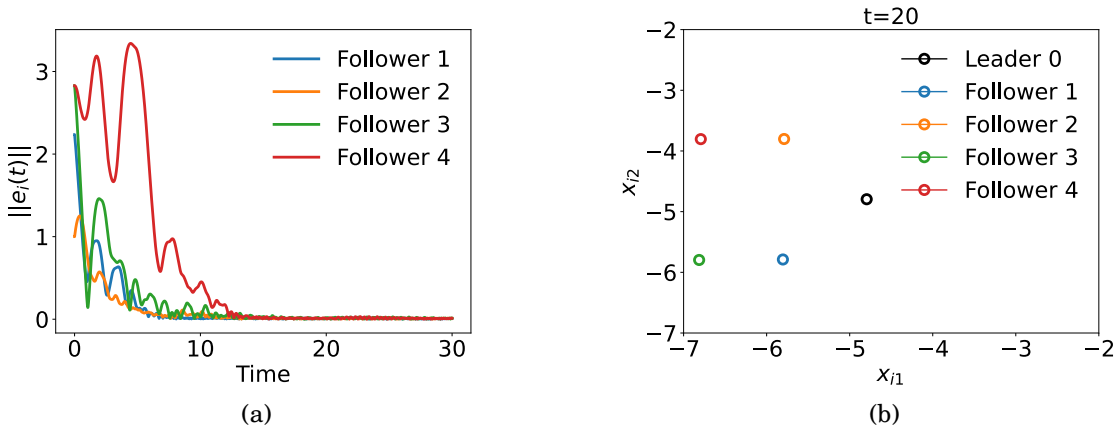

Figure 4.5: (a) The formation tracking error $\|e_i(t)\|$ of agent i, $i = 1,2,3,4$; (b) The position of each agent at time instant $t = 20$.

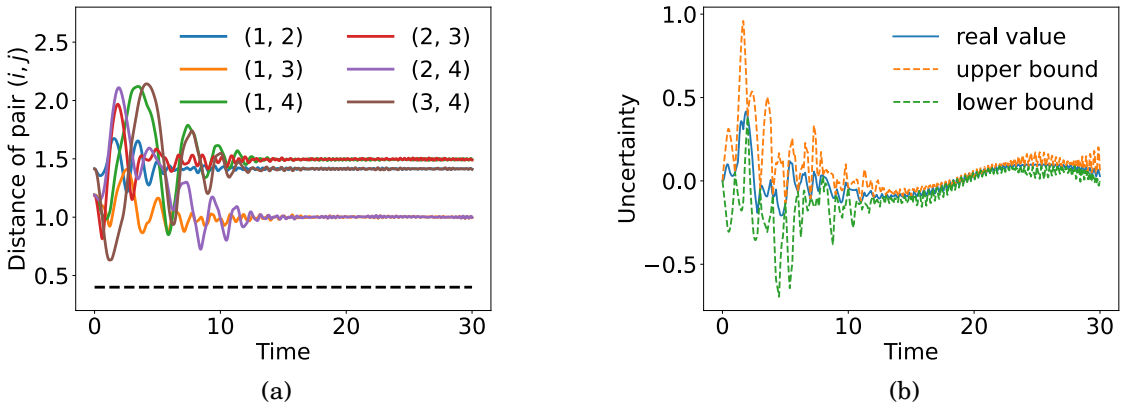

Figure 4.6: (a) The distance of each pair of agents (i,j); (b) The values of uncertainty $\Delta x_{23}^T d_2$.

the upper bound $\mu_{23} + \beta_{23}\sigma_{23}$ and lower bound $\mu_{23} - \beta_{23}\sigma_{23}$. The result illustrates that $|\mu_{ij} - \Delta x_{ij}^T d_i| \leqslant \beta_{ij}\sigma_{ij}$ with high probability, showing the feasibility of GP model for estimating unknown information.

4.5 Conclusion

In this chapter, we investigated safe formation control for MASs by integrating CBF conditions into a QP framework. We first demonstrated the effectiveness of CBF-based QP control in deterministic dynamics. To further address uncertainties, we introduced a GP-CLF-CBF-based QP method, enabling robust safety enforcement under unknown dynamics. This unified and extensible approach offers a practical solution for safe and adaptive control in uncertain MAS environments.

It is worth noting that the CBF used in this chapter, specifically the formulation in (4.9), was adapted from existing literature and represents a valid CBF design for second-order systems. Its key advantage lies in the fact that the first derivative of the barrier function explicitly depends on the control input, making it suitable for use in QP-based control formulations. However, this type of CBF construction typically relies on complex physical model analysis. In practice, such modeling may be difficult, especially when the safety constraints become more intricate or when the physical interpretation is not straightforward.

To address this limitation, we are motivated to explore more intuitive CBF formulations, such as defining a safety function directly in terms of the inter-agent distance, e.g., $h_{ij}(t) = \|x_i(t) - x_j(t)\| - D_{safe}$. While such expressions clearly capture collision avoidance objectives, they are not applicable in second-order systems, as their first derivatives are not affine in the control input. To resolve this issue, the next chapter introduces the concept of high-order control barrier functions, which generalizes the standard CBF

framework for higher-relative-degree systems. In addition, we have observed from the previous two chapters that GP performs well in addressing uncertainties within both CLF and CBF constraints from the perspectives of theoretical analysis and simulation results. Therefore, in the next chapter, we shift our focus to a model-based robustness strategy rather than re-evaluating GP feasibility, to explore an alternative approach for handling system uncertainties.

CHAPTER 5

HIGH-ORDER CBF-BASED QP APPROACH

This chapter revisits the collision avoidance problem in MASs with second-order dynamics. Unlike the previous CBF designs that rely on intricate model-specific construction, this chapter utilizes a straightforward distance-based safety function with relative degree two, offering a more scalable and intuitive formulation. We first consider the deterministic case and propose a HOCBF-based QP controller that guarantees inter-agent safety. Then, this framework is extended to uncertain scenarios. A robust HOCBF formulation is developed to accommodate the uncertainty, ensuring safety with the prior of disturbances. Both theoretical analysis and experimental results demonstrate the feasibility of proposed control methods.

This chapter is based on the academic paper "High-Order Control Barrier Function for Safety in Uncertain Multi-Agent Systems," Preparing to submit.

5.1 Background and Preliminaries

5.1.1 Background

In the previous chapter, the CBF (4.9) is well constructed to ensure compatibility with second-order system dynamics, which requires specific modeling insights and analytical effort. The core motivation of this chapter is to enable the use of intuitive and direct barrier functions, such as $h_{ij}(t) = \|x_i(t) - x_j(t)\| - D_{safe}$, which are easy to define but fail to meet the relative degree condition for second-order or high-order systems. To address this challenge, we employ HOCBFs as an extension of standard CBFs, which enforce forward invariance through high-order derivatives of the barrier function, allowing safety constraints to be encoded for systems with relative degree two or more [105, 176]. Although the concept of HOCBF can be found in the existing literature, our goal is to extend their use to MASs, where the main technical challenge is satisfying the distributed control requirement while managing the increased complexity of continuous derivatives.

In addition to structural generalization, this chapter also presents a robust formulation of HOCBF-based QP control to account for system uncertainties. In previous chapters, GP regression has been employed to estimate unknown dynamics in CLF and CBF constraints, and has proven effective in handling model uncertainty in a probabilistic and data-driven manner. While this approach is suitable when data is available, an alternative path arises when a bound on the uncertainty is known or can be estimated. In this chapter, we shift focus from probabilistic learning-based modeling to model-based robustness. A robust HOCBF-based QP formulation will be developed, incorporating these bounds into the constraints. Although this idea has appeared in earlier literature [177], typically addressing scenarios where disturbances only influence the control input, we extend this formulation to a more general setting in which uncertainties affect the entire system dynamics.

5.1.2 High-order CBF

Attention should be paid to the previous CBF conditions where $L_g h(x) \neq 0$ is required in order to reserve the items containing u. These requirements are satisfied when the function h is of relative degree one, which sometimes may not be applicable in some systems. To deal with this problem, the definition of higher relative degree and its applications are given below.

Definition 5.1. [178] Along with the ACS (3.1), a function $y(x)$ being of relative degree m (m is a positive integer) means that

$$L_g L_f^{m-1} y \neq 0 \quad \text{and} \quad L_g L_f^s y = 0, \quad s = 1, \cdots, m-2 \tag{5.1}$$

where $L_g L_f^s y \triangleq \frac{\partial L_f^{s-1} y}{\partial x} g(x)$ and $L_f^s y \triangleq \frac{\partial L_f^{s-1} y}{\partial x} f(x)$.

As shown in [179], the invariant set for dynamical system is presented by function $h(x) = h_0(x)$. If function $h_0(x)$ is mth-order differentiable, denote the following series of functions:

$$h_s(x) = \dot{h}_{s-1}(x) + \alpha_s h_{s-1}, \quad s = 1, \cdots, m, \tag{5.2}$$

where α_s are positive constants. We further consider a series of sets $\mathscr{C}_s$ with the form:

$$\mathscr{C}_s = \{x \in X | h_s(x) \geqslant 0\}, \quad s = 1, \cdots, m. \tag{5.3}$$

According to the defined $h_s(x)$ in (5.2) and $\mathscr{C}_s$ in (5.3), the definition of high-order control barrier function (HOCBF) is given below.

Definition 5.2. [176] For the ACS (3.1), a function $h(x) : \mathbb{R}^n \to \mathbb{R}$ is a valid HOCBF of relative degree m if there is

$$\sup_{u \in U} [L_f h_{m-1}(x) + L_g h_{m-1}(x) u + \alpha_m h_{m-1}(x)] \geqslant 0. \tag{5.4}$$

5.2 Deterministic Systems

To ensure collision avoidance, the CBF previously introduced in (4.9) was derived based on an analysis of the physical model. However, such a model-dependent approach may not always be feasible in real-world applications due to the presence of unmodeled dynamics. Therefore, in this section, we revisit the second-order MASs discussed earlier and aim to achieve collision avoidance using a more easily constructed function that directly reflects the safety objective.

5.2.1 HOCBF Design

Consider the following second-order MAS dynamics:

$$\begin{cases} \dot{x}_i = v_i \\ \dot{v}_i = u_i, \quad i \in \mathbf{I}[1,N], \end{cases} \tag{5.5}$$

where $x_i, v_i, u_u \in \mathbb{R}^n$ represent the position, velocity and control input of agent i, respectively.

To ensure inter-agent collision avoidance, we define a candidate CBF for the agent pair (i,j) as:

$$h_{ij}(t) = \|x_i(t) - x_j(t)\| - D_{safe}, \quad i \neq j, \tag{5.6}$$

where $D_{safe} > 0$ denotes the prescribed minimum safety distance among agents. Let the relative position and velocity be defined as:

$$\begin{aligned} \Delta x_{ij} &= x_i(t) - x_j(t), \\ \Delta v_{ij} &= v_i(t) - v_j(t), \end{aligned} \tag{5.7}$$

then the time derivative of $h_{ij}(t)$, using the system dynamics (5.5), is:

$$\dot{h}_{ij}(t) = \frac{\Delta x_{ij}^T \Delta v_{ij}}{\|\Delta x_{ij}\|}. \tag{5.8}$$

Note that (5.8) does not depend on the control input, as the relative degree of $h_{ij}(t)$ with respect to the system is 2. Following the HOCBF framework introduced in Section 5.1.2, we define the first and second CBFs as:

$$
\begin{aligned}
&h_{ij}^0(t) = h_{ij}(t) = \|\Delta x_{ij}\| - D_{safe}, \\
&h_{ij}^1(t) = \dot{h}_{ij}^0(t) + \alpha_0 h_{ij}^0(t) = \frac{\Delta x_{ij}^T \Delta v_{ij}}{\|\Delta x_{ij}\|} + \alpha_0(\|\Delta x_{ij}\| - D_{safe}),
\end{aligned} \tag{5.9}
$$

where $\alpha_0 > 0$ is a design parameter. The time derivative of $h_{ij}^1(t)$ along the system dynamics (5.5) yields:

$$
\dot{h}_{ij}^1(t) = \alpha_0 \frac{\Delta x_{ij}^T \Delta v_{ij}}{\|\Delta x_{ij}\|} + \frac{\Delta v_{ij}^T \Delta v_{ij}}{\|\Delta x_{ij}\|} - \frac{(\Delta x_{ij}^T \Delta v_{ij})^2}{\|\Delta x_{ij}\|^3} + \frac{\Delta x_{ij}^T}{\|\Delta x_{ij}\|} \Delta u_{ij}, \tag{5.10}
$$

where $\Delta u_{ij} = u_i(t) - u_j(t)$. By applying the HOCBF condition (5.4) with a positive parameter $\alpha_1 > 0$, we obtain the following safety condition for the agent pair (i, j):

$$
\Delta x_{ij}^T \Delta u_{ij} + \alpha_0 \Delta x_{ij}^T \Delta v_{ij} + \Delta v_{ij}^T \Delta v_{ij} - \frac{(\Delta x_{ij}^T \Delta v_{ij})^2}{\|\Delta x_{ij}\|^2} \geqslant -\alpha_1 \|\Delta x_{ij}\| \left[\frac{\Delta x_{ij}^T \Delta v_{ij}}{\|\Delta x_{ij}\|} + \alpha_0 h_{ij}(t) \right]. \tag{5.11}
$$

This inequality can be rearranged into a more convenient linear form in terms of the control inputs:

$$
\begin{aligned}
-\Delta x_{ij}^T u_i(t) - \Delta x_{ji} u_j(t) \leqslant & \alpha_0 \alpha_1 \|\Delta x_{ij}\| h_{ij}(t) + (\alpha_0 + \alpha_1) \Delta x_{ij}^T \Delta v_{ij} \\
& + \|\Delta v_{ij}\|^2 - \frac{(\Delta x_{ij}^T \Delta v_{ij})^2}{\|\Delta x_{ij}\|^2} \triangleq b_{ij}.
\end{aligned} \tag{5.12}
$$

5.2.2 HOCBF-based QP Controller Design

Analogous to the formulation in (4.12), the HOCBF-based QP controller for agent i, $i \in \mathbf{I}[1, N]$, is defined as:

$$
\begin{aligned}
u_i^* = & \arg\min_{u_i \in U} \frac{1}{2} (u_i - u_i^{nom})^T (u_i - u_i^{nom}) \\
\text{s.t} \quad & -\Delta x_{ij}^T u_i \leqslant \frac{1}{2} b_{ij}, \quad j \neq i,
\end{aligned} \tag{5.13}
$$

where u_i^{nom} is the nominal control input, and b_{ij} is the safety margin defined in (5.12).

Assume that the velocity and acceleration of each agent are bounded such that $\|v_i(t)\| \leqslant b_v$ and $\|u_i(t)\| \leqslant b_u$. With this consideration, we can characterize a set of 'nearby' agents that are relevant for collision avoidance, and exclude distant agents from the constraint set without compromising safety.

Lemma 5.1. *In the MAS described by* (5.5)*, agent i will not collide with any agent j, $j \notin \mathscr{M}_i$ in the near future, regardless of the control input u_i, where*

$$\mathscr{M}_i = \left\{ j \in \boldsymbol{I}[1,N] \middle| \|\Delta x_{ij}\| \leqslant D_{safe} + \frac{2b_v}{\alpha_0}, j \neq i \right\}, \quad i \in \boldsymbol{I}[1,N]. \tag{5.14}$$

Proof: The argument follows similarly to *Lemma* 4.2. Specifically, define

$$D_{near} = D_{safe} + \frac{2b_v}{\alpha_0}. \tag{5.15}$$

For any agent j, $j \notin \mathscr{M}_i$, we have:

$$\dot{h}_{ij}(t) = \dot{D}_{ij} \geqslant -2b_v \geqslant -\alpha_0(D_{near} - D_{safe}) \geqslant -\alpha_0(\|\Delta x_{ij}\| - D_{safe}) = -\alpha_0 h_{ij}(t), \tag{5.16}$$

which implies that the HOCBF condition is satisfied, and hence the safety of agent i and j is guaranteed in the short term regardless of the control input. ■

Based on this observation, the HOCBF-based QP controller for agent i ($i \in \mathbf{I}[1,N]$) can be refined to only consider the relevant nearby agents:

$$\begin{aligned} u_i^* = \underset{u_i \in U}{\arg\min} \frac{1}{2}(u_i - u_i^{nom})^T(u_i - u_i^{nom}) \\ \text{s.t} \quad -\Delta x_{ij}^T u_i \leqslant \frac{1}{2} b_{ij}, \quad j \in \mathscr{M}_i. \end{aligned} \tag{5.17}$$

Theorem 5.1. *Collision avoidance for the second-order MAS* (5.5) *is guaranteed under the control input u_i^* obtained from the HOCBF-based QP problem* (5.17)*.*

Proof: The result follows directly from (4.4) and *Lemma 5.1*. ■

Remark 5.1. *This section demonstrates that high-order dynamical systems can be handled without requiring a meticulously designed, model-specific CBF. Instead, the CBF*

defined in (5.6) *offers a direct and intuitive encoding of the collision avoidance objective. As shown in Theorem 5.1, satisfying the HOCBF constraints ensures safety, highlighting the practicality and generality of the proposed approach.*

5.3 Uncertain Systems

In this section, we extend the previously proposed HOCBF approach to address the uncertain MASs.

5.3.1 Robust HOCBF Design

Consider the following uncertain MASs characterized by second-order dynamics:

$$\begin{cases} \dot{x}_i = v_i + d_{v_i} \\ \dot{v}_i = u_i + d_{u_i}, \quad i \in \mathbf{I}[1,N], \end{cases} \tag{5.18}$$

where d_{v_i} and d_{u_i} represent bounded uncertainties satisfying $\|d_{v_i}\|_\infty \leqslant \bar{b}_v$ and $\|d_{u_i}\|_\infty \leqslant \bar{b}_u$, with $\bar{b}_v > 0$ and $\bar{b}_u > 0$.

To ensure safe inter-agent distances, we adopt the direct CBF defined as $h_{ij}(t) = \|x_i(t) - x_j(t)\| - D_{safe}$ for each agent pair (i,j). The time derivative of $h_{ij}(t)$ along the dynamics in (5.18) is given by

$$\dot{h}_{ij}(t) = \frac{\Delta x_{ij}^T}{\|\Delta x_{ij}\|}\left(\Delta v_{ij} + \Delta d_{v_{ij}}\right), \tag{5.19}$$

where Δx_{ij}^T and Δv_{ij} are defined in (5.7), and $\Delta d_{v_{ij}} = d_{v_i} - d_{v_j}$. We define the high-order CBF as:

$$\begin{aligned} &h_{ij}^0(t) = h_{ij}(t) = \|\Delta x_{ij}\| - D_{safe}, \\ &h_{ij}^1(t) = \dot{h}_{ij}^0(t) + \alpha_0 h_{ij}^0(t) = \frac{\Delta x_{ij}^T(\Delta v_{ij} + \Delta d_{v_{ij}})}{\|\Delta x_{ij}\|} + \alpha_0(\|\Delta x_{ij}\| - D_{safe}), \end{aligned} \tag{5.20}$$

where $\alpha_0 > 0$ is a design parameter. To ensure robustness against uncertainties, we introduce a conservative lower bound:

$$\bar{h}_{ij}^1 = \frac{\Delta x_{ij}^T \Delta v_{ij}}{\|\Delta x_{ij}\|} + \alpha_0(\|\Delta x_{ij}\| - D_{safe}) - 2\sqrt{n}\,\bar{b}_v, \tag{5.21}$$

where n denotes the dimension of the state vector x_i. Note that

$$\frac{\Delta x_{ij}^T \Delta d_{v_{ij}}}{\|\Delta x_{ij}\|} \geqslant -\left\| \frac{\Delta x_{ij}}{\|\Delta x_{ij}\|} \right\|_1 \cdot \|\Delta d_{v_{ij}}\|_\infty \geqslant -\sqrt{n} \left\| \frac{\Delta x_{ij}}{\|\Delta x_{ij}\|} \right\|_2 \cdot (\|d_{v_i}\|_\infty + \|d_{v_j}\|_\infty) \geqslant -2\sqrt{n}\,\bar{b}_v. \tag{5.22}$$

Therefore, we obtain the inequality:

$$\begin{aligned} h_{ij}^1 &= \frac{\Delta x_{ij}^T \Delta v_{ij}}{\|\Delta x_{ij}\|} + \frac{\Delta x_{ij}^T \Delta d_{v_{ij}}}{\|\Delta x_{ij}\|} + \alpha_0(\|\Delta x_{ij}\| - D_{safe}) \\ &\geqslant \frac{\Delta x_{ij}^T \Delta v_{ij}}{\|\Delta x_{ij}\|} - 2\sqrt{n}\,\bar{b}_v + \alpha_0(\|\Delta x_{ij}\| - D_{safe}) = \bar{h}_{ij}^1, \end{aligned} \tag{5.23}$$

which implies that satisfying $\bar{h}_{ij}^1 \geqslant 0$ guarantees $h_{ij}^1 \geqslant 0$, thereby ensuring forward invariance of the safe set.

Next, we compute the time derivative of $\bar{h}_{ij}^1(t)$ under the system dynamics (5.18):

$$\begin{aligned} \dot{\bar{h}}_{ij}^1(t) =& \alpha_0 \frac{\Delta x_{ij}^T(\Delta v_{ij} + \Delta d_{v_{ij}})}{\|\Delta x_{ij}\|} + \frac{\Delta v_{ij}^T(\Delta v_{ij} + \Delta d_{v_{ij}})}{\|\Delta x_{ij}\|} \\ & - \frac{(\Delta x_{ij}^T \Delta v_{ij})[\Delta x_{ij}^T(\Delta v_{ij} + \Delta d_{v_{ij}})]}{\|\Delta x_{ij}\|^3} + \frac{\Delta x_{ij}^T}{\|\Delta x_{ij}\|}(\Delta u_{ij} + \Delta d_{u_{ij}}), \end{aligned} \tag{5.24}$$

where $\Delta u_{ij} = u_i - u_j$ and $\Delta d_{u_{ij}} = d_{u_i} - d_{u_j}$. Accordingly, the CBF condition for the agent pair (i, j) becomes:

$$\dot{\bar{h}}_{ij}^1 \geqslant -\alpha_1 \bar{h}_{ij}^1 = -\alpha_1 \left[\frac{\Delta x_{ij}^T \Delta v_{ij}}{\|\Delta x_{ij}\|} + \alpha_0(\|\Delta x_{ij}\| - D_{safe}) - 2\sqrt{n}\,\bar{b}_v \right], \tag{5.25}$$

where α_1 is a user-defined constant.

5.3.2 Robust HOCBF-based QP Controller Design

Note that the original HOCBF condition in (5.25) is not valid due to the presence of the uncertain terms $\Delta d_{v_{ij}}$ and $\Delta d_{u_{ij}}$. To address this issue, similar to the result in (5.22), we

derive the following bounds:

$$\frac{\Delta x_{ij}^T \Delta d_{u_{ij}}}{\|\Delta x_{ij}\|} \geqslant -\left\| \frac{\Delta x_{ij}}{\|\Delta x_{ij}\|} \right\|_1 \cdot \|\Delta d_{u_{ij}}\|_\infty \geqslant -2\sqrt{n}\bar{b}_u, \tag{5.26}$$

and

$$\begin{aligned}
&\frac{\Delta v_{ij}^T \Delta d_{v_{ij}}}{\|\Delta x_{ij}\|} - \frac{(\Delta x_{ij}^T \Delta v_{ij})(\Delta x_{ij}^T \Delta d_{v_{ij}})}{\|\Delta x_{ij}\|^3} \\
\geqslant& -\left\| \frac{\Delta v_{ij}}{\|\Delta x_{ij}\|} - \frac{\Delta x_{ij}^T \Delta v_{ij} \Delta x_{ij}}{\|\Delta x_{ij}\|^3} \right\|_1 \cdot \|\Delta d_{v_{ij}}\|_\infty \\
=& -\frac{1}{\|\Delta x_{ij}\|} \left\| \Delta v_{ij} - \frac{\Delta x_{ij}^T \Delta v_{ij} \Delta x_{ij}}{\|\Delta x_{ij}\|^2} \right\|_1 \cdot \|\Delta d_{v_{ij}}\|_\infty \\
\geqslant& -\frac{\sqrt{n}}{\|\Delta x_{ij}\|} \left\| \Delta v_{ij} - \frac{\Delta x_{ij}^T \Delta v_{ij} \Delta x_{ij}}{\|\Delta x_{ij}\|^2} \right\|_2 \cdot \|\Delta d_{v_{ij}}\|_\infty \\
=& -\frac{2\sqrt{n}\bar{b}_v}{\|\Delta x_{ij}\|} \sqrt{\|\Delta v_{ij}\|^2 - \frac{(\Delta x_{ij}^T \Delta v_{ij})^2}{\|\Delta x_{ij}\|^2}}.
\end{aligned} \tag{5.27}$$

Substituting (5.22), (5.24), (5.26) and (5.27) into (5.25) yields the following condition for the agent pair (i, j):

$$\begin{aligned}
&\Delta x_{ij}^T \Delta u_{ij} + \alpha_0 \Delta x_{ij}^T \Delta v_{ij} + \Delta v_{ij}^T \Delta v_{ij} - \frac{(\Delta x_{ij}^T \Delta v_{ij})^2}{\|\Delta x_{ij}\|^2} \\
&- 2\sqrt{n}\bar{b}_u \|\Delta x_{ij}\| - 2\alpha_0 \sqrt{n}\bar{b}_v \|\Delta x_{ij}\| - 2\sqrt{n}\bar{b}_v \sqrt{\|\Delta v_{ij}\|^2 - \frac{(\Delta x_{ij}^T \Delta v_{ij})^2}{\|\Delta x_{ij}\|^2}} \\
&\geqslant -\alpha_1 \|\Delta x_{ij}\| \left[\frac{\Delta x_{ij}^T \Delta v_{ij}}{\|\Delta x_{ij}\|} + \alpha_0 (\|\Delta x_{ij}\| - D_{safe}) - 2\sqrt{n}\bar{b}_v \right],
\end{aligned} \tag{5.28}$$

which can be rewritten as:

$$-\Delta x_{ij}^T u_i(t) - \Delta x_{ji} u_j(t) \leqslant b_{ij} - \bar{b}_{ij}, \tag{5.29}$$

where b_{ij} is defined as in (5.12), and the robust compensation term $\bar{b}_{ij}$ is given by:

$$\bar{b}_{ij} = 2\sqrt{n}(\bar{b}_u + \alpha_0 \bar{b}_v + \alpha_1 \bar{b}_v)\|\Delta x_{ij}\| + 2\sqrt{n}\bar{b}_v \sqrt{\|\Delta v_{ij}\|^2 - \frac{(\Delta x_{ij}^T \Delta v_{ij})^2}{\|\Delta x_{ij}\|^2}}. \tag{5.30}$$

Based on the above derivation, the HOCBF-based QP controller for agent i, $i \in \mathbf{I}[1,N]$ is formulated as:

$$\begin{aligned} u_i^* &= \underset{u_i \in U}{\arg\min} \frac{1}{2}(u_i - u_i^{nom})^T(u_i - u_i^{nom}) \\ \text{s.t} \quad & -\Delta x_{ij}^T u_i \leqslant \frac{1}{2}(b_{ij} - \bar{b}_{ij}), \quad j \neq i. \end{aligned} \tag{5.31}$$

We now generalize the concept of 'nearby' agents to account for system uncertainty.

Lemma 5.2. *In the uncertain MAS described by* (5.18)*, agent i will not collide with any agent j, $j \notin \bar{\mathscr{M}}_i$ in the near future, regardless of the control input u_i, where*

$$\bar{\mathscr{M}}_i = \left\{ j \in \boldsymbol{I}[1,N] \middle| \|\Delta x_{ij}\| \leqslant D_{safe} + \frac{2(b_v + \bar{b}_v)}{\alpha_0}, j \neq i \right\}, \quad i \in \boldsymbol{I}[1,N]. \tag{5.32}$$

Proof: The proof is similar to that of *Lemma* 5.1 and is omitted here. ■

Accordingly, the robust HOCBF-based QP controller for agent i ($i \in \mathbf{I}[1,N]$) is updated as follows:

$$\begin{aligned} u_i^* &= \underset{u_i \in U}{\arg\min} \frac{1}{2}(u_i - u_i^{nom})^T(u_i - u_i^{nom}) \\ \text{s.t} \quad & -\Delta x_{ij}^T u_i \leqslant \frac{1}{2}(b_{ij} - \bar{b}_{ij}), \quad j \in \bar{\mathscr{M}}_i. \end{aligned} \tag{5.33}$$

Theorem 5.2. *Under the control input u_i^* obtained by solving the HOCBF-based QP in* (5.33)*, collision avoidance is guaranteed for the uncertain second-order MAS* (5.18)*.*

Proof: This result directly follows from (4.4) and *Lemma 5.2*. ■

Remark 5.2. *In this section, the proposed robust HOCBF method offers a practical alternative for handling safety in uncertain MASs. Compared with learning-based approaches such as those relying on GPs in Chapter 4, the robust HOCBF avoids the need for model learning, thereby reducing computational overhead and simplifying real-time implementation. However, this benefit comes at the cost of increased conservativeness, as the worst-case disturbance is considered in the safety constraint design, which may lead to overly cautious behavior.*

5.4 Numerical Simulation

Example 5-1: We consider the formation tracking control of the deterministic MAS (5.5) in this experiment, where the communication topology is the same as that in Figure 3.3. The control objective is to realize formation tracking while the leader moves towards its destination x_d. The formation shape is defined as s_i for follower i ($i = 1,2,3,4$). We aim to ensure that as $t \to \infty$, there is

$$x_0(t) \to x_d, \quad v_0(t) \to \mathbf{0}_2;$$

$$x_i(t) - x_0(t) - s_i \to \mathbf{0}_2, \quad v_i(t) \to v_0(t), \quad i = 1,2,3,4.$$

The nominal control inputs for leader 0 and follower i ($i = 1,2,3,4$) are, respectively, taken as:

$$u_0^{nom} = -k_1(x_0 - x_d) - k_2 v_0;$$

$$u_i^{nom} = -k_3 \left[\sum_{j=1}^{4} a_{ij}((x_i - s_i) - (x_j - s_j)) + a_{i0}(x_i - x_0 - s_i) \right] - k_4 \left[\sum_{j=1}^{4} a_{ij}(v_i - v_j) + a_{i0}(v_i - v_0) \right],$$

where a_{ij} represents the element of the adjacency matrix of the communication topology, and $a_{i0} = 1$ if follower i receives information from the leader, and $a_{i0} = 0$ otherwise. The gain parameters are $k_1 = 1, k_2 = 0.5, k = 1, k_4 = 1$. The initial positions of followers are

$$[x_1(0), x_2(0), x_3(0), x_4(0)] = [(-2,0),(-2.5,0),(-3,0),(-3.5,0)]$$

and the formation shape is described as follows:

$$[s_1, s_2, s_3, s_4] = [(-1,-1),(-1,1),(-2,-1),(-2,1)].$$

The leader's initial position is $x_0(0) = (-1.5,0)$, and destination is $x_d = (5,0)$. Initially, all agents have zero velocity. The parameter values are set as $b_v = 6$, $b_u = 6$, $\alpha_0 = 1$ and $\alpha_1 = 1$.

Under the HOCBF-based QP controller solved from (5.17), Figure 5.1 (a) illustrates the distances between multiple agents, revealing that safety is not successfully ensured.

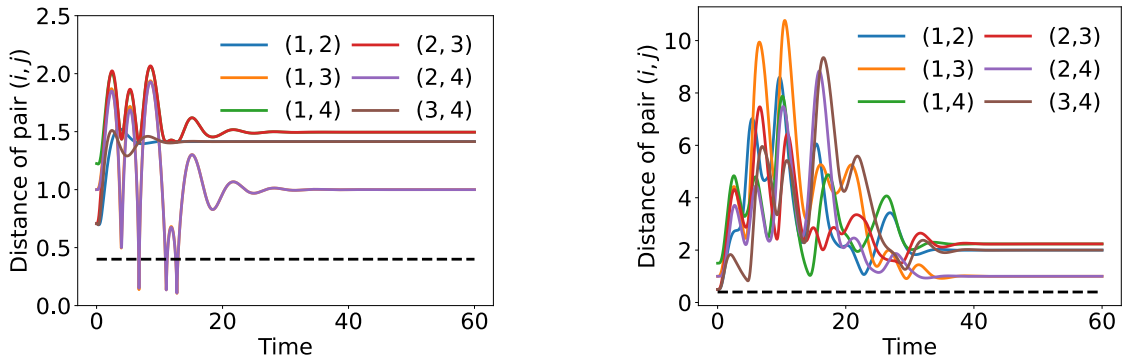

(a) (b)

Figure 5.1: (a) The distance of each pair of agents (i,j) under the nominal control inputs u_0^{nom} and u_i^{nom}; (b) The distance of each pair of agents (i,j) under the HOCBF-based QP controller (5.17).

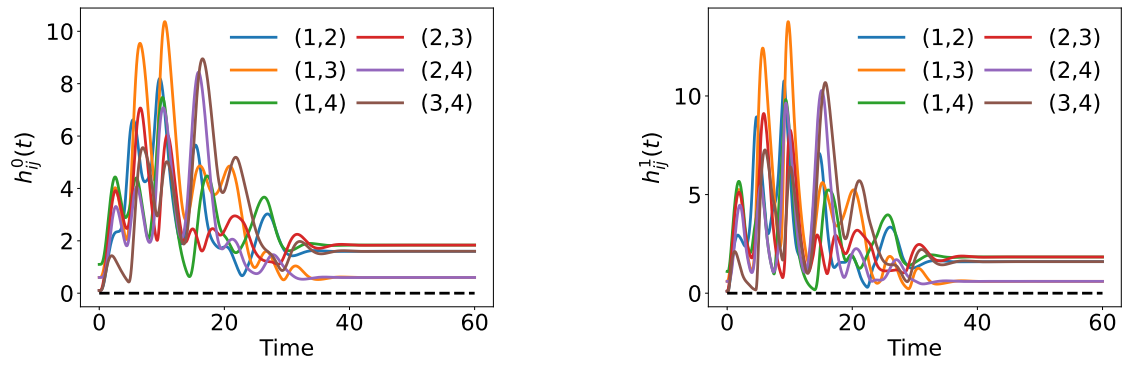

(a) (b)

Figure 5.2: (a) The first-order CBF $h_{ij}^0(t)$; (b) The second-order CBF $h_{ij}^1(t)$.

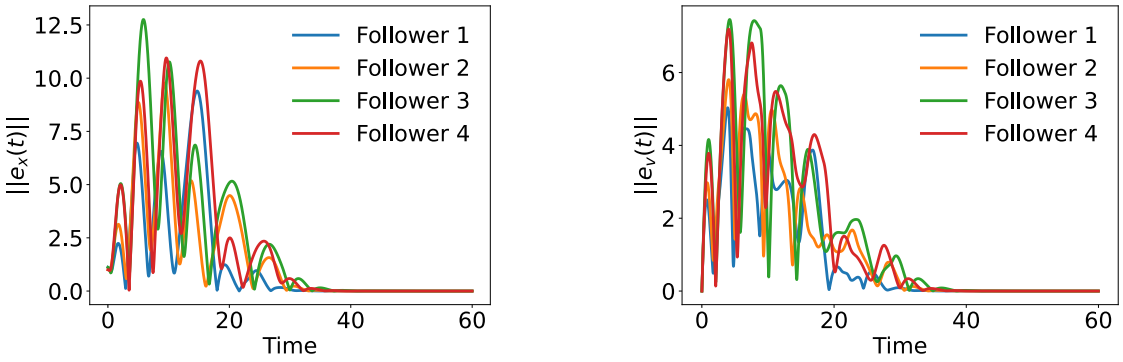

(a) (b)

Figure 5.3: (a) The formation tracking error $\|e_x(t)\|$; (b) The velocity tracking error $\|e_v(t)\|$.

However, when the proposed HOCBF-based QP controller (5.17) is applied, Figure 5.1 (b) shows that the agents maintain a safe distance, ensuring collision avoidance.

Furthermore, Figure 5.2 depicts both the first-order CBF $h^0_{ij}(t)$ and the second-order CBF $h^1_{ij}(t)$ for each agent pair (i,j), demonstrating that both remain non-negative throughout the control process. Additionally, the state tracking error $e_x(t) = x_i(t) - x_0(t) - s_i$ and velocity tracking error $e_v(t) = v_i(t) - v_0(t)$ of each follower, presented in Figure 5.3, confirm the successful achievement of the formation tracking control objective.

Example 5-2: To further validate the robust HOCBF approach, we consider the formation tracking control task for the uncertain MAS described by (5.18), with a state dimension of $n = 2$. The MAS consists of one active leader with time-varying velocity $v_0(t) = 0.5\sin(x_0(t))$, and four followers connected through the communication topology illustrated in Figure 3.3. The nominal controller for follower i, $i = 1,2,3,4$ is designed as follows:

$$u_i^{nom} = -(x_i - \hat{x}_i - s_i) - (v_i - \hat{v}_i), \tag{5.34}$$

where $\hat{x}_i$ and $\hat{v}_i$ denote the local estimates of the leader's position x_0 and velocity v_0, respectively. These estimates are generated by distributed observers governed by the

following dynamics:

$$\begin{cases} \dot{\hat{x}}_i = \hat{v}_i - \left[\sum_{j=1}^{4} a_{ij}(\hat{x}_i - \hat{x}_j) + a_{i0}(\hat{x}_i - x_0)\right] \\ \dot{\hat{v}}_i = -\left[\sum_{j=1}^{4} a_{ij}(\hat{v}_i - \hat{v}_j) + a_{i0}(\hat{v}_i - v_0)\right], \quad i \in \mathbf{I}[1,N]. \end{cases}$$

The bounds of uncertainty are set as $\bar{b}_v = 0.1$ and $\bar{b}_u = 0.1$. All other parameters and initial conditions are kept consistent with those in *Example 5-1*.

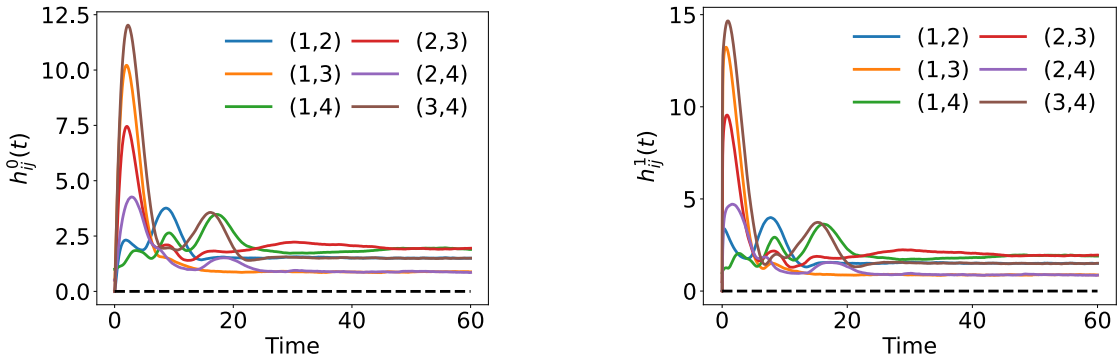

(a) (b)

Figure 5.4: (a) The first-order CBF $h_{ij}^0(t)$; (b) The second-order CBF $h_{ij}^1(t)$.

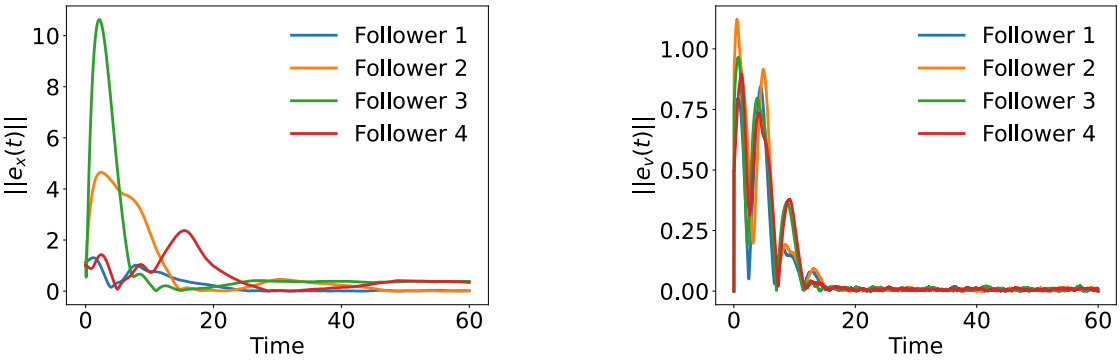

(a) (b)

Figure 5.5: (a) The formation tracking error $\|e_x(t)\|$; (b) The velocity tracking error $\|e_v(t)\|$.

Under the robust HOCBF-based QP controller derived from (5.33), Figure 5.4 illustrates the evolution of both the first-order CBF $h_{ij}^0(t)$ and the second-order CBF $h_{ij}^1(t)$ for

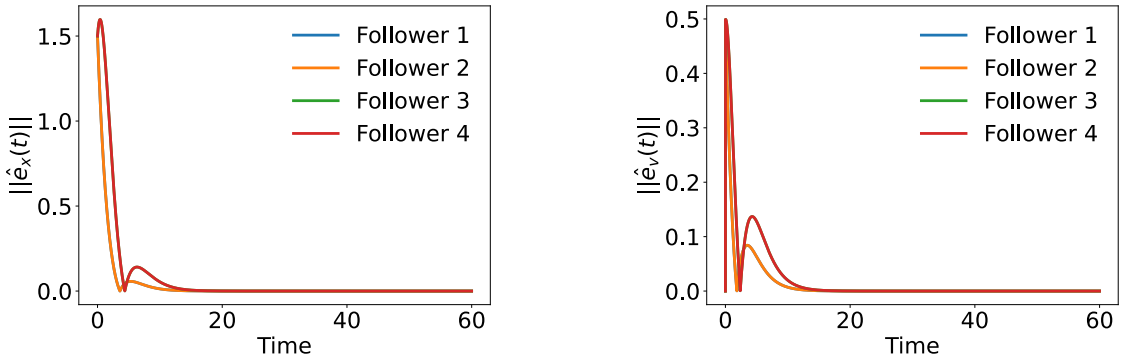

(a) (b)

Figure 5.6: (a) The state estimation error $\|\hat{e}_x(t)\|$; (b) The velocity estimation error $\|\hat{e}_v(t)\|$.

each agent pair (i, j), demonstrating that collision avoidance is consistently maintained. The state tracking error, defined as $e_x(t) = x_i(t) - x_0(t) - s_i$, and the velocity tracking error $e_v(t) = v_i(t) - v_0(t)$ for each follower are shown in Figure 5.5, verifying the achievement of the formation tracking control objective. Slight oscillations are caused by uncertainty at the end of the control process. Furthermore, Figure 5.6 presents the estimation errors $\hat{e}_x = \hat{x}_i - x_0$ and $\hat{e}_v = \hat{v}_i - v_0$, which further clarify the distributed observer design.

5.5 Conclusion

In this chapter, we introduced HOCBFs to enable the use of intuitive, distance-based safety functions in second-order MASs. This approach eliminates the need for complex CBF designs while ensuring the feasibility of safety constraints within a QP framework. Furthermore, we proposed a robust extension of the HOCBF-based QP method, extending its applicability to systems affected by dynamic uncertainties. The resulting framework provides an effective solution for safe control in uncertain MAS environments.

Through the previous three chapters, we have investigated the cooperative control of MASs from three aspects, stability, safety and robustness, by constructing a unified QP

framework that integrates CLF, CBF and uncertainty modeling techniques. While the proposed methods achieve the desired control objectives, our experimental results reveal noticeable differences in control performance. For instance, by comparing the safety results in Figure 4.3 (a) and Figure 4.6 (b), we observe that although both trajectories successfully avoid collisions, the minimum inter-agent distances and their proximity to the predefined safety boundary differ. Specifically, the result in Figure 4.6 (b) demonstrates a more conservative behavior, maintaining a larger buffer zone. While such behavior ensures reliability and tolerance to the effects of uncertainty, it may lead to suboptimal performance in terms of path efficiency or control effort.

In our view, less conservative control behavior is often preferable, as it allows agents to accomplish tasks such as obstacle avoidance with minimal deviation. Performance can also be evaluated from a stability perspective, for example through convergence time, steady-state error, or Lyapunov function decay rates. Motivated by these observations, the next chapter shifts focus to the system-level performance of MASs. We aim to formalize performance evaluation criteria and develop methods to improve control performance without sacrificing control objectives.

CHAPTER 6

HYPERPARAMETER OPTIMIZATION IN SAFE MASS

It is crucial to study the control performance of MASs to balance the control objectives with control efforts. This chapter will demonstrate that the control performance index is closely related to the hyperparameters in the QP control framework, and the Bayesian optimization algorithm is used to optimize and improve performance. First, based on the developed safe control approach, a performance enhancement framework is established to optimize the performance index. Hyperparameters are then explored and categorized, introducing the concept of feasible hyperparameters to describe the attainability of control objectives. Subsequently, the CBO algorithm is employed to identify a set of feasible and optimal hyperparameters in a data-driven manner, even when the functional expressions of performance and constraints are unknown. Finally, experiments are conducted to demonstrate the feasibility of the proposed CBF-CBO algorithm in MASs.

This chapter is based on the academic paper "Safe Control Framework of Multi-Agent Systems From a Performance Enhancement Perspective," in IEEE Transactions on Automation Science and Engineering, 2024. DOI: 10.1109/TASE.2024.3466791.

6.1 Background and Preliminaries

6.1.1 Background

In the preceding chapters, we have developed a control framework for MASs by integrating stability, safety and robustness through a unified QP formulation. While these foundational properties are essential, they do not fully capture the efficiency or effectiveness of the control strategy from a performance perspective. Our simulation results have revealed that their performance varies depending on system configurations and design choices. A closer examination of these results suggests that control performance is sensitive to certain hyperparameters. Motivated by these observations, this chapter aims to investigate the relationship between control performance and hyperparameter selection. We begin by identifying and classifying the key hyperparameters in our QP framework. These hyperparameters are often manually tuned , but they play a crucial role in balancing safety, efficiency, and convergence. To systematically improve performance, we propose treating the performance optimization task as a constrained black-box optimization problem, where the objective is to minimize a performance-related cost subject to safety and stability constraints derived from the control framework.

However, optimizing such black-box functions under constraints, especially when the constraints are defined implicitly by controller feasibility or safety criteria, is a non-trivial challenge. To this end, we adopt a CBO algorithm, a data-efficient and model-free approach well-suited for optimizing expensive or non-analytic functions. We tailor the CBO framework to the context of MAS control by encoding stability and safety constraints, while using performance metrics such as LQR cost as black-box objectives. Through this approach, we are able to automatically tune hyperparameters in a principled and constraint-aware manner, leading to performance improvements without violating safety or stability requirements.

6.1.2 Bayesian Optimization

In this subsection, we will introduce some basic knowledge of Bayesian optimization (BO) algorithm.

Suppose that there is an unknown function $y(\theta)$, $\theta \in \Theta$, and we aim to solve the following optimization problem:

$$\theta^* = \arg\min_{\theta\in\Theta} y(\theta). \tag{6.1}$$

To address this problem, BO is a potential approach that solely requires the input and output dataset instead of the analytic form of y. The essence of BO is to explore the space Θ iteratively to find the optimal solution. The next search point θ_{p+1} is generated through an acquisition function that balances the exploitation of predicted optimum and exploration of unexplored regions. Common acquisition functions include upper confidence bound, entropy search, and expected improvement (EI) [180], *etc*. EI is introduced and used in this section[1].

Based on the dataset $\mathscr{D} = \{\theta_k, y(\theta_k)\}_{k=1}^p$, the current optimum is

$$y_p^* = \min_{k=1,\cdots,p} y(\theta_k). \tag{6.2}$$

Then, EI measures the expected improvement of candidate θ, which is formulated as follows:

$$\mathrm{EI}(\theta|y_p^*) = \mathbb{E}[\max(y_p^* - \hat{y}(\theta), 0)]. \tag{6.3}$$

Here, $\hat{y}(\theta)$ is a surrogate function of unknown $y(\theta)$. Therefore, the next search point determined by EI is

$$\theta_{p+1} = \arg\max_{\theta\in\Theta} \mathrm{EI}(\theta|y_p^*). \tag{6.4}$$

[1]In this chapter, EI is used also because its extension, constraint-weighted EI, is a proven acquisition function in the CBO algorithm.

Remark 6.1. *The surrogate function $\hat{y}(\theta)$ is usually obtained by Gaussian process regression, which is calculated with the mean $\mu(\theta|\mathscr{D})$ and variance $\sigma^2(\theta|\mathscr{D})$ shown as in* (3.9)*. Then (6.3) can be obtained as*

$$\mathrm{EI}(\theta|y_p^*) = \sigma(\theta)[z(\theta)\Phi(z(\theta)) + \phi(z(\theta))],$$

where

$$z(\theta) = \frac{\mu(\theta) - y_p^*}{\sigma(\theta)},$$

$\phi(\cdot)$ is the probability density function, and $\Phi(\cdot)$ is the cumulative distribution function [181].

6.2 Hyperparameter VS Performance

6.2.1 Hyperparameter Analysis

According to the analysis in previous chapter, the solvability of the QP problems requires further investigation. Existing research [116] has shown that the value of α in the CBF constraint influences the minimum distance between the system states and the boundary of set $\mathscr{C}$. Hence, it is reasonable to guess that the CBF-based QP solution is relevant to the values of hyperparameters. For further analysis, we detail the hyperparameters in the QP problems and categorize them into the following two groups:

- **Control hyperparameters** refer to the parameters used in the nominal controller u_i^{nom} to achieve system stability. For instance, gain parameters in the state-feedback controllers serve as hyperparameters, and the communication topology of MASs is considered a kind of control hyperparameter [182]. In the implicit approach, the parameter in the CLF condition c that indicates convergence rate is categorized as a control hyperparameter.

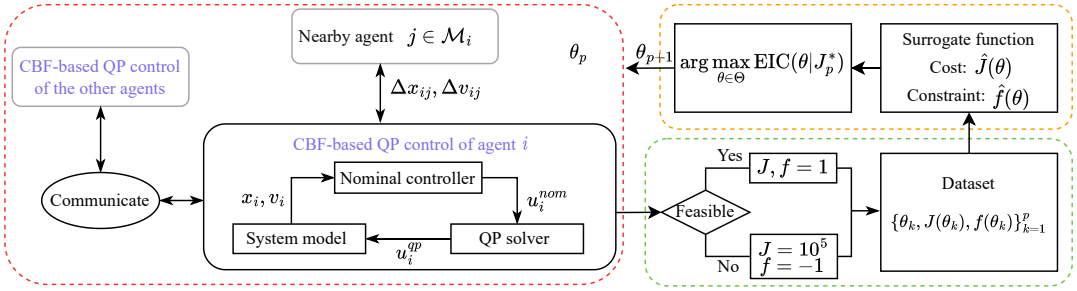

Figure 6.1: An overview of CBF-CBO-based performance enhancement for MASs.

- **Safety hyperparameters** refer to the parameters used in the CBF constraint to ensure system safety. The constant α in is a basic example. Furthermore, in a multiple agents environment, there may be multiple CBF constraints in the QP formulation. Hence, the slack variables for multiple CBFs are also considered safety hyperparameters [183]. Similarly, if exponential CBFs are used for high relative-degree safety constraints, the safety parameters will include more than one hyperparameter to be optimized [105].

Note that the safety objective is ensured under the control input solved from the CBF-based QP problem. We define a set of hyperparameters θ as *feasible* for MASs if they render the QP problems solvable and allow the control objective to be achieved under the resulting QP controller. We aim to find the feasible hyperparameters that can also optimize control performance.

In the following, we will illustrate the relationship between the performance of MASs and the hyperparameters in the QP formulation. Following this, we introduce the constrained Bayesian optimization (CBO) algorithm to search for improved hyperparameters. An overview of the CBF-CBO-based performance enhancement approach for MASs can be found from Figure 6.1.

6.2.2 Control Performance

The performance of control systems can typically be described using the system states, control input, and convergence rate or time. As discussed in Section 2.4.1, the linear quadratic regulator (LQR) is a commonly used performance index that combines quadratic terms of states and control variables. This index is here for clarity. Specifically, define $\eta_i = [x_i^T, v_i^T]^T \in \mathbb{R}^{2n}$ for agent i ($i \in \mathbf{I}[1,N]$). Denote

$$\bar{x} = [\eta_1^T, \cdots, \eta_N^T]^T \in \mathbb{R}^{2nN}, \quad \text{and} \quad \bar{u} = [u_1^T, \cdots, u_N^T]^T \in \mathbb{R}^{nN}. \tag{6.5}$$

To describe the performance of the control process, the LQR cost is formulated as follows:

$$J(\bar{x}, \bar{u}) = \int_0^\infty (\bar{x}^T Q \bar{x} + \bar{u}^T R \bar{u}) \mathrm{d}t, \tag{6.6}$$

where $Q \in \mathbb{R}^{2nN \times 2nN}$ and $R \in \mathbb{R}^{nN \times nN}$ are positive matrices.

Minimizing the LQR cost (6.6) is a meaningful problem from an optimization perspective. While the value of $J(\bar{x}, \bar{u})$ seems to depend on $\bar{x}$ and $\bar{u}$, it ultimately varies from the gain parameters used to determine the control inputs. For clarity, let θ denote the hyperparameters in the QP formulation (4.22). The performance optimization problem is expressed below:

$$\theta^* = \arg\min_{\theta \in \Theta} J(\bar{x}, \bar{u}, \theta), \tag{6.7}$$

where Θ represents the range of hyperparameters θ. An illustrative example is given to demonstrate the impact of hyperparameters on system control performance.

Example 6-1: For the MAS (4.7) with four agents, firstly we focus on the control objective, aiming to ensure that the position x_i and velocity v_i of each agent i ($i = 1,2,3,4$) approach zero over time. The state-feedback controller:

$$u_i^{nom}(t) = -k_1 x_i(t) - k_2 v_i(t)$$

is adopted, where k_1 and k_2 are positive gain parameters. In this experiment, we take Q and R in (6.6) as identity matrices[2], and suppose the initial position and velocity of agent i as

$$x_i(0) = i, \quad \text{and} \quad v_i(0) = 1, \quad i = 1,2,3,4.$$

Considering the gain parameters as the hyperparameters $\theta = (k_1, k_2)$, Figure 6.2 shows the control performance under different values of hyperparameter θ. In Figure 6.2 (a), the time instants t_1, t_2, t_3 corresponding to θ_1, θ_2, θ_3 are the earliest time instants when the neighbor value of J falls below 0.1, indicating convergence. The results in Figure 6.2 (b) indicates the realization of desired control objectives under the controller $u_i^{nom}(t)$. □

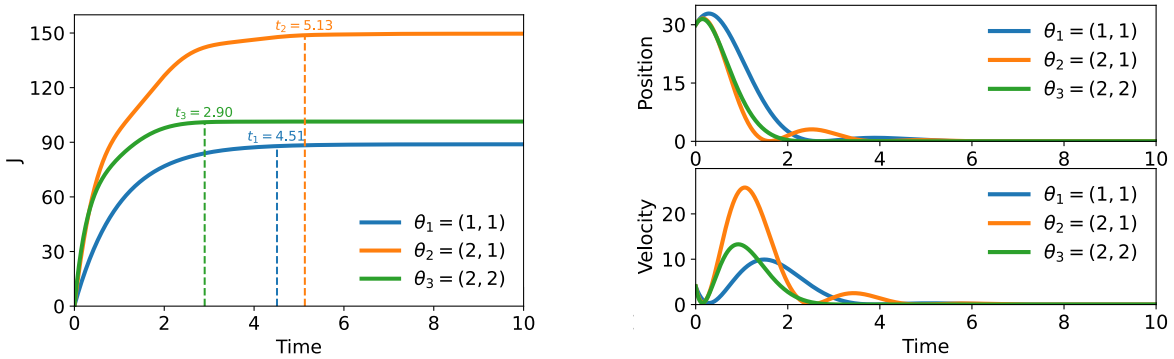

(a) (b)

Figure 6.2: (a) The LQR cost $J(t)$ under different values of θ; (b) The position error $\sum_{i=1}^{4} \|x_i(t) - \mathbf{0}_2\|^2$ and velocity error $\sum_{i=1}^{4} \|v_i(t) - \mathbf{0}_2\|^2$ under different values of θ.

The results of *Example 6-1* demonstrate that the performance J depends on the hyperparameter θ in terms of convergence value and convergence time. When additional constraints, such as limits on velocity and acceleration and the collision avoidance safety constraint, are considered, the nominal controller needs to be modified using the CBF filters at some time, and the accumulated modifications are unknown. In this scenario, we cannot explicitly describe the mathematical relationship between the performance and hyperparameters. In other words, (6.7)presents a black-box optimization problem.

[2]Noting that the value of J is also dependent on Q and R, we fix Q and R to see the relationship between LQR performance and the gain parameters.

Remark 6.2. *It is worth noting that the LQR cost is introduced as an observable illustration to facilitate a clearer comprehension of the simulation examples. Actually, the control performance can be designed with user-specific cost functions (to be minimized) or reward functions (to be maximized).*

6.3 CBF-CBO-based Performance Enhancement

6.3.1 Constrained Bayesian Optimization

Considering the control objective and safety objective for MASs, the unconstrained optimization problem (6.7) is extended to the following constrained optimization problem:

$$\begin{aligned} \theta^* &= \arg\min_{\theta\in\Theta} J(\theta) \\ \text{s.t.} \quad & f(\theta) \geqslant 0, \end{aligned} \tag{6.8}$$

where $f(\theta) \geqslant 0$ serves as a constraint function, indicating the feasibility of hyperparameter θ.

The constrained Bayesian optimization (CBO) algorithm is employed to deal with the constrained optimization problem (6.8), utilizing the *expected improvement with constraints* (EIC) as the acquisition function. Given the absence of an explicit mapping relationship between θ and J or f, the surrogate functions $\hat{J}(\theta)$ and $\hat{f}(\theta)$ are estimated separately using Gaussian processes and incorporated into the EIC as follows:

$$\mathrm{EIC}(\theta|J_p^*) = \Phi(0)\mathrm{EI}(\theta|J_p^*), \tag{6.9}$$

where $J_p^* = \min_{k=1,\cdots,p} J(\theta_k)$ is the optimal value of the current dataset $\{\theta_k, J(\theta_k)\}_{k=1}^p$, and $\Phi(\cdot)$ is the estimated cumulative distribution function of $f(\cdot)$ [152]. Under the dataset $\{\theta_k, J(\theta_k)\}_{k=1}^p$, the next observation θ_{p+1} is given by maximizing the EIC function, which is shown as follows:

$$\theta_{p+1} = \arg\max_{\theta\in\Theta} \mathrm{EIC}(\theta|J_p^*). \tag{6.10}$$

Assumption 6.1. *The Gaussian process models are non-degenerate and adhere to the no-empty-ball property [184].*

In the following, *Example 6-2* demonstrates the impact of the CBO algorithm on the constrained optimization problem (6.8). For comparison, the original BO algorithm introduced in Section 6.1.2 is used to solve the unconstrained optimization problem (6.7), with the next observation determined by the EI (6.4). The results of *Example 6-2* show that the optimal solutions θ^* and J^* can be identified after sufficient evaluations.

Example 6-2: Firstly, recalling *Example 6-1*, under the state-feedback controller $u_i^{nom} = -k_1 x_i - k_2 v_i$, the LQR-based optimal gain $\theta = [k_1, k_2]$ can be theoretically determined as follows. The MAS (4.7) has the linear form

$$\dot{\eta}_i = A\eta_i + Bu_i,$$

where

$$\eta_i = \begin{bmatrix} x_i \\ v_i \end{bmatrix}, \quad A = \begin{bmatrix} \mathbf{0}_{n\times n} & I_n \\ \mathbf{0}_{n\times n} & \mathbf{0}_{n\times n} \end{bmatrix} \quad \text{and} \quad B = \begin{bmatrix} \mathbf{0}_{n\times n} \\ I_n \end{bmatrix}.$$

Then the LQR (6.6) can be expressed as

$$J = \sum_{i=1}^{4} \int_0^\infty (\eta_i^T \eta_i + u_i^T u_i) \mathrm{d}t.$$

Hence, the optimal solution is determined by $\theta^* = B^T P$, where P satisfies the Riccati equation:

$$PA + A^T P - PBB^T P + I = 0.$$

In this setting, we obtain that

$$\theta^* = [1, 1.732] \quad \text{and} \quad J^* = J(\theta^*) = 79.427.$$

Secondly, we verify the feasibility of the BO algorithm in solving the unconstrained optimization problem of *Example 6-1*. The hyperparameter set to be optimized is $\theta =$

$[k_1, k_2]$, and the search space is assumed to be $\Theta = (0,5]^2$. As shown in Figure 6.3 (a), after 40 evaluations, the optimal solutions obtained by BO are

$$\theta^*_{bo} = [0.9982, 1.7346] \quad \text{and} \quad J^*_{bo} = 79.426,$$

which are almost the same as the true optima.

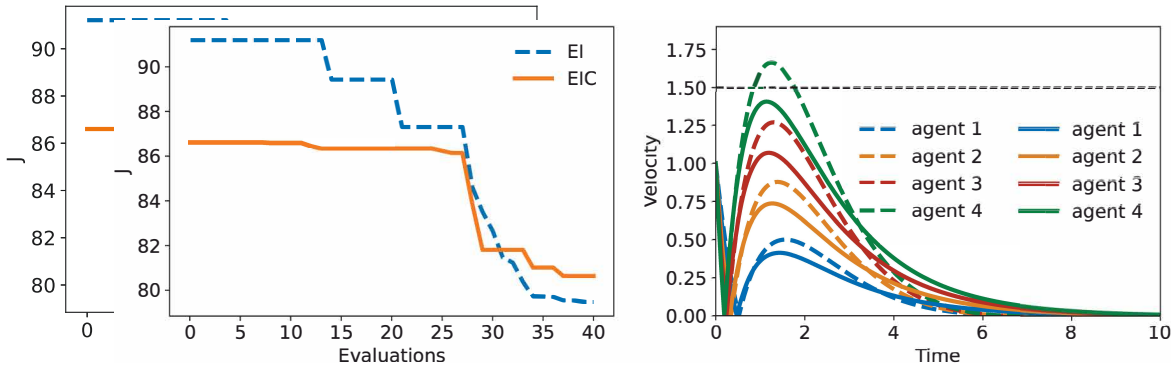

(a) (b)

Figure 6.3: (a) The best LQR cost J observed during function evaluations via EI and EIC; (b) The trajectories of velocity $\|v_i(t)\|$ for all agents.

Furthermore, in Figure 6.3 (b), the black dotted line represents the safe bound of velocity. The colorful dotted lines are controlled with the hyperparameter found by EI, and the colorful curve lines are controlled with the hyperparameter found by EIC. We can find from Figure 6.3 (b) that the velocity of each agent under θ^*_{bo} obtained by BO can successfully converge to zero. However, when considering the control condition $\|v_i(t)\| \leqslant b_v$ ($b_v = 1.5$), the previously obtained optimal hyperparameter, whether derived theoretically or through BO evaluations, is not feasible. In such scenarios, the constrained optimization problem (6.8) is employed, where the constraint function $f(\theta) \geqslant 0$ implicitly ensures the condition $\|v_i\| \leqslant b_v$. Since there is no analytical expression between θ and $\|v_i\| \leqslant b_v$, CBO is used to solve this problem. After 40 evaluations, the optimal hyperparameter found by CBO is

$$\theta^*_{cbo} = [1.0882, 2.2547] \quad \text{and} \quad J^*_{cbo} = 80.641.$$

At this point, the obtained θ^*_{cbo} is feasible, since the resulting velocities of all agents are within their safe ranges, as shown in Figure 6.3 (b). □

Moreover, one can see from this illustrative example that increasing the number of evaluations could bring the optima found by the Bayesian optimization algorithms closer to the true optima, even when the true optima are unknown. According to Bayesian Decision Theory, the following lemma demonstrates the convergence of the CBO algorithm.

Lemma 6.1. *(Theorem 1 in [185]) If the observations are collected with* (θ_1, J_1) *fixed in the space* $\{\theta \in \Theta | f(\theta) \geqslant 0\}$*, and* $\{\theta_k, J(\theta_k)\}_{k=2}^{p}$ *are sequentially chosen by EIC* (6.9)*, then as* $p \to \infty$*, the best observed performance* J^* *almost surely converges to the global optimum of problem* (6.8)*.*

6.3.2 CBF-CBO Algorithm

The above *Example 6-2* demonstrates that CBO can provide a numerical solution to the constrained optimization problem of MASs. This section will provide a detailed explanation of how this method works. As depicted in Figure 6.1, there are two processes: a lower-layer safety control process and an upper-layer hyperparameter optimization process.

- *Control loop:* For the lower-layer safety control, the CBF-based QP controller (4.22) is utilized to ensure collision avoidance in MASs. This controller incorporates the nominal control inputs to achieve desired control objectives and is dependent on the hyperparameter θ. In experiments, we set $f(\theta) = 1$ for feasible θ, and the performance $J(\theta)$ is recorded when the terminal criteria for the control loop of MASs are met. Common termination conditions include reaching the desired state within an acceptable error threshold or exhausting the maximum allowed control time (as used in this chapter). For infeasible θ, the control loop is terminated as

soon as the control or safety objectives are violated. In such cases, we set $f(\theta) = -1$ and $J(\theta) = 10^5$, where the large value of J indicates the infeasibility of θ. Infeasible observations are also included in the dataset to assist in finding the next better θ through CBO.

- *Optimization iteration:* For the upper-layer hyperparameter optimization, the performance function $J(\theta)$ is modeled using Gaussian process regression with the observed dataset $\{\theta_k, J(\theta_k), f(\theta_k)\}_{k=1}^{p}$, and the binary constraint function $f(\theta)$ is modeled using Gaussian process classification with the dataset [186]. The Gaussian process models are updated every time the dataset for CBO is updated following function evaluations. The initial dataset for CBO can be uniformly or randomly sampled from the search space Θ [187]. After each function evaluation, an additional sample $\{\theta_{p+1}, J(\theta_{p+1}), f(\theta_{p+1})\}$ is obtained, updating the dataset. The evaluations will continue until the terminal criteria for CBO are met. These criteria can vary, such as fixing a maximum number of evaluations M (as used in this chapter) or adopting early-stopping strategies [180].

Theorem 6.1. *If the number of evaluations approaches positive infinity, the MAS* (4.7) *can achieve its control objectives while ensuring collision avoidance under the CBF-based QP controller* (4.22) *with the optimal hyperparameter θ^* found by CBO. Moreover, the control performance of the MAS is optimized in this scenario.*

Proof: Firstly, by solving the constrained optimization problem (6.8), the convergence of the observations by CBO ensures the optimality of the hyperparameter, as demonstrated in *Lemma* 6.1. Correspondingly, the control performance of the MAS is optimized under the obtained hyperparameter. Additionally, the constraint in (6.8) is satisfied, indicating the feasibility of the hyperparameter and the achievement of both control and safety objectives.

Specifically, the CBF-based QP (4.22) is solvable with the obtained hyperparameter, providing a controller for each agent. According to the analysis in previous sections, safety between agent i and agent j ($j \in \mathscr{M}_i$) is ensured by satisfying the CBF constraint. Moreover, the control objective of the MAS (4.7) is achieved through the self-designed nominal controller in QPs, as evidenced by the convergence of the control performance value. ■

Algorithm 1 CBF-CBO-based performance enhancement of MASs.

Input: $x_i(t_0)$, $v_i(t_0)$, b_u, b_v, D_{safe}, search space Θ;
Output: Optimal hyperparameter θ^* and performance J^*;
Initialize: Evaluations with p_0 random hyperparameters;
Training dataset $\mathbb{D} = \{\theta_k, J(\theta_k), f(\theta_k)\}_{k=1}^{p_0}$;
for $p = p_0$ to $M + p_0$ **do**
  Update the surrogate function $\hat{J}(\theta)$ with Gaussian process and $\mathbb{D}$;
  Update the surrogate function $\hat{f}(\theta)$ with Gaussian process and $\mathbb{D}$;
  $\theta_{p+1} = \arg\max_{\theta\in\Theta} \mathrm{EIC}(\theta|J_p^*)$ in (6.10);
  while not termination condition **do**
    for $i = 1$ to N **do**
      Calculate the nominal control input u_i^{nom};
      Update nearby neighbor set $\mathscr{M}_i$;
      Obtain the safe control input u_i^*;
      Update the state information x_i, v_i;
    end for
  end while
  $\mathbb{D} \leftarrow \mathbb{D} \cup (\theta_{p+1}, J(\theta_{p+1}), f(\theta_{p+1}))$;
  $p \leftarrow p + 1$;
end for

Computational Complexity. The computational complexity of Algorithm 1 primarily involves two components: training the GP models and maximizing the EIC function (6.10). First, the computational complexity of training a Gaussian process is mainly determined by the number of hyperparameters to be optimized (denoted as N_θ) or the number of training data points (denoted as N_{train}). To be specific, the complexity is $\mathscr{O}(N_\theta^3)$ or $\mathscr{O}(N_{train}^2)$. Additionally, the L-BFGS (Limited-memory Broyden-Fletcher-Goldfarb-Shanno) algorithm is employed to solve the EIC acquisition function. While there is no

rigorous computational complexity analysis for EIC, we set M as its maximum evaluation number.

Remark 6.3. *Although the BO algorithms perform well in solving expensive optimization problems with limited data [188], they are more suited for lower-dimension hyperparameter optimization due to computational complexity. In large-scale MASs, the number of hyperparameters to be optimized may be very high. One straightforward approach is to fix some hyperparameters to be the same across different agents, such as sharing the same CBF parameter α for all agents, as a trade-off between control performance and computational complexity. Another potential approach for large-scale MASs is to concentrate on subsets of agents by prioritizing them based on their contributions to overall performance, such as scoring agents in the literature [189].*

Remark 6.4. *Take the widely used LQR performance as an example. The control hyperparameter usually indicates the convergence rate of state errors, thereby influencing the overall convergence speed of LQR performance. Conversely, the safety hyperparameter may impede the convergence of LQR performance, as the CBF filter adjusts the nominal controller to ensure safety. These effects on control performance are implicit and challenging to quantify. Moreover, the control and safety hyperparameters mutually influence each other during the optimization process, and their relationship can be elucidated through the kernel function of the Gaussian process.*

Remark 6.5. *The proposed CBF-CBO approach is a unified framework that can be adapted to various control tasks, for example, when system dynamics differ or are affected by uncertainties [190]. The key variation lies in the CBF design to match specific system dynamics. Given the high costs of actual experiments in MASs, the CBF-CBO algorithm can initially be employed in simulation experiments to determine optimal hyperparameters, which enables energy-efficient implementation in real-world applications.*

6.4 Deployment in Safe MASs

Two experiments are conducted to validate the theoretical analysis. The first experiment addresses the destination achievement control of MASs, representing a non-cooperative control task. The second experiment considers the formation control of MASs, which is a cooperative control task. Both experiments use four different hyperparameter optimization algorithms: random search (RS), genetic algorithm (GA), covariance matrix adaptation evolution strategy (CMA), and the suggested CBO method presented in this chapter.

We conduct the experiments on a server with an Intel Xeon Gold 6238R CPU and 180GB of memory. Each search for the next observation using EIC (https://botorch.org/) takes about 0.6 seconds. The CBF-based QP is solved using CVXOPT (https://cvxopt.org/), with each solving time being less than 0.001 seconds. In the RS algorithm, candidate observations are uniformly sampled. The population size of both GA and CMA (https://github.com/CMA-ES/pycma) is 5.

6.4.1 Destinations Achievement

In this experiment, we reconsider the safe control scenario in *Example 4-1*. We notice from Figure 4.3 that the control performance is not very good under the self-given hyperparameters. Hence, we test the feasibility of proposed CBO algorithm using this numerical experiment.

Despite the notations given in *Example 4-1*, denote

$$e = [e_1^T, e_2^T, e_3^T, e_4^T]^T \quad \text{and} \quad u = [u_1^T, u_2^T, u_3^T, u_4^T]^T.$$

We aim to minimize the cost function:

$$J = \int_0^{30} (e^T Q e + u^T R u) \mathrm{d}t,$$

where the matrices Q and R are fixed as identity matrices. We choose $b_v = 3.5$ and $b_u = 4$ in this experiment.

Considering the nominal controller $u_i^{nom} = -k_{i1}(x_i - P_i) - k_{i2}v_i$, the hyperparameters to be optimized include eight control parameters and one safety parameter, which are denoted as

$$\theta = [k_{11}, k_{12}, k_{21}, k_{22}, k_{31}, k_{32}, k_{41}, k_{42}, \alpha].$$

The search space is $\Theta = (1, 100)^9$ in the log scale.

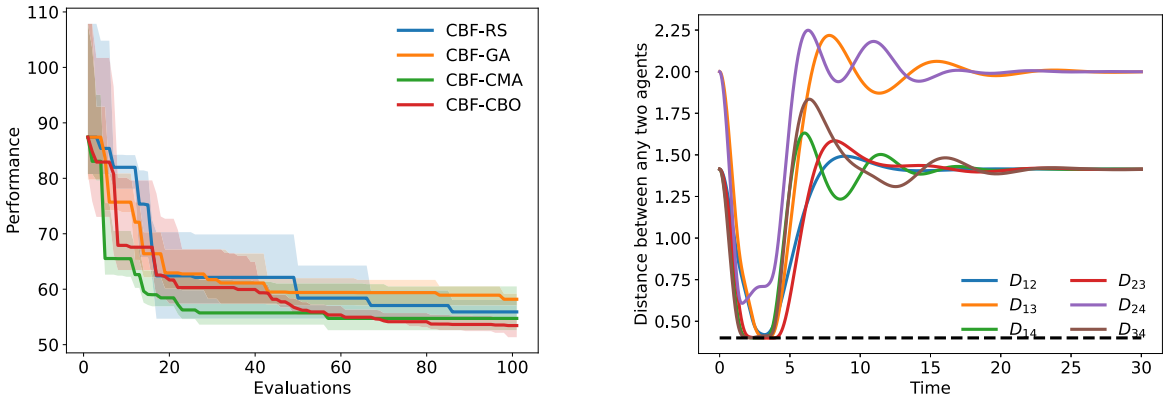

(a) (b)

Figure 6.4: (a) The best LQR cost J observed over 100 evaluations using CBF-RS, CBF-GA, CBF-CMA and CBF-CBO; (b) The distance of each pair of agents (i, j).

The experiment is repeated five times. Figure 6.4 (a) shows the best performance over 100 evaluations with median values and 25th and 75th percentiles plotted, which demonstrates that the CBF-CBO approach outperforms the others. The optimal hyperparameters found by CBF-CBO are

$$\theta^*_{cbo} = [0.4002, 0.3682, 0.6225, 1.3987, 1.0240, 0.6983, 0.4384, 0.5714, 1.6524],$$

resulting in a cost of $J^*_{cbo} = 51.346$. When using the CBF-based QP controller with θ^*_{cbo}, Figure 6.4 (b) demonstrates successful collision avoidance among agents, where the dotted black line indicates the safe bound $D_{safe} = 0.4$. Figures 6.5 (a) shows the

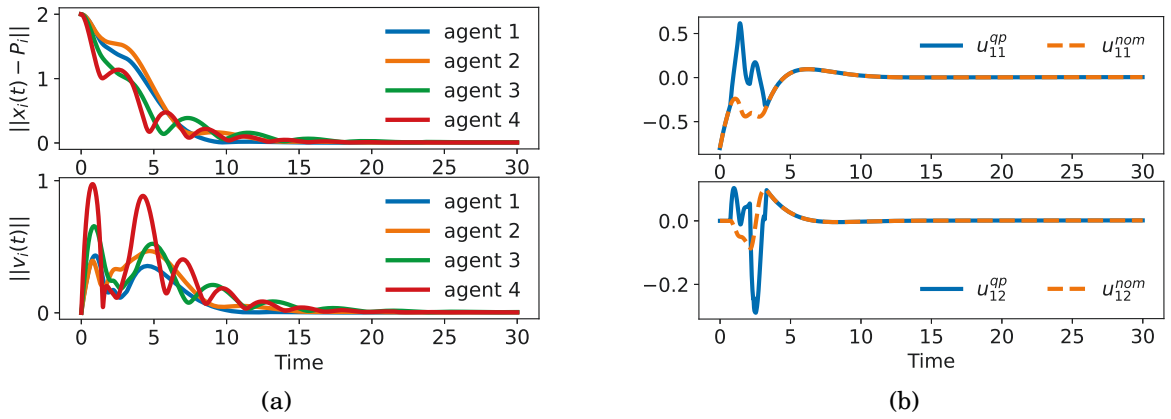

(a) (b)

Figure 6.5: (a) The position and velocity tracking errors for all agents; (b) The control input of Agent 1, with each dimension of $u_1(t)$ shown.

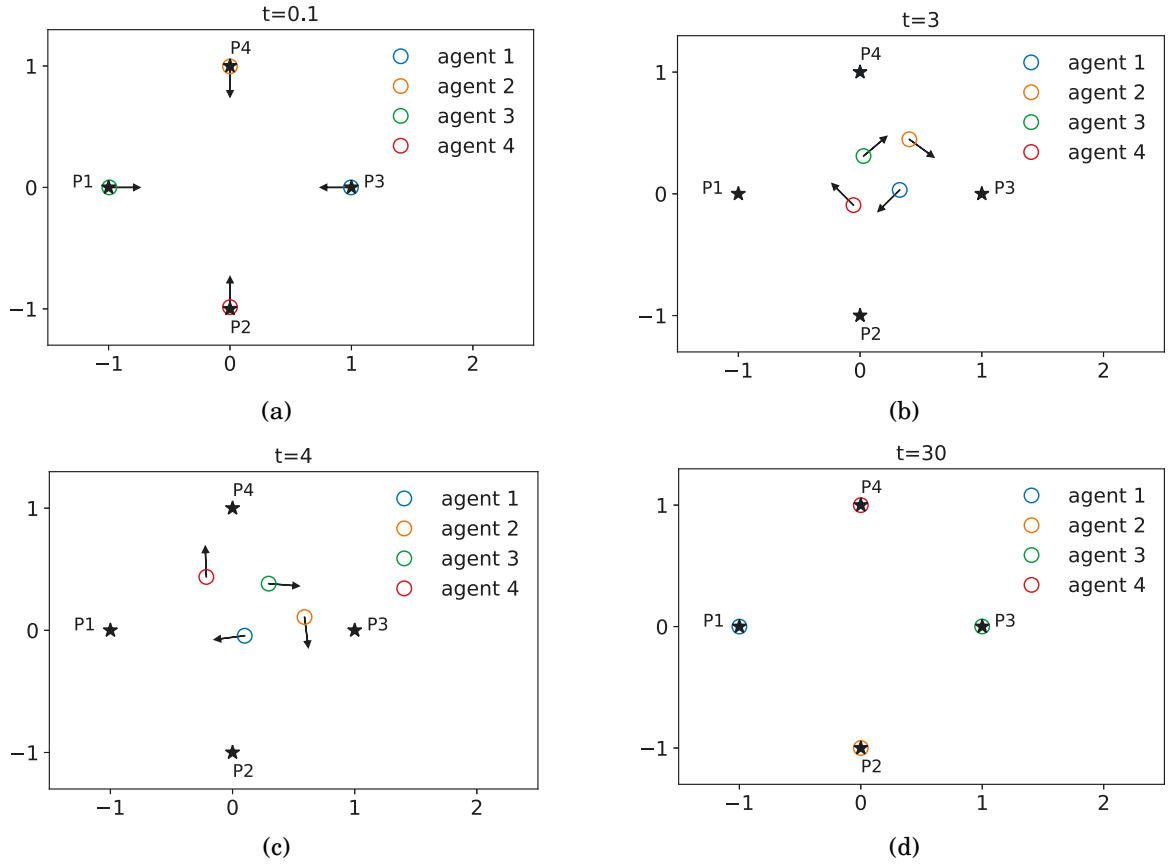

(a) (b) (c) (d)

Figure 6.6: The position of each agent at time instant (a) $t = 0.1$; (b) $t = 3$; (c) $t = 4$; (d) $t = 30$.

achievement of the control objectives, and the CBF filtered u_1^{qp} and the nominal u_1^{nom} are plotted in Figures 6.5 (b) to highlight their differences. In each subplot of Figure 6.6, the x-axis represents the first dimension of position, x_{i1}, and the y-axis represents the second dimension, x_{i2}. Circles indicate the position coordinates of agents, while arrows represent their velocities. The final subplot demonstrates that each agent reaches its destination.

6.4.2 Formation Tracking

In this experiment, we apply the proposed CBO algorithm to the safe formation control of MASs. Specifically, for a system consisting of one leader and four followers, the leader moves towards its destination x_d, and we aim to drive the followers to reach the leader's state while maintaining a formation defined by the relative configurations s_i. The nominal control inputs are

$$u_0^{nom} = -k_1(x_0 - x_d) - k_2 v_0$$

for leader 0, and

$$u_i^{nom} = -k_3[\sum_{j=1}^{4} a_{ij}((x_i - s_i) - (x_j - s_j)) + a_{i0}(x_i - x_0 - s_i)] - k_4[\sum_{j=1}^{4} a_{ij}(v_i - v_j) + a_{i0}(v_i - v_0)]$$

for follower i ($i = 1,2,3,4$). The initial positions of followers are

$$[x_1(0), x_2(0), x_3(0), x_4(0)] = [(-2,0),(-2.5,0),(-3,0),(-3.5,0)]$$

and the formation shape is described as follows:

$$[s_1, s_2, s_3, s_4] = [(-1,-1),(-1,1),(-2,-1),(-2,1)].$$

The leader's initial position is $x_0(0) = (-1.5,0)$, and destination is $x_d = (5,0)$. Initially, all agents have zero velocity. Take $b_v = 6$ and $b_u = 6$. The hyperparameters to be optimized are

$$\theta = [k_1, k_2, k_3, k_4, \alpha],$$

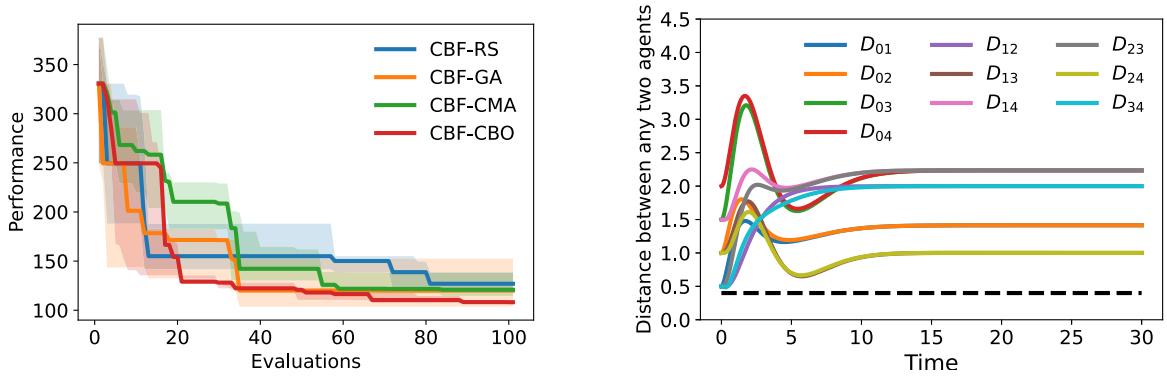

Figure 6.7: (a) The best LQR cost J observed over 100 evaluations using CBF-RS, CBF-GA, CBF-CMA and CBF-CBO; (b) The distance of each pair of agents (i, j).

while the remaining parameters are consistent with those used in the previous destination achievement experiment.

According to Figure 6.7 (a), it is evident that CBF-CBO outperforms CBF-RS, CBF-GA and CBF-CMA. The optimal hyperparameters found by CBF-CBO are

$$\theta^*_{cbo} = [0.7121, 1.7749, 0.9412, 1.9998, 1.6886],$$

yielding an optimal LQR cost of $J^*_{cbo} = 94.979$. When using the CBF-based QP controller with hyperparameter θ^*_{cbo}, Figure 6.7 (b) demonstrates successful collision avoidance among agents. For the positions of all agents at various times, refer to Figure 6.8. The final subplot illustrates the successful formation of the desired shape.

6.5 Conclusion

In this chapter, we introduced a safe control framework for MASs aimed at improving control performance. We categorized performance-related hyperparameters and introduced feasibility criteria aligned with the stability and safety objectives to be achieved. To optimize the unknown performance function with a feasibility constraint, we proposed the CBF-CBO algorithm to identify improved hyperparameters.

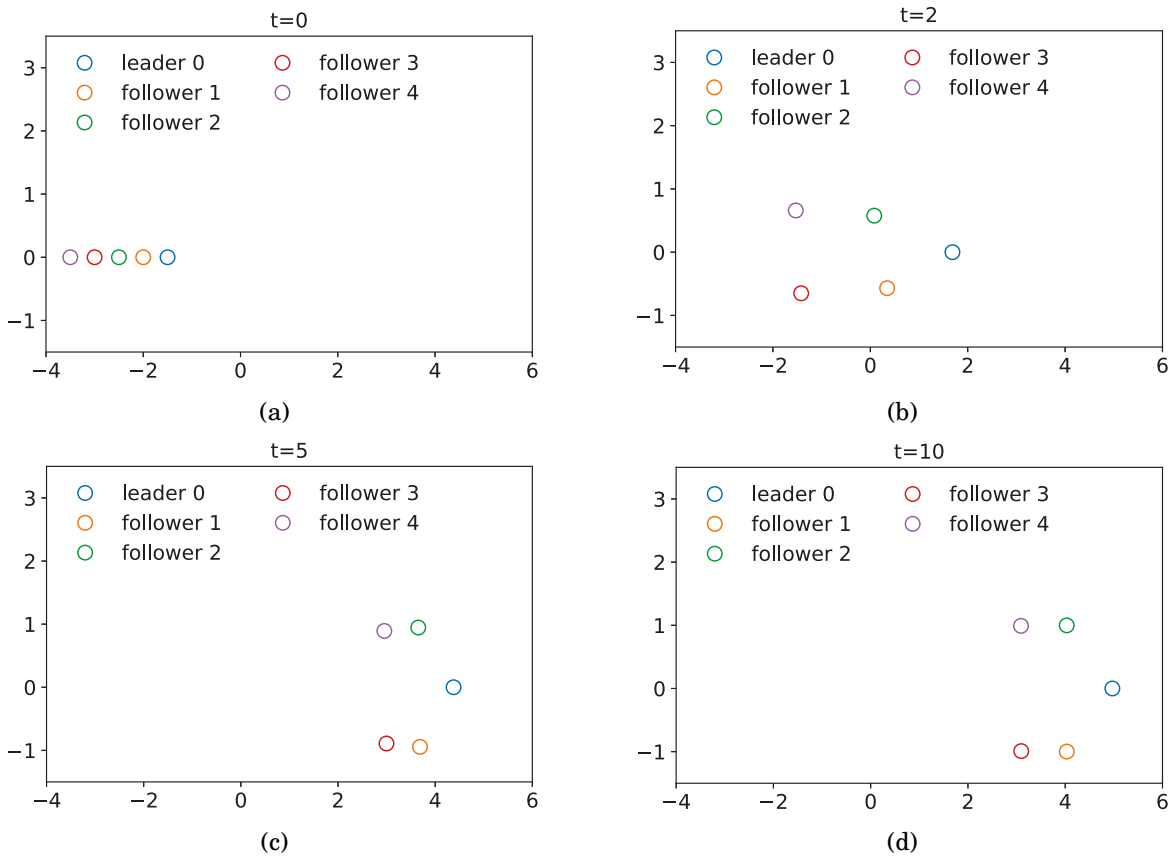

Figure 6.8: The position of each agent at time instant (a) $t = 0$; (b) $t = 2$; (c) $t = 5$; (d) $t = 10$.

Up to now, we have explored the cooperative control of MASs from four key perspectives, stability, safety, robustness, and optimality, progressing step by step from fundamental concepts to more in-depth analyses, thereby enhancing its potential applicability to real-world applications.

CHAPTER 7

CONCLUSION AND FUTURE RESEARCH

This chapter summarizes the main content of this thesis, and outlines future research directions.

7.1 Conclusion

This thesis has presented a comprehensive study on the safe and robust cooperative control of MASs using a constrained QP framework that integrates CLF and/or CBF conditions. The primary objective was to ensure system-wide stability and safety while addressing key challenges such as robustness to uncertainties, computational efficiency, and long-term performance optimization.

To this end, several contributions were made. First, a distributed CLF-based QP control strategy was developed for the stability of MASs, incorporating event-triggered and intermittent control mechanisms to reduce computational burden. Second, to ensure inter-agent collision avoidance, a pairwise CBF-based QP control framework was designed for safe formation control, enhanced with a structured neighboring set to re-

duce the number of CBF conditions. Third, the proposed framework was extended to address scenarios where only simple distance-based safety functions are available. To accommodate such cases, high-order CBFs were introduced, enabling the enforcement of safety constraints for systems with higher relative degrees. Furthermore, robustness was enhanced by incorporating bounded disturbance models, ensuring reliable safety guarantees under worst-case uncertainty. Fourth, the thesis introduced data-driven GP models into both CLF and CBF constraints to estimate unknown system components, thus eliminating the need for predefined uncertainty bounds and enabling a more flexible response to dynamic environments. Moreover, the thesis addressed the problem of performance enhancement under hyperparameter sensitivity by formulating it as a black-box optimization problem. A novel CBF-CBO algorithm was proposed, which effectively achieves performance improvement and safety assurance. Finally, simulation results demonstrated the efficacy and practicality of the proposed approaches in a variety of cooperative control scenarios.

7.2 Future Research

While this dissertation presents some progress in the safe control of MASs using CBF-based approach, there remain several challenges and limitations. We introduce some of them in this section to open up promising directions for future research.

7.2.1 Learning Neural Barrier Functions

One limitation of the CBF-based control framework lies in the necessity of manual design of the barrier function expressions. In the current formulation, the construction of a valid CBF requires prior knowledge of the system dynamics and a clear mathematical characterization of the safe set. For relatively simple environments or systems with known constraints, such design may be feasible. However, in high-dimensional, nonlin-

ear, or partially unknown environments, or in systems operating under dynamic and non-stationary safety constraints, manually specifying an appropriate barrier function becomes a daunting task, if not impossible.

A future research direction is the integration of learning-based methods, particularly neural networks, into the CBF framework to autonomously synthesize safety certificates and controllers. This concept, often referred to as neural barrier functions or learning-based barrier certificates, leverages the powerful function approximation capabilities of deep neural networks to learn suitable barrier functions directly from data or through interaction with the environment. There are several specific avenues within this direction worth exploring:

1. Learning barrier functions from demonstrations or trajectories

   One intuitive approach is to learn the shape of the safe set, and thereby the corresponding CBF, from expert demonstrations or from trajectories known to be safe. A neural network can be trained to approximate the barrier function that remains positive inside the safe set and negative outside, while satisfying the required differentiability and Lipschitz continuity properties. Such an approach reduces the reliance on explicit safe set modeling and may generalize better in environments where human intuition or classical analysis fails.

2. Learning of safe controllers

   Beyond learning the CBF itself, another direction is to jointly learn the control policy that satisfies the safety constraints implied by a learned barrier function. This could be formulated as a constrained optimization problem embedded in a neural network architecture, or approached via constrained reinforcement learning. Here, the barrier condition acts as a regularizer or hard constraint, guiding the controller towards safe actions during training and inference. Note that the design

of loss function may be an important factor during this process.

3. Ensuring theoretical guarantees

   A significant challenge in learning-based methods is the lack of formal guarantees. Therefore, a vital research avenue is to embed formal safety guarantees within the learning process. For example, one may use hybrid methods that combine analytical CBF constraints with learnable parameters, or apply verification techniques (e.g., neural network reachability analysis) to ensure that the learned neural barrier function adheres to required properties such as forward invariance and control feasibility under bounded disturbances.

4. Multi-agent and distributed learning frameworks

   In MASs, learning barrier functions introduces additional complexity due to agent interactions and the need for distributed computation. Research can be directed towards decentralized training of neural barrier functions, enabling each agent to learn local safety certificates while coordinating with others to maintain global safety. This requires addressing issues such as communication constraints, partial observability, and scalable learning architectures.

In summary, neural barrier functions offer the potential to automate the design of safety constraints, adapt to complex environments, and provide scalable solutions to high-dimensional control problems. Nonetheless, ensuring theoretical rigor, robustness, and interpretability remains an open and vital challenge. Addressing these issues will require a multidisciplinary effort combining control theory, machine learning, formal methods, and systems engineering. The outcome of this research direction may significantly broaden the applicability of barrier-function-based control frameworks, pushing them toward practical deployment in safe systems.

7.2.2 Event-triggered Safe Control in MASs

In addition to the challenge of constructing appropriate CBFs, another key limitation of the current CBF-based safe control framework, especially in MASs, is the computational burden associated with solving QP problems at every control update. In most CBF implementations, safety is ensured by formulating and solving a constrained QP at every time step to compute the control input. While this real-time optimization framework guarantees safety and performance, it also incurs significant computational overhead, which may become prohibitive in large-scale or resource-constrained systems.

To address this limitation, a future research direction is the exploration of event-triggered control (ETC) mechanisms within the context of CBF-based safety control. Unlike conventional time-triggered control schemes, where the control input is updated at fixed and typically high frequencies, ETC aims to update the controller only when necessary, based on the occurrence of specific state-dependent events. This paradigm has the potential to substantially reduce the computational load, leading to energy-efficient and scalable safe control strategies for MASs. Several challenges and opportunities exist in this direction, motivating a wide array of research tasks:

1. Design of safety-preserving event-triggering conditions

   The central problem in integrating ETC with CBFs is the design of a triggering function that ensures safety at all times, despite the fact that the control input is not continuously updated. The triggering condition must be formulated such that between two triggering events, the system trajectory remains within the safe set. This typically involves deriving bounds on the system's evolution using worst-case analysis, Lipschitz constants, or robust invariance techniques. Future research could explore tight and computationally tractable formulations of such conditions, particularly for nonlinear, coupled MASs with complex dynamics.

2. Co-design of event triggers and control laws in MASs

   In MASs, agents often interact and influence each other's safety constraints. Designing event-triggered mechanisms in such a context requires a co-design of the triggering logic and the decentralized control laws. This includes dealing with asynchronous triggering, communication delays, and distributed triggering rules. Future research should focus on creating scalable, distributed ETC-CBF frameworks where each agent independently determines when to update its control input while still ensuring global safety. Additional challenges include developing inter-agent triggering protocols and analyzing their stability properties.

3. Theoretical analysis and performance guarantees

   One concern in ETC is the possibility of Zeno behavior, where an infinite number of events occur in a finite time. Future research must establish strict lower bounds on inter-event times, known as minimum dwell-time conditions, to ensure physical realizability. Moreover, rigorous performance guarantees (e.g., bounded suboptimality, guaranteed convergence to goals, resilience to disturbances) must be established to ensure that the ETC-based control strategy not only preserves safety but also achieves the system's primary control objectives.

4. Simulation and real-world implementation in resource-constrained systems

   Beyond theoretical development, it is essential to validate the proposed ETC-CBF framework through comprehensive simulations and real-world experiments. Future research should demonstrate how event-triggered QP control scales with increasing number of agents and how much computation, energy, and bandwidth savings can be achieved without sacrificing safety. Application domains such as vehicle fleets, swarms, networked agents, and smart manufacturing systems serve as ideal testbeds to benchmark the practical advantages of ETC-based safety control.

In summary, the integration of ETC into the CBF framework represents a powerful approach to alleviate computational burdens in safety MASs, particularly under real-time constraints and limited resources. However, this approach introduces new challenges in guaranteeing safety under sporadic updates, requiring a rigorous redesign of triggering functions, safety conditions, and control synthesis mechanisms. Addressing these challenges opens a broad and impactful research agenda, aiming to make CBF-based safe control not only theoretically sound but also practically viable for large-scale deployment in complex and distributed environments.

7.2.3 Transferable Barrier Functions for Cross-task Safety

A fundamental challenge in deploying CBF-based safe control strategies in real-world scenarios lies in their limited generalization and transferability across different environments and tasks. Traditional CBF design is highly problem-specific: the barrier function is typically handcrafted or finely tuned based on prior knowledge of the environment's geometry, obstacle layout, and system dynamics. As a result, a CBF controller that works effectively in one scenario may fail to generalize when deployed in a new environment with different obstacles, terrain structures, or agent configurations. This lack of adaptability may constrain the applicability of CBF-based methods in dynamic or unknown environments, particularly in domains such as navigation, 3D scene reconstruction, search and rescue, or intelligent surveillance.

A promising direction for overcoming this limitation lies in augmenting CBF design with meta learning, enabling the rapid adaptation and transfer of safe control capabilities across a wide variety of tasks and environments. The core idea is to develop a CBF-based controller that not only performs well in a specific environment but also learns a generalizable prior, a set of parameters or features, that can be efficiently fine-tuned to new environments using minimal data or few-shot adaptation. This research direction

sits at the intersection of safe control, transfer learning, and meta learning, and has the potential to greatly extend the versatility and autonomy of intelligent agents operating in complex, uncertain, or unstructured environments. Key aspects of this research include:

1. Meta-learning frameworks for CBF parameterization

   One potential approach is to represent the CBF (and optionally the associated safe controller) using a parameterized function, such as a neural network, and apply gradient-based meta-learning algorithms to learn a set of meta-parameters that can be quickly adapted to new tasks. The meta-training phase involves exposing the model to a diverse set of simulated environments or scenarios, such that it learns a shared structure of safety constraints (e.g., common patterns in obstacle geometry or agent dynamics). When faced with a novel environment, the agent can then fine-tune the barrier function using only a few samples from the new environment, significantly reducing the data and time required for deployment.

2. CBF-driven exploration in meta-reinforcement learning

   Another exciting possibility is to use meta-learned CBFs not only for safety enforcement, but also to guide exploration in RL tasks. In many RL problems, safety constraints discourage agents from exploring unknown or high-risk states, leading to overly conservative behaviors. However, a meta-CBF trained across many environments can encode a prior over safe-but-informative exploration strategies, allowing the agent to balance safety with curiosity. This could accelerate learning in tasks like 3D scene reconstruction, where the agent must actively explore a space while avoiding collisions, or multi-agent coordination tasks where exploration risks inter-agent conflicts.

3. Applications in real-world systems

   The practical significance of this research direction lies in its potential to enable

plug-and-play safe controllers for a wide range of robotics and AI applications. For example, in autonomous driving, a meta-learned CBF could rapidly adapt to different urban layouts, weather conditions, or traffic norms with minimal retraining. In robotic swarms, such as UAV teams performing search and mapping, each robot could locally adapt its safety controller based on the terrain features while maintaining global coordination protocols. Similarly, in human-robot interaction, CBFs that adapt to user-specific behavior or environment constraints can enable safer and more personalized assistance.

In summary, improving the adaptability, generalization, and transferability of CBFs represents a transformative step toward safe, intelligent, and autonomous agents capable of operating in complex, heterogeneous, and rapidly changing environments. By integrating meta learning techniques, agents can not only avoid collisions in previously unseen scenarios but also contribute to broader tasks such as 3D scene understanding, efficient exploration, and semantic navigation, thereby bridging the gap between safe control and general AI autonomy. This line of research has the potential to extend the usability of CBFs beyond rigid, model-specific deployments, opening up new frontiers in safe and flexible MASs.

References

[1] C. E. Adu, C. E. R. Chuquiure, B. Zhang, and R. Vasudevan, "Bring the heat: Rapid trajectory optimization with pseudospectral techniques and the affine geometric heat flow equation," *IEEE Robotics and Automation Letters*, vol. 10, no. 4, pp. 4148–4155, 2025.

[2] L. Weng, Z. Li, and L. Gao, "Affine formation maneuver control of multiagent systems with disturbances based on rise controller," *IEEE Systems Journal*, vol. 19, no. 1, pp. 142–151, 2025.

[3] P. Su, Z. Shi, J. Yu, X. Dong, Z. Ren, and D. Wang, "Distributed time-varying optimization-based protocols for affine formation maneuver," *IEEE Transactions on Industrial Electronics*, pp. 1–9, 2025.

[4] K. Yang, S. Li, M. Wang, and X. Tang, "Interactive decision-making integrating graph neural networks and model predictive control for autonomous driving," *IEEE Transactions on Intelligent Transportation Systems*, vol. 26, no. 5, pp. 6991–7005, 2025.

[5] F. C. Schweppe, *Uncertain dynamic systems*. Prentice Hall, 1973.

[6] H. I. Ugurlu, A. Redder, and E. Kayacan, "Lyapunov-inspired deep reinforcement learning for robot navigation in obstacle environments," in *2025 IEEE Symposium on Computational Intelligence on Engineering/Cyber Physical Systems (CIES)*, 2025, pp. 1–8.

[7] J. Liu, Y. Meng, M. Fitzsimmons, and R. Zhou, "Compositionally verifiable vector neural lyapunov functions for stability analysis of interconnected nonlinear systems," in *2024 American Control Conference (ACC)*, 2024, pp. 4789–4794.

[8] V. Debauche, A. Edwards, R. M. Jungers, and A. Abate, "Stability analysis of switched linear systems with neural lyapunov functions," in *Proceedings of*

the AAAI Conference on Artificial Intelligence, vol. 38, no. 19, 2024, pp. 21 010–21 018.

[9] B. Zhong, S. Liu, M. Caccamo, and M. Zamani, "Secure-by-construction synthesis for control systems," *IEEE Transactions on Automatic Control*, vol. 70, no. 6, pp. 4170–4177, 2025.

[10] A. Forsgren, P. E. Gill, and M. H. Wright, "Interior methods for nonlinear optimization," *SIAM Review*, vol. 44, no. 4, pp. 525–597, 2002. [Online]. Available: https://doi.org/10.1137/S0036144502414942

[11] P. Wieland and F. Allgower, "Constructive safety using control barrier functions," *IFAC Proceedings Volumes*, vol. 40, no. 12, pp. 462–467, 2007, 7th IFAC Symposium on Nonlinear Control Systems. [Online]. Available: https://www.sciencedirect.com/science/article/pii/S1474667016355690

[12] P.-O. Gutman and P. Hagander, "A new design of constrained controllers for linear systems," *IEEE Transactions on Automatic Control*, vol. 30, no. 1, pp. 22–33, 1985.

[13] Q. Nguyen and K. Sreenath, "L1 adaptive control for bipedal robots with control lyapunov function based quadratic programs," in *2015 American Control Conference (ACC)*, 2015, pp. 862–867.

[14] B. Li, Z. Guo, C. Hu, S. Zhu, and S. Wen, "Safe formation control of uncertain multiagent systems from a bayesian perspective," *IEEE Transactions on Automatic Control*, vol. 70, no. 3, pp. 1929–1934, 2025.

[15] Y. Ouyang, L. Xue, L. Dong, and C. Sun, "Neural network-based finite-time distributed formation-containment control of two-layer quadrotor uavs," *IEEE Transactions on Systems, Man, and Cybernetics: Systems*, vol. 52, no. 8, pp. 4836–4848, 2022.

[16] M. Abbasi and H. J. Marquez, "Observer-based event-triggered consensus control of multi-agent systems with time-varying communication delays," *IEEE Transactions on Automation Science and Engineering*, vol. 21, no. 4, pp. 6336–6346, 2024.

[17] Y. Yang, X. Si, D. Yue, and Y.-C. Tian, "Time-varying formation tracking with prescribed performance for uncertain nonaffine nonlinear multiagent systems,"

IEEE Transactions on Automation Science and Engineering, vol. 18, no. 4, pp. 1778–1789, 2021.

[18] R. Olfati-Saber, J. A. Fax, and R. M. Murray, "Consensus and cooperation in networked multi-agent systems," *Proceedings of the IEEE*, vol. 95, no. 1, pp. 215–233, 2007.

[19] L. An, G.-H. Yang, C. Deng, and C. Wen, "Event-triggered reference governors for collisions-free leader-following coordination under unreliable communication topologies," *IEEE Transactions on Automatic Control*, vol. 69, no. 4, pp. 2116–2130, 2024.

[20] S. Wang, Y. Cao, Z. Guo, Z. Yan, S. Wen, and T. Huang, "Periodic event-triggered synchronization of multiple memristive neural networks with switching topologies and parameter mismatch," *IEEE Transactions on Cybernetics*, vol. 51, no. 1, pp. 427–437, 2021.

[21] Y. Zhang, G. Wen, A. Rahmani, and B. Li, "Aperiodically intermittent adaptive dynamic event-triggered control for linear multi-agent systems," in *2022 13th Asian Control Conference (ASCC)*, 2022, pp. 1848–1853.

[22] C. Song, Y. Li, Y. Sheng, Z. Zeng, and N. R. Pal, "Sampled-data-based event-triggered output-feedback consensus for uncertain heterogeneous high-order multiagent systems," *IEEE Transactions on Systems, Man, and Cybernetics: Systems*, pp. 1–15, 2025.

[23] H. Wang, K. Xu, and H. Zhang, "Adaptive finite-time tracking control of nonlinear systems with dynamics uncertainties," *IEEE Transactions on Automatic Control*, vol. 68, no. 9, pp. 5737–5744, 2023.

[24] X.-G. Guo, D.-Y. Zhang, J.-L. Wang, J. H. Park, and L. Guo, "Observer-based event-triggered composite anti-disturbance control for multi-agent systems under multiple disturbances and stochastic fdias," *IEEE Transactions on Automation Science and Engineering*, vol. 20, no. 1, pp. 528–540, 2023.

[25] B. Li, G. Wen, Z. Peng, S. Wen, and T. Huang, "Time-varying formation control of general linear multi-agent systems under markovian switching topologies and communication noises," *IEEE Transactions on Circuits and Systems II: Express Briefs*, vol. 68, no. 4, pp. 1303–1307, 2021.

[26] M. Khan and A. Chatterjee, "Gaussian control barrier functions: Safe learning and control," in *2020 59th IEEE Conference on Decision and Control (CDC)*, 2020, pp. 3316–3322.

[27] B. Li, S. Wang, Z. Guo, S. Zhu, J. Huang, J. Sun, G. Wen, and S. Wen, "Safe control framework of multi-agent systems from a performance enhancement perspective," *IEEE Transactions on Automation Science and Engineering*, vol. 22, pp. 7622–7631, 2025.

[28] G. Pappas and S. Simic, "Consistent abstractions of affine control systems," *IEEE Transactions on Automatic Control*, vol. 47, no. 5, pp. 745–756, 2002.

[29] H. Zhang, Y. Luo, and D. Liu, "Neural-network-based near-optimal control for a class of discrete-time affine nonlinear systems with control constraints," *IEEE Transactions on Neural Networks*, vol. 20, no. 9, pp. 1490–1503, 2009.

[30] N. Nakamura, H. Nakamura, Y. Yamashita, and H. Nishitani, "Homogeneous stabilization for input affine homogeneous systems," *IEEE Transactions on Automatic Control*, vol. 54, no. 9, pp. 2271–2275, 2009.

[31] I. Kanellakopoulos, P. V. Kokotovic, and A. S. Morse, "Systematic design of adaptive controllers for feedback linearizable systems," in *1991 American Control Conference*, 1991, pp. 649–654.

[32] Y.-B. Wang, J.-Y. Hang, and M.-L. Zhang, "Stable label-specific features generation for multi-label learning via mixture-based clustering ensemble," *IEEE/CAA Journal of Automatica Sinica*, vol. 9, no. 7, pp. 1248–1261, 2022.

[33] A. Shariati and Q. Zhao, "Robust leader-following output regulation of uncertain multi-agent systems with time-varying delay," *IEEE/CAA Journal of Automatica Sinica*, vol. 5, no. 4, pp. 807–817, 2018.

[34] F. Mazenc, M. Maghenem, and A. Loria, "A strict iss-lyapunov function for ltv systems with non-time-differentiable dynamics," *IEEE Control Systems Letters*, pp. 1–1, 2025.

[35] Y. Wang, X. Li, and S. Song, "Input-to-state stabilization of nonlinear impulsive delayed systems: An observer-based control approach," *IEEE/CAA Journal of Automatica Sinica*, vol. 9, no. 7, pp. 1273–1283, 2022.

[36] H. Min, S. Xu, B. Zhang, Q. Ma, and D. Yuan, "Fixed-time lyapunov criteria and state-feedback controller design for stochastic nonlinear systems," *IEEE/CAA Journal of Automatica Sinica*, vol. 9, no. 6, pp. 1005–1014, 2022.

[37] W. He, Z. Yin, and C. Sun, "Adaptive neural network control of a marine vessel with constraints using the asymmetric barrier lyapunov function," *IEEE Transactions on Cybernetics*, vol. 47, no. 7, pp. 1641–1651, 2017.

[38] S. Mohammad Khansari-Zadeh and A. Billard, "Learning control lyapunov function to ensure stability of dynamical system-based robot reaching motions," *Robotics and Autonomous Systems*, vol. 62, no. 6, pp. 752–765, 2014. [Online]. Available: https://www.sciencedirect.com/science/article/pii/S0921889014000372

[39] N. Gaby, F. Zhang, and X. Ye, "Lyapunov-net: A deep neural network architecture for lyapunov function approximation," in *2022 IEEE 61st Conference on Decision and Control (CDC)*, 2022, pp. 2091–2096.

[40] Y. Wan, G. Wen, X. Yu, and T. Huang, "Distributed consensus tracking of networked agent systems under denial-of-service attacks," *IEEE Transactions on Systems, Man, and Cybernetics: Systems*, vol. 51, no. 10, pp. 6183–6196, 2021.

[41] L. Xing, C. Wen, F. Guo, Z. Liu, and H. Su, "Event-based consensus for linear multiagent systems without continuous communication," *IEEE Transactions on Cybernetics*, vol. 47, no. 8, pp. 2132–2142, 2017.

[42] G. Zhao and C. Hua, "Leader-following consensus of multiagent systems via asynchronous sampled-data control: A hybrid system approach," *IEEE Transactions on Automatic Control*, vol. 67, no. 5, pp. 2568–2575, 2022.

[43] Y. Zhou, G. Wen, J. Zhou, H. Liu, and J. Lv, "Data-driven output consensus tracking control for heterogeneous multi-agent systems with a dynamic leader," *IEEE Transactions on Control of Network Systems*, pp. 1–10, 2025.

[44] W. Su, C. Mu, X. Yang, J. Bian, and C. Sun, "Optimal tracking control for leader-following consensus of nonlinear multiagent systems," *IEEE Transactions on Systems, Man, and Cybernetics: Systems*, vol. 55, no. 5, pp. 3098–3107, 2025.

[45] Y. Zhou, G. Wen, J. Zhou, and T. Yang, "Data-driven fault-tolerant bipartite consensus tracking for multi-agent systems with a non-autonomous leader," *IEEE/-CAA Journal of Automatica Sinica*, vol. 12, no. 1, pp. 279–281, 2025.

[46] X. Zhang, Q. Yang, F. Xiao, H. Fang, and J. Chen, "Linear formation control of multi-agent systems," *Automatica*, vol. 171, p. 111935, 2025. [Online]. Available: https://www.sciencedirect.com/science/article/pii/S0005109824004291

[47] X.-J. Peng, Y. He, H. Li, and S. Tian, "Robust time-varying formation control of one-sided lipschitz nonlinear multiagent system with delays via optimization algorithm," *IEEE Transactions on Cybernetics*, vol. 55, no. 4, pp. 1801–1813, 2025.

[48] C. Tang, L. Ji, S. Yang, and X. Guo, "Adaptive bipartite time-varying formation tracking control for heterogeneous multi-agent systems with dos attacks," *ISA Transactions*, vol. 157, pp. 56–67, 2025. [Online]. Available: https://www.sciencedirect.com/science/article/pii/S0019057824006141

[49] Z. Zhu, Y. Jiang, Z. Liu, and F. Wang, "Fuzzy adaptive group formation-containment tracking control of nonlinear multiagent systems with intermittent actuator faults," *IEEE Transactions on Fuzzy Systems*, vol. 33, no. 5, pp. 1455–1465, 2025.

[50] J. Yu and Y. Shi, "Scaled group consensus in multiagent systems with first/second-order continuous dynamics," *IEEE Transactions on Cybernetics*, vol. 48, no. 8, pp. 2259–2271, 2018.

[51] W. Yu, G. Chen, M. Cao, and J. Kurths, "Second-order consensus for multiagent systems with directed topologies and nonlinear dynamics," *IEEE Transactions on Systems, Man, and Cybernetics, Part B (Cybernetics)*, vol. 40, no. 3, pp. 881–891, 2010.

[52] N. Wang, Y. Wang, G. Wen, M. Lv, and F. Zhang, "Fuzzy adaptive constrained consensus tracking of high-order multi-agent networks: A new event-triggered mechanism," *IEEE Transactions on Systems, Man, and Cybernetics: Systems*, vol. 52, no. 9, pp. 5468–5480, 2022.

[53] R. Yang, L. Liu, and G. Feng, "Leader-following output consensus of heterogeneous uncertain linear multiagent systems with dynamic event-triggered strategy," *IEEE Transactions on Systems, Man, and Cybernetics: Systems*, vol. 52, no. 3, pp. 1626–1637, 2022.

[54] C.-E. Ren, J. Zhang, and Y. Guan, "Prescribed performance bipartite consensus control for stochastic nonlinear multiagent systems under event-triggered strategy," *IEEE Transactions on Cybernetics*, vol. 53, no. 1, pp. 468–482, 2023.

[55] J. Fu, G. Wen, X. Yu, and Z.-G. Wu, "Distributed formation navigation of constrained second-order multiagent systems with collision avoidance and connectivity maintenance," *IEEE Transactions on Cybernetics*, vol. 52, no. 4, pp. 2149–2162, 2022.

[56] Y. Lu, X. Dong, Q. Li, J. Lv, and Z. Ren, "Time-varying group formation-containment tracking control for general linear multiagent systems with unknown inputs," *IEEE Transactions on Cybernetics*, vol. 52, no. 10, pp. 11 055–11 067, 2022.

[57] D. Shevitz and B. Paden, "Lyapunov stability theory of nonsmooth systems," *IEEE Transactions on Automatic Control*, vol. 39, no. 9, pp. 1910–1914, 1994.

[58] Z. Artstein, "Stabilization with relaxed controls," *Nonlinear Analysis: Theory, Methods & Applications*, vol. 7, no. 11, pp. 1163–1173, 1983. [Online]. Available: https://www.sciencedirect.com/science/article/pii/0362546X83900494

[59] E. D. Sontag, "A 'universal' construction of artstein's theorem on nonlinear stabilization," *Systems & Control Letters*, vol. 13, no. 2, pp. 117–123, 1989. [Online]. Available: https://www.sciencedirect.com/science/article/pii/0167691189900285

[60] R. A. Freeman and P. V. Kokotovic, "Inverse optimality in robust stabilization," *SIAM Journal on Control and Optimization*, vol. 34, no. 4, pp. 1365–1391, 1996. [Online]. Available: https://doi.org/10.1137/S0363012993258732

[61] A. D. Ames and M. Powell, "Towards the unification of locomotion and manipulation through control lyapunov functions and quadratic programs," in *Control of Cyber-Physical Systems: Workshop held at Johns Hopkins University*. Springer, 2013, pp. 219–240.

[62] A. D. Ames, K. Galloway, K. Sreenath, and J. W. Grizzle, "Rapidly exponentially stabilizing control lyapunov functions and hybrid zero dynamics," *IEEE Transactions on Automatic Control*, vol. 59, no. 4, pp. 876–891, 2014.

[63] R. Freeman and J. Primbs, "Control lyapunov functions: new ideas from an old source," in *Proceedings of 35th IEEE Conference on Decision and Control*, vol. 4, 1996, pp. 3926–3931 vol.4.

[64] H. Yuqing and H. Jianda, "Generalized point wise min-norm control based on control lyapunov functions," in *2007 Chinese Control Conference*, 2007, pp. 404–408.

[65] R. Furqon, Y.-J. Chen, M. Tanaka, K. Tanaka, and H. O. Wang, "An sos-based control lyapunov function design for polynomial fuzzy control of nonlinear systems," *IEEE Transactions on Fuzzy Systems*, vol. 25, no. 4, pp. 775–787, 2017.

[66] B. Li, S. Wen, Z. Yan, G. Wen, and T. Huang, "A survey on the control lyapunov function and control barrier function for nonlinear-affine control systems," *IEEE/CAA Journal of Automatica Sinica*, vol. 10, no. 3, pp. 584–602, 2023.

[67] F. Castaneda, J. J. Choi, B. Zhang, C. J. Tomlin, and K. Sreenath, "Gaussian process-based min-norm stabilizing controller for control-affine systems with uncertain input effects and dynamics," in *2021 American Control Conference (ACC)*, 2021, pp. 3683–3690.

[68] B. Li, G. Wen, Z. Peng, T. Huang, and A. Rahmani, "Fully distributed consensus tracking of stochastic nonlinear multiagent systems with markovian switching topologies via intermittent control," *IEEE Transactions on Systems, Man, and Cybernetics: Systems*, vol. 52, no. 5, pp. 3200–3209, 2022.

[69] Z.-W. Liu, X. Yu, Z.-H. Guan, B. Hu, and C. Li, "Pulse-modulated intermittent control in consensus of multiagent systems," *IEEE Transactions on Systems, Man, and Cybernetics: Systems*, vol. 47, no. 5, pp. 783–793, 2017.

[70] S. He, X. Liu, P. Lu, C. Du, and H. Liu, "Distributed finite-time consensus algorithm for multiagent systems via aperiodically intermittent protocol," *IEEE Transactions on Circuits and Systems II: Express Briefs*, vol. 69, no. 7, pp. 3229–3233, 2022.

[71] H.-J. Ma, G.-H. Yang, and T. Chen, "Event-triggered optimal dynamic formation of heterogeneous affine nonlinear multiagent systems," *IEEE Transactions on Automatic Control*, vol. 66, no. 2, pp. 497–512, 2021.

[72] B. Li, Y. Cao, Y. Yang, S. Zhu, Z. Guo, T. Huang, and S. Wen, "Quadratic programming consensus tracking control of uncertain multiagent systems via event-triggered mechanism," *IEEE Transactions on Systems, Man, and Cybernetics: Systems*, vol. 54, no. 12, pp. 7861–7870, 2024.

[73] P. Tabuada, "Event-triggered real-time scheduling of stabilizing control tasks," *IEEE Transactions on Automatic Control*, vol. 52, no. 9, pp. 1680–1685, 2007.

[74] P. Ong, G. Bahati, and A. D. Ames, "Stability and safety through event-triggered intermittent control with application to spacecraft orbit stabilization," in *2022 IEEE 61st Conference on Decision and Control (CDC)*, 2022, pp. 453–460.

[75] Y. H. Choi and S. J. Yoo, "Neural-network-based distributed asynchronous event-triggered consensus tracking of a class of uncertain nonlinear multi-agent systems," *IEEE Transactions on Neural Networks and Learning Systems*, vol. 33, no. 7, pp. 2965–2979, 2022.

[76] S. Prajna, A. Jadbabaie, and G. J. Pappas, "A framework for worst-case and stochastic safety verification using barrier certificates," *IEEE Transactions on Automatic Control*, vol. 52, no. 8, pp. 1415–1428, 2007.

[77] J. Sun, J. Yang, and Z. Zeng, "Safety-critical control with control barrier function based on disturbance observer," *IEEE Transactions on Automatic Control*, vol. 69, no. 7, pp. 4750–4756, 2024.

[78] M. H. Cohen, T. G. Molnar, and A. D. Ames, "Safety-critical control for autonomous systems: Control barrier functions via reduced-order models," *Annual Reviews in Control*, vol. 57, p. 100947, 2024. [Online]. Available: https://www.sciencedirect.com/science/article/pii/S1367578824000166

[79] A. Isaly, M. Ghanbarpour, R. G. Sanfelice, and W. E. Dixon, "On the feasibility and continuity of feedback controllers defined by multiple control barrier functions," *IEEE Transactions on Automatic Control*, vol. 69, no. 11, pp. 7326–7339, 2024.

[80] M. Rauscher, M. Kimmel, and S. Hirche, "Constrained robot control using control barrier functions," in *2016 IEEE/RSJ International Conference on Intelligent Robots and Systems (IROS)*, 2016, pp. 279–285.

[81] W. Shaw-Cortez, D. Oetomo, C. Manzie, and P. Choong, "Tactile-based blind grasping: A discrete-time object manipulation controller for robotic hands," *IEEE Robotics and Automation Letters*, vol. 3, no. 2, pp. 1064–1071, 2018.

[82] W. Shaw Cortez, D. Oetomo, C. Manzie, and P. Choong, "Control barrier functions for mechanical systems: Theory and application to robotic grasping," *IEEE Transactions on Control Systems Technology*, vol. 29, no. 2, pp. 530–545, 2021.

[83] S. Kousik, S. Vaskov, F. Bu, M. Johnson-Roberson, and R. Vasudevan, "Bridging the gap between safety and real-time performance in receding-horizon trajectory design for mobile robots," *The International Journal of Robotics Research*, vol. 39, no. 12, pp. 1419–1469, 2020. [Online]. Available: https://doi.org/10.1177/0278364920943266

[84] J. Zeng, B. Zhang, and K. Sreenath, "Safety-critical model predictive control with discrete-time control barrier function," in *2021 American Control Conference (ACC)*, 2021, pp. 3882–3889.

[85] W. Jiang, G. Wen, Z. Peng, T. Huang, and A. Rahmani, "Fully distributed formation-containment control of heterogeneous linear multiagent systems," *IEEE Transactions on Automatic Control*, vol. 64, no. 9, pp. 3889–3896, 2019.

[86] A. Mondal, C. Bhowmick, L. Behera, and M. Jamshidi, "Trajectory tracking by multiple agents in formation with collision avoidance and connectivity assurance," *IEEE Systems Journal*, vol. 12, no. 3, pp. 2449–2460, 2018.

[87] N. Lashkari, M. Biglarbegian, and S. X. Yang, "Development of a novel robust control method for formation of heterogeneous multiple mobile robots with autonomous docking capability," *IEEE Transactions on Automation Science and Engineering*, vol. 17, no. 4, pp. 1759–1776, 2020.

[88] S. Prajna and A. Rantzer, "Convex programs for temporal verification of nonlinear dynamical systems," *SIAM Journal on Control and Optimization*, vol. 46, no. 3, pp. 999–1021, 2007. [Online]. Available: https://doi.org/10.1137/050645178

[89] R. Wisniewski and C. Sloth, "Converse barrier certificate theorems," *IEEE Transactions on Automatic Control*, vol. 61, no. 5, pp. 1356–1361, 2016.

[90] C. Tomlin, G. Pappas, and S. Sastry, "Conflict resolution for air traffic management: a study in multiagent hybrid systems," *IEEE Transactions on Automatic Control*, vol. 43, no. 4, pp. 509–521, 1998.

[91] L. Wang, A. D. Ames, and M. Egerstedt, "Safety barrier certificates for collisions-free multirobot systems," *IEEE Transactions on Robotics*, vol. 33, no. 3, pp. 661–674, 2017.

[92] Y. Chen, A. Singletary, and A. D. Ames, "Guaranteed obstacle avoidance for multi-robot operations with limited actuation: A control barrier function approach," *IEEE Control Systems Letters*, vol. 5, no. 1, pp. 127–132, 2021.

[93] L. Wang, A. Ames, and M. Egerstedt, "Safety barrier certificates for heterogeneous multi-robot systems," in *2016 American Control Conference (ACC)*, 2016, pp. 5213–5218.

[94] J. Fu, G. Wen, and X. Yu, "Safe consensus tracking with guaranteed full state and input constraints: A control barrier function-based approach," *IEEE Transactions on Automatic Control*, vol. 68, no. 12, pp. 8075–8081, 2023.

[95] S. Yan, L. Shi, H. Zhang, S. Yao, and Y. Zhou, "Safety-critical model-free adaptive iterative learning control for multi-agent consensus using control barrier functions," *IEEE Transactions on Circuits and Systems II: Express Briefs*, vol. 71, no. 1, pp. 221–225, 2024.

[96] J. Long, W. Wang, J. Huang, J. Lv, and K. Liu, "Adaptive leaderless consensus for uncertain high-order nonlinear multiagent systems with event-triggered communication," *IEEE Transactions on Systems, Man, and Cybernetics: Systems*, vol. 52, no. 11, pp. 7101–7111, 2022.

[97] E. Sabouni, C. G. Cassandras, W. Xiao, and N. Meskin, "Optimal control of connected automated vehicles with event/self-triggered control barrier functions," *Automatica*, vol. 162, p. 111530, 2024. [Online]. Available: https://www.sciencedirect.com/science/article/pii/S0005109824000220

[98] S.-C. Hsu, X. Xu, and A. D. Ames, "Control barrier function based quadratic programs with application to bipedal robotic walking," in *2015 American Control Conference (ACC)*, 2015, pp. 4542–4548.

[99] G. Wu and K. Sreenath, "Safety-critical and constrained geometric control synthesis using control lyapunov and control barrier functions for systems evolving on manifolds," in *2015 American Control Conference (ACC)*, 2015, pp. 2038–2044.

[100] Q. Nguyen and K. Sreenath, "Exponential control barrier functions for enforcing high relative-degree safety-critical constraints," in *2016 American Control Conference (ACC)*, 2016, pp. 322–328.

[101] X. Xu, "Constrained control of input-output linearizable systems using control sharing barrier functions," *Automatica*, vol. 87, pp. 195–201, 2018. [Online]. Available: https://www.sciencedirect.com/science/article/pii/S0005109817305046

[102] W. Xiao and C. Belta, "Control barrier functions for systems with high relative degree," in *2019 IEEE 58th Conference on Decision and Control (CDC)*, 2019, pp. 474–479.

[103] A. D. Ames, J. W. Grizzle, and P. Tabuada, "Control barrier function based quadratic programs with application to adaptive cruise control," in *53rd IEEE Conference on Decision and Control*, 2014, pp. 6271–6278.

[104] X. Xu, P. Tabuada, J. W. Grizzle, and A. D. Ames, "Robustness of control barrier functions for safety critical control," *IFAC-PapersOnLine*, vol. 48, no. 27, pp. 54–61, 2015, analysis and Design of Hybrid Systems ADHS. [Online]. Available: https://www.sciencedirect.com/science/article/pii/S2405896315024106

[105] W. Xiao and C. Belta, "High-order control barrier functions," *IEEE Transactions on Automatic Control*, vol. 67, no. 7, pp. 3655–3662, 2022.

[106] Y. Xiong, D.-H. Zhai, M. Tavakoli, and Y. Xia, "Discrete-time control barrier function: High-order case and adaptive case," *IEEE Transactions on Cybernetics*, vol. 53, no. 5, pp. 3231–3239, 2023.

[107] S. Liu, J. Zeng, K. Sreenath, and C. A. Belta, "Iterative convex optimization for model predictive control with discrete-time high-order control barrier functions," in *2023 American Control Conference (ACC)*, 2023, pp. 3368–3375.

[108] M. Hajiahmadi, B. De Schutter, and H. Hellendoorn, "Design of stabilizing switching laws for mixed switched affine systems," *IEEE Transactions on Automatic Control*, vol. 61, no. 6, pp. 1676–1681, 2016.

[109] Z. Peng, D. Wang, T. Li, and M. Han, "Output-feedback cooperative formation maneuvering of autonomous surface vehicles with connectivity preservation and collision avoidance," *IEEE Transactions on Cybernetics*, vol. 50, no. 6, pp. 2527–2535, 2020.

[110] E. Gilbert and I. Kolmanovsky, "A generalized reference governor for nonlinear systems," in *Proceedings of the 40th IEEE Conference on Decision and Control (Cat. No.01CH37228)*, vol. 5, 2001, pp. 4222–4227 vol.5.

[111] J. Wolff and M. Buss, "Invariance control design for nonlinear control affine systems under hard state constraints," *IFAC Proceedings Volumes*, vol. 37, no. 13, pp. 555–560, 2004, 6th IFAC Symposium on Nonlinear Control Systems 2004 (NOLCOS 2004), Stuttgart, Germany, 1-3 September, 2004. [Online]. Available: https://www.sciencedirect.com/science/article/pii/S147466701731282X

[112] K. Ngo, R. Mahony, and Z.-P. Jiang, "Integrator backstepping using barrier functions for systems with multiple state constraints," in *Proceedings of the 44th IEEE Conference on Decision and Control*, 2005, pp. 8306–8312.

[113] K. P. Tee, S. S. Ge, and E. H. Tay, "Barrier lyapunov functions for the control of output-constrained nonlinear systems," *Automatica*, vol. 45, no. 4, pp. 918–927, 2009. [Online]. Available: https://www.sciencedirect.com/science/article/pii/S0005109808005608

[114] M. Z. Romdlony and B. Jayawardhana, "Uniting control lyapunov and control barrier functions," in *53rd IEEE Conference on Decision and Control*, 2014, pp. 2293–2298.

[115] A. D. Ames, X. Xu, J. W. Grizzle, and P. Tabuada, "Control barrier function based quadratic programs for safety critical systems," *IEEE Transactions on Automatic Control*, vol. 62, no. 8, pp. 3861–3876, 2017.

[116] T. G. Molnar, R. K. Cosner, A. W. Singletary, W. Ubellacker, and A. D. Ames, "Model-free safety-critical control for robotic systems," *IEEE Robotics and Automation Letters*, vol. 7, no. 2, pp. 944–951, 2022.

[117] S. K. Sahoo, S. Dasgupta, S. K. Panda, and J.-X. Xu, "A lyapunov function-based robust direct torque controller for a switched reluctance motor drive system," *IEEE Transactions on Power Electronics*, vol. 27, no. 2, pp. 555–564, 2012.

[118] R. Cheng, M. J. Khojasteh, A. D. Ames, and J. W. Burdick, "Safe multi-agent interaction through robust control barrier functions with learned uncertainties," in *2020 59th IEEE Conference on Decision and Control (CDC)*, 2020, pp. 777–783.

[119] A. Alan, A. J. Taylor, C. R. He, G. Orosz, and A. D. Ames, "Safe controller synthesis with tunable input-to-state safe control barrier functions," *IEEE Control Systems Letters*, vol. 6, pp. 908–913, 2022.

[120] S. Kolathaya and A. D. Ames, "Input-to-state safety with control barrier functions," *IEEE Control Systems Letters*, vol. 3, no. 1, pp. 108–113, 2019.

[121] P. Zhao, Y. Mao, C. Tao, N. Hovakimyan, and X. Wang, "Adaptive robust quadratic programs using control lyapunov and barrier functions," in *2020 59th IEEE Conference on Decision and Control (CDC)*, 2020, pp. 3353–3358.

[122] R. Takano and M. Yamakita, "Robust constrained stabilization control using control lyapunov and control barrier function in the presence of measurement noises," in *2018 IEEE Conference on Control Technology and Applications (CCTA)*, 2018, pp. 300–305.

[123] M. Jankovic, "Robust control barrier functions for constrained stabilization of nonlinear systems," *Automatica*, vol. 96, pp. 359–367, 2018. [Online]. Available: https://www.sciencedirect.com/science/article/pii/S0005109818303509

[124] A. Alan, T. G. Molnar, E. Das, A. D. Ames, and G. Orosz, "Disturbance observers for robust safety-critical control with control barrier functions," *IEEE Control Systems Letters*, vol. 7, pp. 1123–1128, 2023.

[125] D. Zeng, Y. Jiang, Y. Wang, H. Zhang, and Y. Feng, "Robust adaptive control barrier functions for input-affine systems: Application to uncertain manipulator safety constraints," *IEEE Control Systems Letters*, vol. 8, pp. 279–284, 2024.

[126] A. Isaly, O. S. Patil, R. G. Sanfelice, and W. E. Dixon, "Adaptive safety with multiple barrier functions using integral concurrent learning," in *2021 American Control Conference (ACC)*, 2021, pp. 3719–3724.

[127] M. H. Cohen, C. Belta, and R. Tron, "Robust control barrier functions for nonlinear control systems with uncertainty: A duality-based approach," in *2022 IEEE 61st Conference on Decision and Control (CDC)*, 2022, pp. 174–179.

[128] Q. Nguyen and K. Sreenath, "Optimal robust control for constrained nonlinear hybrid systems with application to bipedal locomotion," in *2016 American Control Conference (ACC)*, 2016, pp. 4807–4813.

[129] B. T. Lopez and J.-J. E. Slotine, "Unmatched control barrier functions: Certainty equivalence adaptive safety," in *2023 American Control Conference (ACC)*, 2023, pp. 3662–3668.

[130] M. Black, E. Arabi, and D. Panagou, "A fixed-time stable adaptation law for safety-critical control under parametric uncertainty," in *2021 European Control Conference (ECC)*, 2021, pp. 1328–1333.

[131] J. Buch, S.-C. Liao, and P. Seiler, "Robust control barrier functions with sector-bounded uncertainties," *IEEE Control Systems Letters*, vol. 6, pp. 1994–1999, 2022.

[132] Y. Emam, P. Glotfelter, S. Wilson, G. Notomista, and M. Egerstedt, "Data-driven robust barrier functions for safe, long-term operation," *IEEE Transactions on Robotics*, vol. 38, no. 3, pp. 1671–1685, 2022.

[133] Z. Jin, M. Khajenejad, and S. Z. Yong, "Robust data-driven control barrier functions for unknown continuous control affine systems," *IEEE Control Systems Letters*, vol. 7, pp. 1309–1314, 2023.

[134] A. J. Taylor, V. D. Dorobantu, H. M. Le, Y. Yue, and A. D. Ames, "Episodic learning with control lyapunov functions for uncertain robotic systems," in *2019 IEEE/RSJ International Conference on Intelligent Robots and Systems (IROS)*, 2019, pp. 6878–6884.

[135] A. Taylor, A. Singletary, Y. Yue, and A. Ames, "Learning for safety-critical control with control barrier functions," in *Proceedings of the 2nd Conference on Learning for Dynamics and Control*, vol. 120. PMLR, 10–11 Jun 2020, pp. 708–717.

[136] J. Choi, F. Castaneda, C. J.Tomlin, and K. Sreenath, "Reinforcement learning for safety-critical control under model uncertainty, using control lyapunov functions and control barrier functions," 2020.

[137] C. Dawson, Z. Qin, S. Gao, and C. Fan, "Safe nonlinear control using robust neural lyapunov-barrier functions," in *Proceedings of the 5th Conference on Robot Learning*, vol. 164. PMLR, 08–11 Nov 2022, pp. 1724–1735.

[138] P. Jagtap, G. J. Pappas, and M. Zamani, "Control barrier functions for unknown nonlinear systems using gaussian processes," in *2020 59th IEEE Conference on Decision and Control (CDC)*, 2020, pp. 3699–3704.

[139] F. Castaneda, J. J. Choi, B. Zhang, C. J. Tomlin, and K. Sreenath, "Pointwise feasibility of gaussian process-based safety-critical control under model uncertainty," in *2021 60th IEEE Conference on Decision and Control (CDC)*, 2021, pp. 6762–6769.

[140] P. Mestres and J. Cortes, "Feasibility and regularity analysis of safe stabilizing controllers under uncertainty," *Automatica*, vol. 167, p. 111800, 2024.

[141] A. Lederer, Z. Yang, J. Jiao, and S. Hirche, "Cooperative control of uncertain multiagent systems via distributed gaussian processes," *IEEE Transactions on Automatic Control*, vol. 68, no. 5, pp. 3091–3098, 2023.

[142] Y. Hu, J. Fu, and G. Wen, "Decentralized robust collision-avoidance for cooperative multirobot systems: A gaussian process-based control barrier function approach," *IEEE Transactions on Control of Network Systems*, vol. 10, no. 2, pp. 706–717, 2023.

[143] Q. Wei, Z. Yang, H. Su, and L. Wang, "Online adaptive dynamic programming for optimal self-learning control of vtol aircraft systems with disturbances," *IEEE Transactions on Automation Science and Engineering*, vol. 21, no. 1, pp. 343–352, 2024.

[144] H. Wang, H. Zhang, L. Li, and M. Fu, "Lqr and stabilization for discrete-time systems with multiplicative noises and input delays," *IEEE Transactions on Automatic Control*, vol. 69, no. 6, pp. 3515–3530, 2024.

[145] T. Feng, J. Zhang, Y. Tong, and H. Zhang, "Consensusability and global optimality of discrete-time linear multiagent systems," *IEEE Transactions on Cybernetics*, vol. 52, no. 8, pp. 8227–8238, 2022.

[146] C. An, H. Su, and S. Chen, "Inverse-optimal consensus control of fractional-order multiagent systems," *IEEE Transactions on Systems, Man, and Cybernetics: Systems*, vol. 52, no. 8, pp. 5320–5331, 2022.

[147] J. Ma, Z. Cheng, X. Li, W. Wang, M. Tomizuka, and T. H. Lee, "Data-driven linear quadratic optimization for controller synthesis with structural constraints," *IEEE Transactions on Cybernetics*, vol. 54, no. 4, pp. 2295–2307, 2024.

[148] A. S. Sathya, H. Bruyninckx, W. Decre, and G. Pipeleers, "Efficient constrained dynamics algorithms based on an equivalent lqr formulation using gauss' principle of least constraint," *IEEE Transactions on Robotics*, vol. 40, pp. 729–749, 2024.

[149] A. Komaee, "Dynamic gain adaptation in linear quadratic regulators," *IEEE Transactions on Automatic Control*, vol. 69, no. 8, pp. 5094–5108, 2024.

[150] R. Garnett, *Bayesian optimization*. Cambridge University Press, 2023.

[151] C. E. Rasmussen, C. K. Williams *et al.*, *Gaussian processes for machine learning*. The MIT Press, 2006, vol. 1.

[152] M. A. Gelbart, J. Snoek, and R. P. Adams, "Bayesian optimization with unknown constraints," in *Proc. of the 13th Conference on Uncertainty in Artificial Intelligence*, 2014, pp. 250–259.

[153] M. Khosravi, C. Konig, M. Maier, R. S. Smith, J. Lygeros, and A. Rupenyan, "Safety-aware cascade controller tuning using constrained bayesian optimization," *IEEE Transactions on Industrial Electronics*, vol. 70, no. 2, pp. 2128–2138, 2023.

[154] R. Cosner, M. Tucker, A. Taylor, K. Li, T. Molnar, W. Ubelacker, A. Alan, G. Orosz, Y. Yue, and A. Ames, "Safety-aware preference-based learning for safety-critical control," in *Proceedings of The 4th Annual Learning for Dynamics and Control Conference*, vol. 168. PMLR, 23–24 Jun 2022, pp. 1020–1033.

[155] M. Arcak and A. Teel, "Input-to-state stability for a class of lurie systems," *Automatica*, vol. 38, no. 11, pp. 1945–1949, 2002. [Online]. Available: https://www.sciencedirect.com/science/article/pii/S0005109802001000

[156] H. Zhang, F. L. Lewis, and A. Das, "Optimal design for synchronization of cooperative systems: State feedback, observer and output feedback," *IEEE Transactions on Automatic Control*, vol. 56, no. 8, pp. 1948–1952, 2011.

[157] A. I. Paredes, E. Nuno, and A. Loria, "Output-feedback consensus-formation control of nonholonomic vehicles with input constraints and time-varying delays," *IEEE Transactions on Control of Network Systems*, pp. 1–11, 2025.

[158] A. D. Ames, K. Galloway, and J. W. Grizzle, "Control lyapunov functions and hybrid zero dynamics," in *2012 IEEE 51st IEEE Conference on Decision and Control (CDC)*, 2012, pp. 6837–6842.

[159] M. V. Minniti, R. Grandia, F. Farshidian, and M. Hutter, "Adaptive clf-mpc with application to quadrupedal robots," *IEEE Robotics and Automation Letters*, vol. 7, no. 1, pp. 565–572, 2022.

[160] R. Freeman and P. V. Kokotovic, *Robust nonlinear control design: state-space and Lyapunov techniques*. Springer Science & Business Media, 2008.

[161] Z. Li, X. Liu, W. Ren, and L. Xie, "Distributed tracking control for linear multiagent systems with a leader of bounded unknown input," *IEEE Transactions on Automatic Control*, vol. 58, no. 2, pp. 518–523, 2013.

[162] Z. Qu, *Cooperative control of dynamical systems: applications to autonomous vehicles*. Springer, 2009, vol. 3.

[163] N. Srinivas, A. Krause, S. M. Kakade, and M. W. Seeger, "Information-theoretic regret bounds for gaussian process optimization in the bandit setting," *IEEE Transactions on Information Theory*, vol. 58, no. 5, pp. 3250–3265, 2012.

[164] N. Pang, X. Wang, and Z. Wang, "Observer-based event-triggered adaptive control for nonlinear multiagent systems with unknown states and disturbances," *IEEE Transactions on Neural Networks and Learning Systems*, vol. 34, no. 9, pp. 6663–6669, 2023.

[165] J. Umlauft, L. Pohler, and S. Hirche, "An uncertainty-based control lyapunov approach for control-affine systems modeled by gaussian process," *IEEE Control Systems Letters*, vol. 2, no. 3, pp. 483–488, 2018.

[166] G. Chowdhary, H. A. Kingravi, J. P. How, and P. A. Vela, "Bayesian nonparametric adaptive control using gaussian processes," *IEEE Transactions on Neural Networks and Learning Systems*, vol. 26, no. 3, pp. 537–550, 2015.

[167] H. Abdi, G. Raja, and R. Ghabcheloo, "Safe control using vision-based control barrier function (v-cbf)," in *2023 IEEE International Conference on Robotics and Automation (ICRA)*, 2023, pp. 782–788.

[168] S. Wang and S. Wen, "Safe control against uncertainty: A comprehensive review of control barrier function strategies," *IEEE Systems, Man, and Cybernetics Magazine*, vol. 11, no. 1, pp. 34–47, 2025.

[169] M. Desai and A. Ghaffari, "Clf-cbf based quadratic programs for safe motion control of nonholonomic mobile robots in presence of moving obstacles," in *2022 IEEE/ASME International Conference on Advanced Intelligent Mechatronics (AIM)*, 2022, pp. 16–21.

[170] T. Gurriet, A. Singletary, J. Reher, L. Ciarletta, E. Feron, and A. Ames, "Towards a framework for realizable safety critical control through active set invariance," in *2018 ACM/IEEE 9th International Conference on Cyber-Physical Systems (ICCPS)*, 2018, pp. 98–106.

[171] B. J. Morris, M. J. Powell, and A. D. Ames, "Continuity and smoothness properties of nonlinear optimization-based feedback controllers," in *2015 54th IEEE Conference on Decision and Control (CDC)*, 2015, pp. 151–158.

[172] Y. Hong, J. Hu, and L. Gao, "Tracking control for multi-agent consensus with an active leader and variable topology," *Automatica*, vol. 42, no. 7, pp. 1177–1182, 2006. [Online]. Available: https://www.sciencedirect.com/science/article/pii/S0005109806001063

[173] G. Wahba, *Spline models for observational data*. Philadelphia, PA,USA: Siam, 1990.

[174] I. Steinwart and A. Christmann, *Support vector machines*. New York, NY, USA: Springer-Verlag, 2008.

[175] T. Beckers, D. Kulifá, and S. Hirche, "Stable gaussian process based tracking control of euler-lagrange systems," *Automatica*, vol. 103, pp. 390–397,

2019. [Online]. Available: https://www.sciencedirect.com/science/article/pii/S0005109819300305

[176] X. Tan, W. S. Cortez, and D. V. Dimarogonas, "High-order barrier functions: Robustness, safety, and performance-critical control," *IEEE Transactions on Automatic Control*, vol. 67, no. 6, pp. 3021–3028, 2022.

[177] D. Liu and J. Fu, "High-order control barrier function based robust collision avoidance formation tracking of constrained multi-agent systems," in *International Conference on Neural Information Processing*. Springer, 2023, pp. 253–264.

[178] S. Sastry, *Nonlinear systems: analysis, stability, and control*. Springer Science & Business Media, 2013, vol. 10.

[179] L. Lindemann and D. V. Dimarogonas, "Control barrier functions for signal temporal logic tasks," *IEEE Control Systems Letters*, vol. 3, no. 1, pp. 96–101, 2019.

[180] D. R. Jones, M. Schonlau, and W. J. Welch, "Efficient global optimization of expensive black-box functions," *Journal of Global optimization*, vol. 13, no. 4, p. 455, 1998.

[181] Q. Liang, A. E. Gongora, Z. Ren, A. Tiihonen, Z. Liu, S. Sun, J. R. Deneault, D. Bash, F. Mekki-Berrada, S. A. Khan *et al.*, "Benchmarking the performance of bayesian optimization across multiple experimental materials science domains," *npj Computational Materials*, vol. 7, no. 1, p. 188, 2021.

[182] J. Ma, Y. Zheng, and L. Wang, "Lqr-based optimal topology of leader-following consensus," *International Journal of Robust and Nonlinear Control*, vol. 25, no. 17, pp. 3404–3421, 2015.

[183] L. Lindemann and D. V. Dimarogonas, "Control barrier functions for multi-agent systems under conflicting local signal temporal logic tasks," *IEEE Control Systems Letters*, vol. 3, no. 3, pp. 757–762, 2019.

[184] E. Vazquez and J. Bect, "Convergence properties of the expected improvement algorithm with fixed mean and covariance functions," *Journal of Statistical Planning and inference*, vol. 140, no. 11, pp. 3088–3095, 2010.

[185] F. Bachoc, C. Helbert, and V. Picheny, "Gaussian process optimization with failures: classification and convergence proof," *Journal of Global Optimization*, vol. 78, pp. 483–506, 2020.

[186] H.-C. Kim and Z. Ghahramani, "Bayesian gaussian process classification with the em-ep algorithm," *IEEE Transactions on Pattern Analysis and Machine Intelligence*, vol. 28, no. 12, pp. 1948–1959, 2006.

[187] M. Feurer, J. Springenberg, and F. Hutter, "Initializing bayesian hyperparameter optimization via meta-learning," in *Proceedings of the AAAI Conference on Artificial Intelligence*, vol. 29, no. 1, 2015.

[188] S. Wang and K. Li, "Constrained bayesian optimization under partial observations: Balanced improvements and provable convergence," in *Proceedings of the AAAI Conference on Artificial Intelligence*, vol. 38, no. 14, 2024, pp. 15 607–15 615.

[189] Q. Fu, T. Qiu, J. Yi, Z. Pu, and S. Wu, "Concentration network for reinforcement learning of large-scale multi-agent systems," in *Proceedings of the AAAI Conference on Artificial Intelligence*, vol. 36, no. 9, 2022, pp. 9341–9349.

[190] S. Wang, K. Li, Y. Yang, Y. Cao, T. Huang, and S. Wen, "Model-assisted probabilistic safe adaptive control with meta-bayesian learning," 2023. [Online]. Available: https://doi.org/10.48550/arXiv.2307.00828